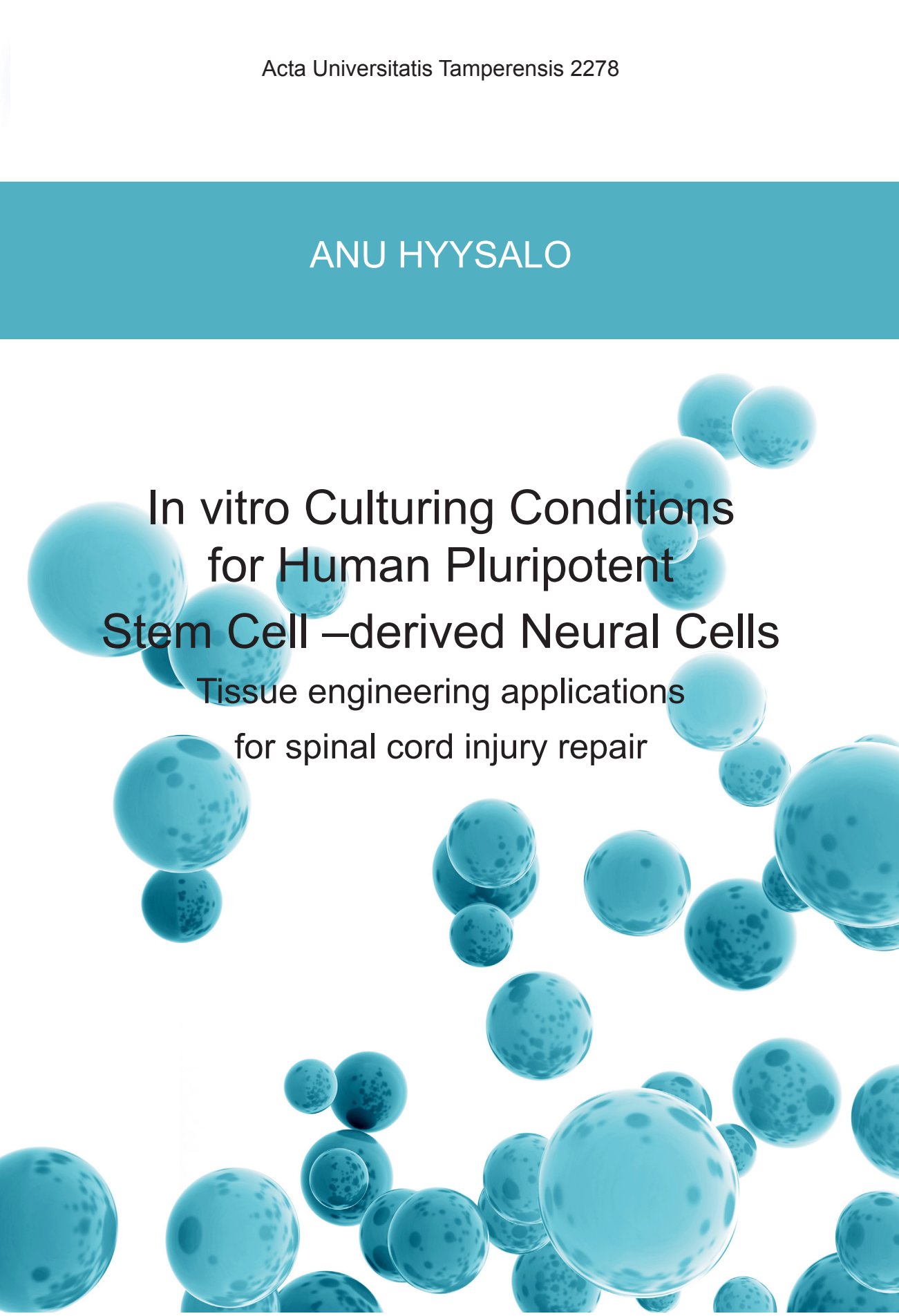


ANU HYYSALO



In vitro Culturing Conditions for Human Pluripotent Stem Cell –derived Neural Cells

Tissue engineering applications
for spinal cord injury repair



ANU HYYSALO

In vitro Culturing Conditions
for Human Pluripotent
Stem Cell –derived Neural Cells

Tissue engineering applications
for spinal cord injury repair



ACADEMIC DISSERTATION

To be presented, with the permission of
the Faculty council of the Faculty of Medicine and Life Sciences
of the University of Tampere,
for public discussion in the auditorium F114 of the Arvo building,
Lääkärintäti 1, Tampere,
on 9 June 2017, at 12 o'clock.

UNIVERSITY OF TAMPERE

ANU HYYSALO

In vitro Culturing Conditions
for Human Pluripotent
Stem Cell –derived Neural Cells

Tissue engineering applications
for spinal cord injury repair

Acta Universitatis Tamperensis 2278
Tampere University Press
Tampere 2017

ACADEMIC DISSERTATION

University of Tampere, Faculty of Medicine and Life Sciences
Finland

Supervised by

Docent Susanna Narkilahti
University of Tampere
Finland

Reviewed by

Professor Cecilia Sahlgren
Åbo Akademi
Finland
Professor Meng Li
Cardiff University
United Kingdom

The originality of this thesis has been checked using the Turnitin OriginalityCheck service in accordance with the quality management system of the University of Tampere.

Copyright ©2017 Tampere University Press and the author

Cover design by
Mikko Reinikka

Acta Universitatis Tamperensis 2278
ISBN 978-952-03-0431-7 (print)
ISSN-L 1455-1616
ISSN 1455-1616

Acta Electronica Universitatis Tamperensis 1780
ISBN 978-952-03-0432-4 (pdf)
ISSN 1456-954X
<http://tampub.uta.fi>

Suomen Yliopistopaino Oy – Juvenes Print
Tampere 2017



The most exciting phrase to hear in science, the one that heralds new discoveries, is not "Eureka!" (I found it!) but "That's funny..."

~Isaac Asimov

Contents

1	Introduction.....	19
2	Literature review.....	21
2.1	The human central nervous system	21
2.1.1	Development of the human central nervous system.....	21
2.1.2	Central nervous system cells <i>in vitro</i>	23
2.2	Human pluripotent stem cells.....	24
2.2.1	Neural differentiation <i>in vitro</i>	26
2.2.2	Astrocyte differentiation <i>in vitro</i>	27
2.2.3	Oligodendrocyte differentiation <i>in vitro</i>	28
2.3	Defined extracellular matrix for hPSC-derived neural cells.....	30
2.3.1	Extracellular matrix composition in the human central nervous system .	30
2.3.2	Defined extracellular matrix substrates for 2D culturing of hPSC-derived neural cells	32
2.3.3	Guiding 2D culture platforms for hPSC-derived neural cells.....	33
2.3.4	Guiding 3D culture platforms for hPSC-derived neural cells.....	36
2.4	Stem cell-based clinical applications for spinal cord injury repair.....	38
2.4.1	Spinal cord injury.....	38
2.4.2	Stem cell-based clinical trials for spinal cord injury repair.....	39
3	Aims of the study.....	43
4	Materials and methods.....	45
4.1	hPSC culturing and differentiation.....	45
4.1.1	Ethical considerations.....	45
4.1.2	hPSC lines and culture.....	45

4.1.3	Production of neurons and astrocytes	47
4.1.4	Production of oligodendrocytes.....	48
4.2	Recombinant human laminins	50
4.3	Nanofiber platform.....	50
4.3.1	Nanofiber-hydrogel scaffolds.....	50
4.4	Characterization of differentiated neural cells.....	51
4.4.1	Morphology and time-lapse imaging.....	51
4.4.2	Cell viability	51
4.4.3	Gene expression analysis.....	52
4.4.4	Protein expression analysis	54
4.4.5	Flow cytometry	56
4.4.6	Scanning electron microscopy.....	56
4.4.7	Microelectrode array measurements.....	57
4.5	Statistical analyses	57
5	Results.....	59
5.1	Differentiation capacities of individual hESC and iPSC lines	59
5.2	Differentiation of iPSC-derived oligodendrocytes and culturing of produced OPCs on nanofiber platforms	62
5.3	Specific laminin isoforms for <i>in vitro</i> culturing of iPSC-derived neurons and astrocytes	64
5.3.1	Functional development of iPSC-derived neuronal networks on different laminin substrates	66
5.4	Nanofiber platform for <i>in vitro</i> culturing of iPSC-derived neurons and astrocytes	67
5.4.1	iPSC-derived neurons and astrocytes on nanofiber platform.....	67
5.4.2	iPSC-derived neurons on nanofiber-hydrogel scaffolds.....	69
6	Discussion	71
6.1	Differentiation propensity of individual iPSC lines	71
6.1.1	Comparison of hESC and iPSC lines	71

6.1.2	Transgene expression of hPSC lines.....	72
6.2	Differentiation of the central nervous system cells from hPSCs	73
6.2.1	Neurons and astrocytes	73
6.2.2	OPCs and oligodendrocytes	74
6.3	Effect of defined laminin substrates on <i>in vitro</i> culturing of hPSC-derived neural cells.....	77
6.3.1	Supporting growth of neurons and astrocytes with specific laminin substrates.....	77
6.3.2	Functional development of neuronal networks.....	78
6.4	Effect of mechanically altered environment on <i>in vitro</i> culturing of hPSC-derived neural cells.....	79
6.4.1	Guiding cell orientation with nanofibers in 2D culture conditions	79
6.4.2	Nanofiber guided neuronal orientation in 3D culture conditions.....	80
6.5	Future perspectives.....	81
7	Conclusions.....	85

Abstract

Human pluripotent stem cells (hPSCs) are capable of self-renewal and differentiation into any cell type found in the human body. hPSCs include embryonic stem cells (ECs), which are derived from the embryonic inner cell mass, as well as induced pluripotent stem cells (iPSCs), derived from somatic cells and reprogrammed using specific transcription factors to induce pluripotency. hPSCs can be directed to differentiate into the main cell types of the central nervous system (CNS), neurons, astrocytes, and oligodendrocytes *in vitro*. hPSC-derived neural cells provide an excellent approach to model CNS development and deficits *in vitro* and furthermore treat injuries and degenerative conditions by replacing damaged tissues. Spinal cord injury (SCI) describes damage to the spinal cord that leads to the loss of muscle function, sensation, or autonomic functions to different extents. CNS cells have limited capacity for regeneration, and cell replacement therapies have been extensively studied for SCI repair, as no efficient treatment for SCI currently exists.

This thesis focused on studying various aspects, including genetic background and chemical and mechanical inductions, of hPSC-derived neural cell differentiation and behavior *in vitro*. The results were aimed to be applicable for developing tissue engineering products for SCI repair. First, the neural differentiation potentials of several hPSC lines were compared *in vitro* in order to discover the presence of potential systematic differences between hESCs and hiPSCs. Previous studies have demonstrated that despite their considerable resemblance, the different genetic backgrounds of hESCs and hiPSCs may affect to their differentiation potential. Our results revealed cell line-specific variations in neural differentiation efficiency. However, the variation between individual hESC and hiPSC lines was higher than the variation between cell lines of different origins, indicating the lack of systematic differences between the two hPSC types.

Next, chemical induction was studied for the differentiation of hPSC-derived oligodendrocytes. Differentiation was induced by a variety of growth factors and morphogens in a temporally defined manner to direct the differentiation through the neural precursor cell stage into oligodendrocyte precursor cells (OPCs), and finally to maturing oligodendrocytes. Although efficient differentiation of OPCs was achieved, the maturation of the cells into oligodendrocytes should be further

stabilized and enhanced. The differentiation process was initially performed under xeno-free and defined culture conditions, enabling clinical applications of the produced cells. The protocol was also adapted into a more cost-effective research-grade method.

Cellular responses to different extracellular matrix (ECM) molecules *in vitro* was studied using hPSC-derived neurons and astrocytes. ECM is found at the intercellular space *in vivo* and it provides both structural support and chemical cues for cell survival, differentiation, migration, and growth. Neurons and astrocytes were cultured on defined substrates using different isoforms or fragments of ECM component laminin. hPSC-derived neurons and astrocytes were shown to attach and grow most efficiently on substrates containing laminin α 5-chain. These substrates also enhanced the functional development of neuronal networks. The studied substrates were both defined and xeno-free and thus can be used as platforms for the efficient production of clinical-grade neural cells from hPSCs.

Finally, the effects of mechanical alterations in the culture conditions were studied using hPSC-derived neurons, astrocytes, and OPCs. The cells were cultured on aligned nanofiber platforms mimicking the aligned cellular orientation in the spinal cord. All cell types were observed to orient according to the underlying fiber alignment. However, ECM protein-coating for the nanofibers was required for efficient growth of the neurons and astrocytes, and previously identified laminin α 5-chain substrates were successfully applied here. As the 3D cultures resemble *in vivo* conditions more accurately than traditional 2D culturing surfaces, orientation guidance of hPSC-derived neurons was also demonstrated in 3D culture conditions consisting of nanofiber platform and hydrogel component.

In conclusion, the results of this thesis provide new insights for the culturing of hPSC-derived neural cells *in vitro*. Obtained knowledge can be utilized for tissue engineering applications, as the novel combination of hPSC-derived CNS cells, clinically relevant ECM substrates, 3D environment of the hydrogel and guiding features of the nanofibers would be beneficial for the development of functional cell grafts for SCI repair.

Tiivistelmä

Ihmisen monikykyiset kantasolut ovat kykeneviä jakaantumaan loputtomasti sekä erilaistumalla tuottamaan mitä tahansa ihmiskehon solutyyppejä. Monikykyisiä kantasoluja ovat sekä alkion sisäsolumassasta eristetyt alkion kantasolut, että erilaistuneista soluista geneettisesti muokatut indusoidut monikykyiset kantasolut. Monikykyiset kantasolut voidaan laboratorio-olosuhteissa tehokkaasti ohjata erilaistumaan keskushermoston tärkeimmiksi solutyypeiksi; hermosoluiksi, astrozyyteiksi, ja oligodendrosyyteiksi. Monikykyisistä kantasoluista erilaistettuja keskushermoston soluja voidaan hyödyntää keskushermoston kehityksen ja häiriöiden *in vitro* mallinnuksessa. Lisäksi monikykyisistä kantasoluista voidaan tuottaa soluja korvaamaan vahingoittunutta kudosta keskushermoston vaurioiden ja sairauksien hoidossa. Keskushermostoon kuuluvan selkäytimen vaurioituminen johtaa tahdonalaisen lihastoiminnan, tuntoaistin, ja autonomisten toimintojen häiriöihin tai katoamiseen. Keskushermoston solujen rajallisen uusiutumiskyvyn vuoksi kantasolusiirteitä on tutkittu paljon yhtenä vaihtoehtona selkäydinvaurion hoitoon. Tällä hetkellä tehokasta hoitoa selkäydinvaurioon ei ole.

Tämän väitöskirjatyön tavoitteena oli tutkia eri tekijöiden, kuten solujen geneettisen taustan sekä kemiallisen ja mekaanisen induktion, vaikutusta monikykyisistä kantasoluista erilaistettujen keskushermoston solujen erilaistumiseen ja käyttäytymiseen *in vitro* kasvatusolosuhteissa. Tuloksia voidaan hyödyntää kehitettäessä kudosteknologisia sovelluksia selkäydinvaurion hoitoon. Ensimmäisessä osatyössä tutkittiin useiden monikykyisien kantasolulinjojen hermosoluerilaistustehokkuutta, ja pyrittiin selvittämään systemaattisia eroja alkion kantasolujen ja indusoidujen monikykyisien kantasolujen välillä. Aiemmat tutkimukset ovat osoittaneet että huolimatta näiden solutyyppeiden samankaltaisuudesta, niiden alkuperästä johtuvat geneettiset eroavaisuudet saattavat vaikuttaa solujen erilaistumistehokkuuteen. Tulokset osoittivat että solulinjojen välillä on selvästi linjakohtaisia eroja erilaistumistehokkuudessa. Vaihtelua on kuitenkin huomattavasti enemmän yksittäisten solulinjojen kuin eri lähteistä peräisin olevien monikykyisien kantasolutyyppeiden välillä.

Seuraavaksi monikykyisten kantasolujen erilaistusta pyrittiin ohjaamaan kemiallisella induktiolla tarkasti määritellyissä kasvatusolosuhteissa. Erilaisia

kasvutekijöitä käytettiin tarkoin ajoitettuna suuntaamaan solujen erilaistumista ensin keskushermoston esiastesoluiksi ja myöhemmin oligodendrosyyttien esiastesoluiksi ja oligodendrosyyteiksi. Menetelmällä saavutettiin oligodendrosyyttien esiastesolujen tehokas erilaistuminen, mutta solujen kypsymistä oligodendrosyyteiksi pitäisi edelleen vakauttaa ja tehostaa. Solujen kohdennettu erilaistus tapahtui ilman eläinperäisiä tekijöitä sisältäviä yhdisteitä, mikä mahdollistaa tällä menetelmällä tuotettujen solujen käytön kliinisissä sovelluksissa. Erilaistusmenetelmästä muokattiin myös kustannustehokkaampi, tutkimustasoinen menetelmä.

Soluväliaineen molekyylien vaikutusta monikykyisistä kantasoluista erilaistettujen hermosolujen ja astrosyyttien käyttäytymiseen ja kehitykseen *in vitro* tutkittiin useilla laminiini-molekyylin isoformeilla. Soluväliaine on solunulkoinen matriisi, joka tukee solujen erilaistumista, kasvua, ja kehitystä sekä rakenteellisesti että kemiallisesti. Tulokset osoittivat että sekä hermosolut että astrosyytit kiinnittyvät ja kasvavat parhaiten pinnoitteilla, jotka sisältävät laminiinin $\alpha 5$ -ketjurakenteen. Nämä pinnoitteet myös tehostivat hermosolujen verkostotason toiminnallista kehitystä. Tässä työssä käytetyt pinnoitteet ovat myös kliiniseen käyttöön sopivia, ja niitä voidaan hyödyntää monikykyisistä kantasoluista erilaistettujen keskushermoston solujen tuottoon kudosteknologisia sovelluksia varten.

Lopuksi kasvatusolosuhteiden mekaanisen muokkauksen vaikutusta tutkittiin monikykyisistä kantasoluista erilaistetuilla hermosoluilla, astrosyyteillä, ja oligodendrosyyttien esiastesoluilla. Soluja kasvatettiin nanokuitupinnoilla, joiden topografia vastaa selkäytimen solujen suuntautumista *in vivo*. Nanokuitujen havaittiin vaikuttavan kaikkien solutyypin kasvuun, ja solujen nähtiin suuntautuvan kasvatusalustan nanokuitujen mukaisesti. Pelkät nanokuidut eivät tukeneet hermosolujen ja astrosyyttien kasvua, mutta kuitujen pintakäsittely väitöskirjan aiemmassa osatyössä tutkituilla $\alpha 5$ -ketjurakenteen sisältävillä laminiini-pinnoitteilla paransi huomattavasti molempien solutyypin kasvua. Lisäksi osoitettiin, että monikykyisistä kantasoluista erilaistettujen hermosolujen kasvua voidaan ohjata nanokuiduilla myös hydrogeelipohjaisessa 3D-ympäristössä, joka vastaa *in vivo* kasvuolosuhteita keskushermostossa paremmin kuin 2D pinta.

Tämän väitöskirjan tulokset tuovat merkittävää lisätietoa ihmisen monikykyisistä kantasoluista erilaistettujen keskushermoston solujen *in vitro* -kasvatuksesta. Tulokset ovat hyödynnettävissä kudosteknologisissa sovelluksissa sillä yhdistämällä ihmisperäisiä keskushermoston tärkeimpiä solutyyppejä, kliiniseen käyttöön sopivia kasvatuspinnoitteita, hydrogeelistä koostuva 3D kasvu-ympäristö sekä nanokuitujen ohjaava vaikutus, voidaan edistää toiminnallisen solusiirteen kehitystä selkäydinvaurion hoitoon.

List of original publications

This thesis is based on four original publications, referred to in the text by Roman numerals (I-IV).

- I Toivonen S*, Ojala M*, **Hyysalo A***, Ilmarinen T, Rajala K, Pekkanen-Mattila M, Äänismaa R, Lundin K, Palgi J, Weltner J, Trokovic R, Silvennoinen O, Skottman H, Narkilahti S, Aalto-Setälä K and Otonkoski T. Comparative analysis of targeted differentiation of human induced pluripotent stem cells (hiPSCs) and human embryonic stem cells reveals variability associated with incomplete transgene silencing in retrovirally derived hiPSC lines. *Stem Cells Translational Medicine*. 2013. 2(2):83-93.
- II Sundberg M, **Hyysalo A**, Skottman H, Shin S, Vemuri M, Suuronen R, Narkilahti S. A xeno-free culturing protocol for pluripotent stem cell-derived oligodendrocyte precursor cell production. *Regenerative Medicine*. 2011. 6(4):449-60.
- III **Hyysalo A**, Ristola M, Mäkinen M, Häyrynen S, Nykter M, Narkilahti S. Laminin $\alpha 5$ substrates promote survival, network formation and functional development of human pluripotent stem cell-derived neurons *in vitro*. *Submitted*.
- IV **Hyysalo A**, Ristola M, Joki T, Honkanen M, Vippola M, Narkilahti S. Aligned poly(ϵ -caprolactone) nanofibers guide orientation and migration of human pluripotent stem cell –derived neurons, astrocytes, and oligodendrocyte precursor cells *in vitro*. *Macromolecular Bioscience*. 2017. *In press*.

* Authors contributed equally.

The original publications included in this thesis are reproduced with permission of the copyright holders.

Additional unpublished data, indicated separately in the text, are presented.

Abbreviations

AA	Ascorbic acid
APC	Allophycocyanin
BDNF	Brain-derived neurotrophic factor
bFGF/FGF2	Basic fibroblast growth factor
BMP	Bone morphogenetic protein
CD	Cluster of differentiation
C-MYC	V-Myc avian myelocytomatosis viral oncogene homolog
CNP	2', 3'-cyclic nucleotide 3'-phosphodiesterase
CNS	Central nervous system
CNTF	Ciliary neurotrophic factor
DAPI	4',6-diamidino-2-phenylindole
DIC	Differential interference contrast
DMEM	Dulbecco's Modified Eagle Medium
EB	Embryoid body
ECM	Extracellular matrix
EGF	Epidermal growth factor
EpCAM	Epithelial cell adhesion molecule
FACS	Fluorescence associated cell sorting
FDA	Food and Drug Administration
FESEM	Field emission scanning electron microscope
GalC	Galactocerebroside
GAPDH	Glyceraldehyde 3-phosphate dehydrogenase
GFAP	Glial fibrillary acidic protein
GMP	Good manufacturing practise
H-CAM	Homing cell adhesion molecule
hESC	Human embryonic stem cell
hiPSC	Human induced pluripotent stem cell
HLA	Human leukocyte antigen
hPSC	Human pluripotent stem cell
IC	Immunocytochemistry
IGF-1	Insulin-like growth factor-1

KLF4	Kruppel-like factor 4
LN	Laminin
MACS	Magnetic associated cell sorting
MAG	Myelin-associated glycoprotein
MAP-2	Microtubule-associated protein 2
MBP	Myelin basic protein
MCS	Multichannel Systems GmbH
MEA	Microelectrodearray
MSC	Mesenchymal stem cell
NCAM	Neural cell adhesion molecule
NDM	Neural differentiation medium
Nkx2.2	NK2 homeobox 2
Nkx6.2	NK6 homeobox 2
NF-68	Neurofilament light chain
NG2	Chondroitin sulphate proteoglycan 4
NPC	Neural precursor cell
NS	Neural stem cell medium
NT3	Neurotrophin-3
O4	Oligodendrocyte marker O4
OCT3/4	Octamer-binding transcription factor 3/4
Olig	Oligodendrocyte transcription factor
OMG	Oligodendrocyte myelin glycoprotein
OPC	Oligodendrocyte precursor cell
PAX6	Paired box 6
PC	Phase contrast
PCL	Poly(ϵ -caprolactone)
PDGF-AA	Platelet-derived growth factor- AA
PDGF- α	Platelet-derived growth factor receptor α
PE	Phycoerythrin
PEI	Polyethyleneimine
PLP	Proteolipid protein
qPCR	Quantitative real time PCR
RA	Retinoic acid
RPE	Retinal pigment epithelium
RT	Room temperature
RT-PCR	Reverse transcription –polymerase chain reaction
SEM	Scanning electron microscopy

S.E.M.	Standard error of mean
SHH	Sonic hedgehog
SOX	SRY (Sex Determining Region Y)-Box
T3	3,3',5-triiodo-L-thyronine
TEM	Transmission electron microscopy
Tra	Tumor-related antigen
TGF β	Transforming growth factor beta
WNT	Wingless-INT
XF	Xeno-free
XF-NSC	Xeno-free neural stem cell –supplement

1 Introduction

Human pluripotent stem cells (hPSCs) are defined by their capacity to self-renew and differentiate into derivatives of all three germ layers. They are thus capable to form all cell types in the human body (Fortier 2005). hPSCs constitute of human embryonic stem cells (hESCs) and human induced pluripotent stem cells (hiPSCs). hESCs are derived from the inner cell mass of blastocyst stage embryos, whereas hiPSCs can be generated from somatic cells using specific transcription factors to induce pluripotency (Wobus and Boheler 2005, Takahashi et al. 2007).

hiPSCs can be targeted to differentiate into the main cell types of human central nervous system (CNS), namely neurons, astrocytes, and oligodendrocytes. Neural differentiation of hPSCs was first described in 2001, and since then, a vast number of *in vitro* differentiation protocols have been published (Carpenter et al. 2001, Reubinoff et al. 2001, Zhang et al. 2001, Dhara and Stice 2008). Afterwards, separate methods for production of astrocytes and oligodendrocytes have been developed (Nistor et al. 2005, Krencik et al. 2011). Differentiation methods for all CNS cell types are constantly being developed and optimized in order to efficiently produce more defined cell populations for research and clinical applications.

Various factors are known to influence differentiation and behavior of hPSC-derived CNS cells *in vitro*. Traditionally, specific chemical compositions of the culture media have been used to induce differentiation into the desired cell type (Yap et al. 2015). *In vitro* culturing substrates, that mimic the *in vivo* extracellular matrix (ECM), are used to guide stem cell differentiation, and support the development and maturation of the differentiated cells (Ma et al. 2008, Kirkeby et al. 2017). Recently, the mechanical properties of the culture environment have also been shown to influence differentiation and behavior of neural cells *in vitro* (Xie et al. 2009, Franze et al. 2013). The mechanical properties of the *in vitro* cultures can be altered using biomaterials, to more closely resemble the characteristics of the CNS tissue (Edmondson et al. 2014). The most exploited biomaterials for CNS tissue engineering are fibrous structures and hydrogels (Bosworth et al. 2013). Nanofiber platforms have been used to direct cell growth in order to, for example, enhance neural network formation or mimic cellular orientation in the spinal cord (Cao et al.

2009). Furthermore, hydrogels resemble relatively soft ECM structures in the CNS and provide a feasible 3D environment (Li et al. 2012).

hPSC-derived CNS cells provide an excellent approach to model CNS development and deficits *in vitro*, and furthermore treat injuries and degenerative conditions by replacing damaged tissue. Spinal cord injury (SCI) is damage to the spinal cord that leads to the loss of muscle function, sensation, or autonomic functions to various extents (Yu and He 2015). The symptoms of SCI are highly variable ranging from pain or numbness to paralysis (<http://asia-spinalinjury.org>). Rehabilitation exercises and physical therapy may have some effects on the recovery of motion, but currently no efficient treatment for SCI exists. Due to the limited regeneration capacity of CNS cells, cell replacement therapies have been extensively studied for SCI repair (Sabapathy et al. 2015). Few clinical trials utilizing stem cell-derived neural cell transplantations are ongoing. While the results from the safety studies are encouraging, the efficacy of these transplantation therapies has not been reported thus far (<https://clinicaltrials.gov>). However, previous preclinical studies have shown that transplantation of dissociated cells often results in poor cell survival and spatial disorganization, leading to inefficient functionality and engraftment *in vivo* (Carlson et al. 2016). The combination of transplanted cells and supporting biomaterial scaffolds could enhance cell survival, guide cellular organization and facilitate the formation of new connections at the injury site (McMurtrey 2014).

The focus of this thesis was to study various aspects, including genetic background and chemical and mechanical inductions, of hPSC-derived CNS cell differentiation and behavior *in vitro*. The results were aimed to be applicable for tissue engineering, as the combination of hPSC-derived CNS cells, clinically relevant ECM substrates, 3D environment of the hydrogel and guiding features of the nanofibers could be beneficial in the development of functional cell grafts for SCI repair.

2 Literature review

2.1 The human central nervous system

The human central nervous system (CNS) consists of the brain and spinal cord. The main cell types in the CNS are neurons and glial cells, including astrocytes and oligodendrocytes. Neurons and glial cells consist of a cell body (soma) and cellular extensions (processes). Neurons transmit information through electrical and chemical signals to and from different organs. Typically, every neuron has one longer axonal process that sends information from the soma to the target tissue. The remaining dendritic processes are shorter and highly branched collecting information from the surrounding tissue. (Franze et al. 2013) Astrocytes have traditionally been considered as supporting cells for neurons since they maintain cellular homeostasis. However, during the past few years, emerging evidence has suggested the role of astrocytes in a range of other functions, for example, in the modulation of synaptic transmission in the CNS (Nedergaard et al. 2003). Oligodendrocytes provide support and enhance the functionality of the neuronal network by producing insulating myelin sheaths around neuronal axons (Goldman and Kuypers 2015).

2.1.1 Development of the human central nervous system

The development of the CNS is initiated by neural induction of multipotent cells in the ectoderm germ layer. The “default pathway model” for neural induction has proposed the propensity of ectodermal cells to differentiate into neural fate. The “default development” is inhibited by suppressive extrinsic signals via bone morphogenetic proteins (BMPs) and Nodal signalling, and thus inhibition of these pathways leads to neural induction. (Wilson and Hemmati-Brivanlou 1995, Munoz-Sanjuan and Brivanlou 2002) However, this model is likely oversimplified, as additional signaling processes such as Wnt and FGF -pathways have been shown to affect neural induction (Zirra et al. 2016). Neural induction results in the formation of neuroepithelial cells that compose the neuroectoderm, which further develops into neural tube in a process called neurulation (Zhang and Jiao 2015).

Neural induction is followed by rostrocaudal and dorsoventral specification of the cells in the developing neural tube. These specifications are required for the development of different CNS regions (forebrain, midbrain, hindbrain, and spinal cord), as well as specific cell-type diversity within each region. Intricate signaling is involved in these processes and the main factors affecting regional patterning are presented in Figure 1.

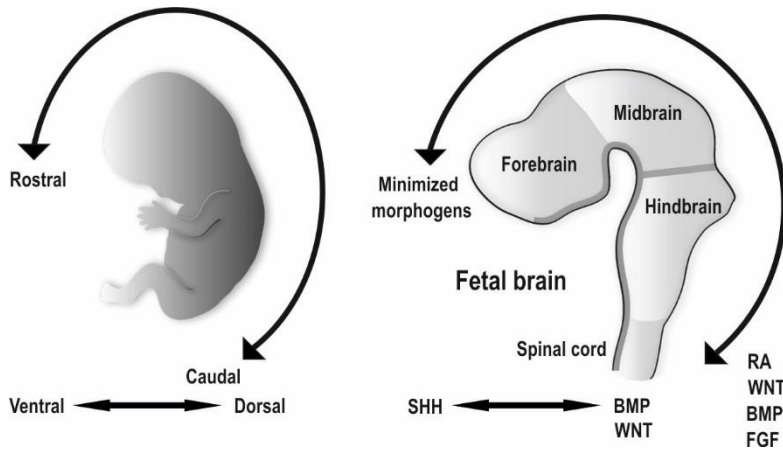


Figure 1. Regional specification of the developing CNS. The rostrocaudal and dorsoventral axes are presented with arrows in the developing fetus and fetal brain. Gradients of different morphogens direct CNS patterning. RA, WNT, BMP, and FGF mediated signaling results in caudal identity, whereas minimized morphogens enable “default” rostral identity. Ventral patterning is strongly induced by SHH, while dorsal fate is specified by BMP and WNT. Abbreviations: RA, retinoic acid; WNT, Wingless-INT; BMP, bone morphogenetic protein; FGF, fibroblast growth factor; SHH, sonic hedgehog.

Neural tube formation induces the transition of neuroepithelial cells into neural precursor cells (NPCs). The NPCs further acquire the phenotype of radial glial precursor cells and give rise to differentiating neurons in the CNS through asymmetric cell division. They also form long radial processes to the outer surface of the neural tube, guiding the migration of the newly born neural precursor cells and neurons. Closing to the date of birth, neurogenesis is followed by gliogenesis when radial glial cells start to produce precursor cells committed to astrocytic and oligodendrocytic lineages. (Martynoga et al. 2012) A summary of cell development during neurogenesis is presented in Figure 2.

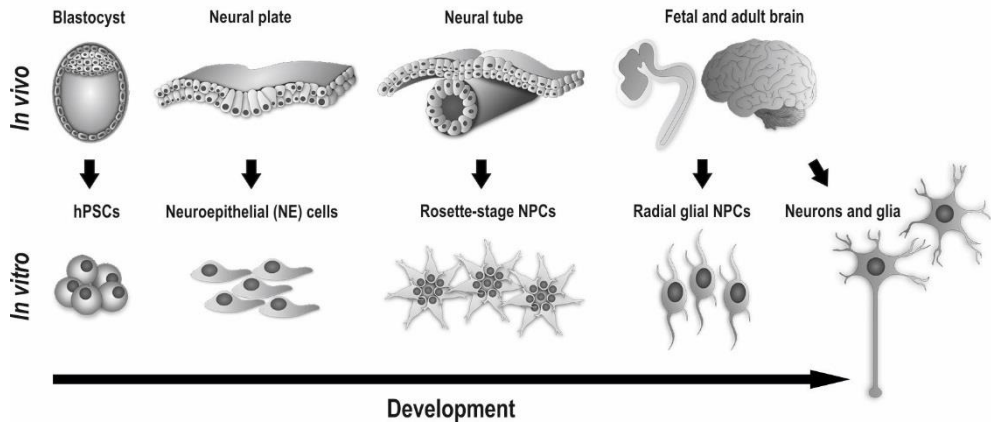


Figure 2. Neurogenesis *in vivo* and resembling neural development *in vitro*. Modified from (Mertens et al. 2016).

The molecular mechanisms behind the neuro-glial switch are complex and currently not fully known (Genethliou et al. 2009). For example, neuronal-oligodendroglial switch in the motor neuron progenitor domain of the spinal cord is regulated by Sonic hedgehog (SHH) signaling and activity of Olig transcription factors; downregulation of proneural transcription factors such as SRY (sex determining region Y)-box 1 (SOX1); acquisition of the glial precursors through Notch-signaling; and activity of proglial transcription factors such as SRY-box 9 (SOX9) (Rowitch 2004). The terminal differentiation and maturation into neuronal and glial cells in the human CNS is a long-term process that may take weeks or months to even years (Yang et al. 2013, Barateiro and Fernandes 2014).

2.1.2 Central nervous system cells *in vitro*

CNS cells have been cultured *in vitro* for decades. Primary CNS cells can be acquired from animal origins, but due to differences between the species, the results of the studies performed using animal cells cannot always be extrapolated to human CNS (Monaco et al. 2015). Primary human tissue can be obtained following major surgical procedures or *post mortem*. In addition, fetal tissues can also be used as a cell source. Nevertheless, there are limitations regarding the availability of primary human tissue, along with ethical considerations, especially regarding the use of fetal material. (Cefalo et al. 1994, Quadrato et al. 2016) The use of immortalized neuronal cell lines derived from neuronal tumors overcomes the issues of limited cell availability. Due

to their pathophysiology, however, these cells do not necessarily resemble those in native tissue. (Gordon et al. 2013)

Stem cells have been utilized for *in vitro* production of CNS cells since they are capable of self-renewal, thus providing an abundant cell source (Fortier 2005). These cells also follow developmental principles *in vivo* and can be directed to differentiate into desired cell populations (Wobus and Boheler 2005). Stem cells can be obtained from embryonic, fetal and adult tissues and directed to differentiate into desired cell populations. The production of CNS cells from human pluripotent stem cells (hPSCs) is reviewed in chapter 2.2. Recent methodological developments have also enabled direct conversion of other somatic cells into CNS cells as well as transcription factor-mediated neural induction of hPSCs (Velasco et al. 2014, Gopalakrishnan et al. 2015, Mertens et al. 2016).

2.2 Human pluripotent stem cells

hPSCs are defined with their capacity to self-renew and differentiate into derivatives of all three germ layers: endoderm, mesoderm, and ectoderm. Thus these cells are capable of forming all cell types in the human body, but lack the ability to form extraembryonic tissues. (Fortier 2005)

hPSCs constitute of human embryonic stem cells (hESCs) and human induced pluripotent stem cells (hiPSCs). hESCs are derived from the inner cell mass of blastocyst stage embryos (Wobus and Boheler 2005). In Finland, hESC derivation is performed using donated, surplus embryos of poor quality from *in vitro* fertilization treatments (Skottman 2010). hiPSCs are derived from somatic cells using specific transcription factors to inducing the pluripotent state. The derivation of hiPSCs was described for the first time in 2007 with the transcription factors octamer-binding transcription factor 3/4 (*OCT3/4*), SRY-box 2 (*SOX2*), Kruppel-like factor 4 (*KLF4*), and V-Myc avian myelocytomatosis viral oncogene homolog (*C-MYC*) (Takahashi et al. 2007). These transcription factors were termed “Yamanaka factors”, and this combination has since been widely utilized in the derivation of hiPSCs (Gonzalez et al. 2009). However, shortly after the discovery of Yamanaka’s group, Yu and colleagues reported the derivation of hiPSCs using transcription factors *OCT3/4*, *NANOG*, *SOX2*, and *LIN28* (Yu et al. 2007). Schematic presentation of the derivation and differentiation potential of hPSCs is shown in Figure 3.

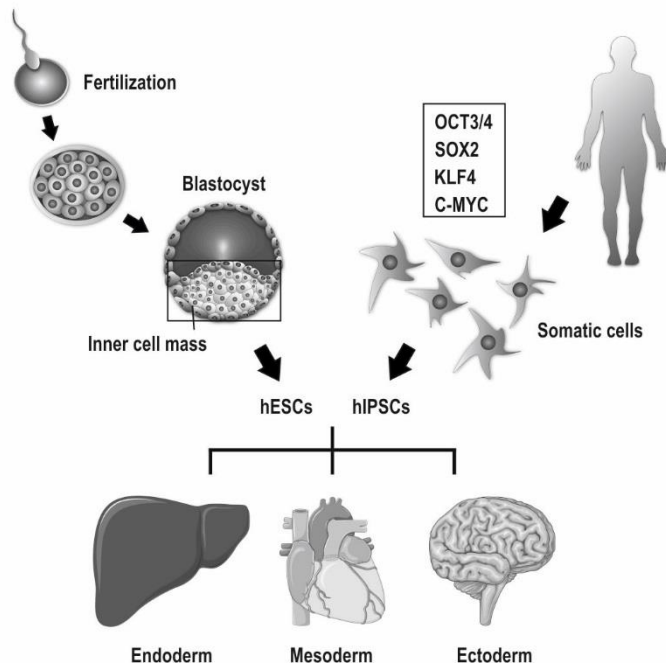


Figure 3. Origins and differentiation capacity of hPSCs. hESCs are derived from the inner cell mass of blastocyst stage embryos, while hPSCs are genetically reprogrammed using specific transcription factors. All hPSCs can be directed to differentiate into derivatives of the endoderm, mesoderm, and ectoderm. Some images in the figure are from Servier Medical Art image bank (<http://servier.com/Powerpoint-image-bank>).

The first hPSCs were derived using retrovirus-based vectors, which integrate genetic material into the host genome. However, the transduced cells are exposed to the risks of insertional mutagenesis, uncontrolled gene expression, and reactivation of the reprogramming factors, which can lead to tumorigenicity of the cells. (Nakagawa et al. 2008) Thus, new approaches for hPSC derivation have been studied and established in order to reduce these disadvantages. Non-integrating viral vectors based on Sendai or adenoviruses have been used (Stadtfield et al. 2008, Fusaki et al. 2009, Zhou and Freed 2009). In addition, a wide variety of techniques utilizing non-viral approaches for introducing DNA, micro-RNA, synthetic mRNA, or recombinant proteins to the cells have also been reported (Hu 2014, Park et al. 2014).

Previously, the equivalence of hESCs and hPSCs has been debated due to their considerably different origins. Similarity in terms of morphology, feeder cell dependence, surface marker expression, and *in vivo* teratoma formation capacity were challenged by studies investigating their gene expression profiles, DNA methylation patterns, and proteomes (Narsinh et al. 2011, Kim et al. 2012, Kyttilä et al. 2016).

The current consensus suggests that while hPSC lines display inherent variations, these are higher within hESC and hiPSC populations than between the populations (Robinton and Daley 2012, Yamanaka 2012).

Directed differentiation of somatic cells from hPSCs requires knowledge about the underlying developmental principles. Activation and inhibition of signaling mechanisms influencing differentiation are chemically acquired by combinations of growth factors and morphogens *in vitro* (Yap et al. 2015). The differentiation processes of neurons, astrocytes, and oligodendrocytes from hPSCs are reviewed in chapters 2.2.1 – 2.2.3.

2.2.1 Neural differentiation *in vitro*

Neural differentiation of hPSCs was first described in 2001 (Carpenter et al. 2001, Reubinoff et al. 2001, Zhang et al. 2001). These protocols were based on the embryoid body (EB) formation step prior to adherent cell culturing in neural differentiation-inducing media. Since then, a vast number of differentiation protocols directing neural development from hPSCs have been published, many of them utilizing the principle of EB formation (Erceg et al. 2009). EBs are 3D cell aggregates that produce a mixed population of differentiating cells, including neural cells. In adherent culture conditions, the cells differentiating towards neural lineage produce radially arranged structures called rosettes, mimicking neural tube formation *in vivo*. Rosettes can be selectively isolated for further culturing, in order to enhance the purity of the produced neural population. (Dhara and Stice 2008, Muratore et al. 2014) The 3D aggregates can also be formed in neural induction media. In this case, the aggregates are considered to produce mostly cells committed to the neural lineage and are termed neurospheres (Nat et al. 2007).

Fibroblast growth factors (FGFs), mainly basic FGF also known as FGF2, are the main growth factors used for neural differentiation *in vitro* (Dhara and Stice 2008). FGFs have been shown to influence neural induction, patterning, survival, proliferation, differentiation, and most recently, axon pathfinding and synapse formation (Mason 2007). In addition to bFGF, epidermal growth factor (EGF) has routinely been used in neural differentiation media to enhance proliferation and differentiation of NPCs (Zhou et al. 2016). Development of differentiation methods has resulted in the use of a variety of additional media components, aiming for the production of more defined neural phenotype (Mertens et al. 2016).

In 2009, Chambers and colleagues introduced an efficient neural differentiation method, which was fully based on adherent cell culture. The key element in this protocol was the inhibition of BMP signaling with Noggin and Activin/Nodal/transforming growth factor beta (TGF β) signaling by small molecule SB431542 (Chambers et al. 2009). This principle, termed “dual-SMAD inhibition”, was thereafter adapted to various differentiation protocols, and dual-SMAD inhibition and EB formation were also combined to acquire the benefits of both culture systems (Patani et al. 2011, Kirkeby et al. 2012, Shi et al. 2012, Doi et al. 2014, Muguruma et al. 2015, Pasca et al. 2015, Yuan et al. 2015). Adherent monolayer cultures often result in a more homogenous cell differentiation due to uniform cellular environment (Dhara and Stice 2008, Lippmann et al. 2014). Nevertheless, the cellular microenvironment within 3D cell aggregates has been considered more natural due to presence of different cell-cell and ECM interactions (Chandrasekaran et al. 2016).

Regional specification of hPSC-derived neurons has an effect on the differentiation potential of the cells and can be controlled during *in vitro* development (Suzuki and Vanderhaeghen 2015). Kirkeby and colleagues have elegantly demonstrated the effects of dose-dependent activation of Wnt signaling by glycogen synthase kinase 3 inhibitors CT99021 or CHIR99021. In their study, progressive caudalization of the cell regional identity was induced, corresponding to the developmental *in vivo* signaling. Furthermore, dorsoventral patterning of the differentiating cells was demonstrated with an SHH gradient, where high concentration of SHH led to the expression of floor plate markers in the cells. (Kirkeby et al. 2012, Kirkeby et al. 2013) Regional patterning has recently been addressed in several neural differentiation studies (Zirra et al. 2016).

Moreover, protocols for efficient neural differentiation under xeno-free and defined conditions have been reported in recent years (Lippmann et al. 2014, Yuan et al. 2015, RW.ERROR - Unable to find reference:164). These conditions enable clinical applications of hPSC-derived neurons.

2.2.2 Astrocyte differentiation *in vitro*

Directed differentiation of hPSCs towards the astrocytic lineage has only been performed during the past few years. Prior to this, astrocytes were usually developed as a result of long-term neural differentiation, resembling the *in vivo* development in the CNS. hNPC differentiation into astrocytes has been demonstrated in several

publications, but these were aiming to prove the astrocytic differentiation capacity of the hNPCs rather than producing pure astrocyte populations. (Itsykson et al. 2005, Johnson et al. 2007, Hu et al. 2010, Lappalainen et al. 2010)

The efficient differentiation of hPSCs into astrocytes positive for glial fibrillary acidic protein (GFAP) and S100 β was first described in 2011 (Krencik et al. 2011). Krencik and colleagues induced the hPSCs into neuroepithelial cells, patterned them into different regional specifications in the brain with SHH, retinoic acid (RA), and FGF8, and finally differentiated the cells into astrocytes using FGF, EGF, and ciliary neurotrophic factor (CNTF). Similar approaches have also been utilized in later differentiation protocols with additional components such as ascorbic acid (AA), brain-derived neurotrophic factor (BDNF), BMP, and insulin-like growth factor-1 (IGF-1) to induce astrocyte fate (Chandrasekaran et al. 2016).

2.2.3 Oligodendrocyte differentiation *in vitro*

Oligodendrocyte differentiation from hPSCs has been successfully performed for over a decade (Nistor et al. 2005, Izrael et al. 2007, Kang et al. 2007, Hu et al. 2009, Sundberg et al. 2010). A summary of the key components used in these early differentiation protocols is presented in Figure 4.

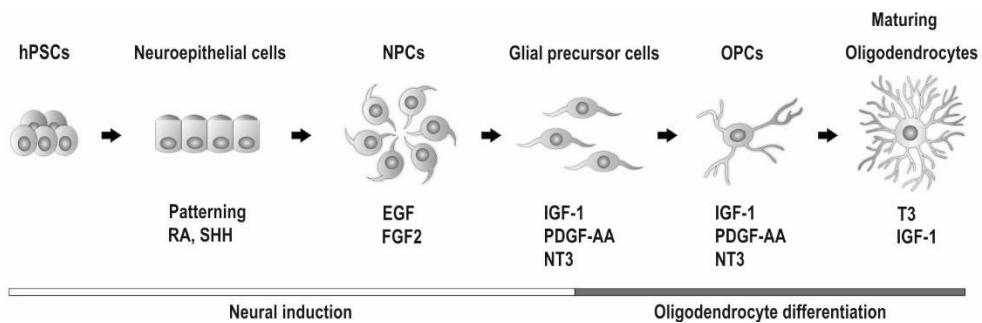


Figure 4. Differentiation of oligodendrocytes from hPSCs. Schematic presentation of the key components used for oligodendrocyte production *in vitro*. Abbreviations: hPSC, human pluripotent stem cell; NPC, neural precursor cell; RA, retinoic acid; SHH, sonic hedgehog; EGF, epidermal growth factor; FGF2, basic fibroblast growth factor; IGF-1, insulin-like growth factor 1; PDGF-AA, platelet-derived growth factor-AA; NT3, Neurotrophin-3; T3, triiodothyronine

Oligodendrocyte production in mouse CNS has been shown to emerge in temporally distinct stages. The first stage is detected in the ventral spinal cord at embryonic day 12.5 under the control of SHH signaling. (Vallstedt et al. 2005) Although the development in human is not as specifically defined, RA and SHH have been used with hPSCs for regional specification of developing oligodendrocyte precursor cells (OPCs) *in vitro* to mimic this developmental stage (Goldman and Kuypers 2015). SHH induces oligodendrocyte lineage specification and proliferation, but based on rodent studies, SHH signaling has also proposed to be involved in later oligodendrocyte differentiation (Oh et al. 2005, Wang and Almazan 2016). EGF and FGF2 have been used for the production of early CNS precursor cells as these factors are known to enhance both neural and glial development at early stages (Zhang et al. 2000, Dhara and Stice 2008, Li and Leung 2015). In addition, Hu and colleagues proposed that FGF2 induces pre-OPC production from hPSCs, but inhibits further OPC development at later stages (Hu et al. 2009). A vast number of studies with both human and murine cells have demonstrated that platelet-derived growth factor-AA (PDGF-AA) and IGF-1 increase OPC proliferation, whereas IGF-1 also enhances the development from OPCs to oligodendrocytes (McMorris and Dubois-Dalcq 1988, Armstrong et al. 1992, Wilson et al. 2003, Hsieh et al. 2004, Cui et al. 2010). Furthermore, neurotrophin 3 (NT3) has been shown to induce both OPC differentiation from NPCs, by enhancing the expression of Olig1, and OPC proliferation (Wilson et al. 2003, Hu et al. 2004). Growth factor withdrawal and thyroid hormone (triiodothyronine, T3) supplementation have been utilized for the final maturation of human OPCs into oligodendrocytes *in vitro*. Thyroid hormone receptor mediates oligodendrocyte differentiation and upregulation of myelin basic protein (MBP), 2', 3'-cyclic nucleotide 3'-phosphodiesterase (CNP), and myelin-associated glycoprotein (MAG) (Baxi et al. 2014).

Although oligodendrocytes have been produced from hPSCs for years using the same essential chemical compounds, the differentiation protocols are still under development, with the aim of gaining more defined and pure oligodendrocyte population within a shorter time frame. Further optimization of differentiation methods has introduced additional growth factors and morphogens for more efficient oligodendrocyte production (Goldman and Kuypers 2015, Li and Leung 2015). Recently, dual-SMAD inhibition has also been incorporated into oligodendrocyte differentiation protocols (Douvaras et al. 2014, Piao et al. 2015, Livesey et al. 2016). Nevertheless, oligodendrocyte differentiation using aforementioned factors is performed, following the neural induction step.

As previously mentioned, OPC production *in vivo* is known to occur in several developmental stages (Gallo and Deneen 2014). After the initial development in the ventral spinal cord, OPCs are also known to arise from the dorsal neural tube independently of SHH signaling. Stacpoole and colleagues demonstrated for the first time *in vitro* that equally efficient production of oligodendrocytes can be performed with NPCs that are regionally specified towards spinal cord and forebrain. Interestingly, OPC differentiation from forebrain but not spinal cord NPCs was dependent on FGF2. (Stacpoole et al. 2013)

In conclusion, a substantial number of protocols directing hPSCs towards OPCs and oligodendrocytes have been published. A majority of these protocols are based on controlling chemical signaling with specific supplements in the media, and the effects of the varying timing, concentration, and addition or withdrawal of single factors to the culturing conditions are difficult to detect and compare. Moreover, to our knowledge oligodendrocyte differentiation under xeno-free and defined culture conditions have not been described. Traditionally, the focus on directed differentiation towards all CNS cells has been on finding chemical factors controlling differentiation, whereas less attention has been given to the physical microenvironment. In recent years the effects and opportunities in modulating cellular physical microenvironment have been increasingly recognized (Kshitiz et al. 2012).

2.3 Defined extracellular matrix for hPSC-derived neural cells

2.3.1 Extracellular matrix composition in the human central nervous system

Extracellular matrix (ECM) is located within the intercellular space in all tissues. The ECM not only provides structural support for the cells but also participates in chemical signaling that regulates cell survival, migration, growth, and activity (Burnside and Bradbury 2014). *In vitro* differentiation of stem cells can also be affected by ECM molecules (Singh and Schwarzbauer 2012).

The ECM in the CNS is organized to form basement membrane, perineuronal nets and interstitial matrix (Figure 5A). The basement membrane separates CNS cells from the surrounding tissue on the CNS pial surface and participates in the formation of the blood-brain barrier (Engelhardt 2003). Perineuronal nets are formed on the neuronal cell surface, and interstitial matrix molecules are dispersed

within the intercellular space. The basement membrane is mainly composed of collagen, laminin, nidogen, and fibronectin. (Lau et al. 2013) The composition of the perineuronal nets differs from that of the basement membrane, due to the presence of large amounts of glycoproteins and proteoglycans such as tenascins and chondroitin sulfate proteoglycans linked to hyaluronan (Bonneh-Barkay and Wiley 2009). The same components are found in the interstitial matrix, in addition to small amounts of molecules from the basement membrane such as laminin, collagen and fibronectin (Haggerty et al. 2016). This composition and organization of the ECM molecules in the CNS results in a considerably soft ECM structure (Franze et al. 2013).

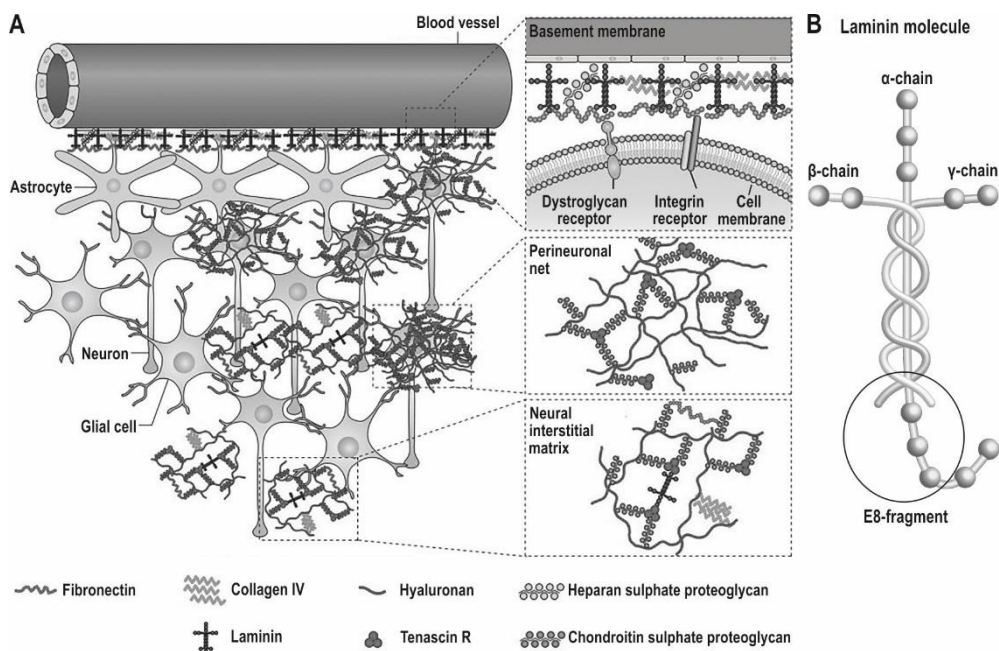


Figure 5. ECM structure in the CNS. (A) ECM forms basement membranes, perineuronal nets and interstitial matrix. Major components in the ECM of the CNS are glycoproteins and proteoglycans linked to hyaluronan. Other than in the basement membrane, very little fibrillary components such as collagen or fibronectin are present. Modified from (Lau et al. 2013). (B) Schematic presentation of the molecular structure of laminin with highlighted E8-fragment.

Laminin is a prominent component of the basement membrane and is known to affect neural tube formation, cell migration, CNS histogenesis, and myelination during development (Miner et al. 1998, Halfter et al. 2002, Chun et al. 2003). The laminins are a family of large heterotrimeric multidomain proteins consisting of α , β , and γ -chains (Figure 5B). Five types of α , three types of β , and three types of γ -chains have been identified and different combinations of these chains form at least 15 different laminin isoforms in mammalian cells. (Fusaoka-Nishioka et al. 2011) The isoforms are named based on their chain compositions, e.g. laminin (LN)511 containing α 5, β 1, and γ 1-chains (Aumailley et al. 2005). The expressions and functions of several laminin chains and isoforms have been demonstrated in the CNS (Domogatskaya et al. 2012). These results not only suggest that specific laminin isoforms could be utilized for *in vitro* culturing of CNS cells but also raise the question of whether the differentiation and culturing of defined cell populations could be enhanced by using certain laminin isoforms.

2.3.2 Defined extracellular matrix substrates for 2D culturing of hPSC-derived neural cells

hPSC-derived neurons, astrocytes and oligodendrocytes have been cultured *in vitro* using a selection of different substrates. The traditionally used substrates, including laminins, collagens, vitronectin, and fibronectin, are derived from human or mouse cells or tissues. These substrate compositions are undefined and can display batch to batch variation (Tsai et al. 2015). Thus, the defined substrates have been studied in order to develop culture conditions that are more suitable for stem cell-based clinical applications. Undifferentiated hPSCs and hPSC-derived neural cells have previously been cultured on recombinant human laminin isoforms 511 and 521, LN511 fragment E8, recombinant vitronectin, vitronectin-based synthetic peptide, and synthetic polymer coatings (Rodin et al. 2010, Rodin et al. 2014b, Miyazaki et al. 2012, Nakagawa et al. 2014, Lu et al. 2014, Doi et al. 2014, Chen et al. 2011, Lippmann et al. 2014, Melkounian et al. 2010, Villa-Diaz et al. 2010, Tsai et al. 2015). In this chapter, the focus is on defined human laminin substrates and their use in neural differentiation of hPSCs.

The successful derivation of hPSCs and long-term culturing of undifferentiated hPSCs have been reported on LN521, LN511 and LN511-E8 substrates (Rodin et al. 2010, Rodin et al. 2014b, Miyazaki et al. 2012, Nakagawa et al. 2014, Kele et al. 2016). However, Rodin and colleagues also described the clonal expansion and

derivation of hESCs on LN521/E-cadherin substrate, which was not enabled by LN511 (Rodin et al. 2014b). Controversial reports on hPSC culturing efficiency using LN511 and LN511-E8 have also been published arguing whether LN511-E8 is more or less supportive culture substrate compared to the full-length LN511 isoform (Miyazaki et al. 2012, Rodin et al. 2014a). E8 is composed of C-terminal regions of LN511 α , β , and γ -chains (Figure 5B). It is easier to produce compared to full-length laminin molecule, but the truncated structure limits the biological activities of LN511-E8 (Miyazaki et al. 2012). Thus, the comprehensive knowledge of the biological functions and differences between these substrates are still lacking.

Directed differentiation into dopaminergic neurons have been demonstrated with hIPSCs that were derived and cultured on LN521 and LN511-E8 (Lu et al. 2014, Nakagawa et al. 2014). Undifferentiated hIPSCs and differentiating neurons were cultured on same substrates. Doi and colleagues did not perform hIPSC derivation on defined substrates, but adapted undifferentiated hIPSCs from feeder cells to LN511-E8 (Doi et al. 2014, Nishimura et al. 2016). They also performed directed dopaminergic differentiation on LN511-E8 with a suspension culture maturation phase. The differentiated cells were characterized more extensively compared to previous studies, including functional analysis using patch clamp measurements and transplantation into 6-OHDA-lesioned rats of hemi-Parkinsonian model. A recent study of Kirkeby and colleagues demonstrated that hPSC-derived ventral mesencephalic progenitor cells can be differentiated on LN111, LN421, LN511, and LN521. However, of these substrates, LN111 selectively supported the differentiation of neural cells over the expansion of hPSCs. (Kirkeby et al. 2017) Thus far, studies of hPSC-derived astrocytes or oligodendrocytes on defined laminin substrates have not been reported.

2.3.3 Guiding 2D culture platforms for hPSC-derived neural cells

The physical properties of the cellular environment can induce chemical signaling in the cells by a process called mechanotransduction (Kolind et al. 2012). The effects of the mechanical environment on cells *in vitro* have been reported with various cell types, including stem cell differentiation and neural cell behavior (Xie et al. 2009, Franze et al. 2013, Shah et al. 2014). The physical properties of the cell culture environment have been remodeled using nanofiber platforms and microgrooves to induce orientation of neural cells (Xia et al. 2014, Yang et al. 2014). The aligned nanofiber-based culture conditions mimic the *in vivo* structure of the human spinal

cord, thus offering a relevant platform for *in vitro* modeling and clinical applications for the treatment of spinal cord injury (SCI) (Straley et al. 2010, Xiao et al. 2016).

Neurons, astrocytes and oligodendrocytes have been cultured on aligned nanofibers generated from synthetic, natural, or combinatorial biosynthetic materials (Cao et al. 2009). Cell viability, orientation, migration and axonal guidance were demonstrated. However, a majority of these studies have been performed with cells of animal origins. Previous studies on the behavior of hPSC-derived neural cells on nanofiber platforms are listed in Table 1.

Table 1. hPSC-derived neural cells studied on nanofiber platforms.

Fibers	Cell type	Studied fiber characteristics/ functionalization	Reference
Random and aligned, poly(<i>L</i> -lactic acid)	Neural cells	Absorbed and heparin-bound FGF2 and EGF, PORN/LN-coating	(Lam et al. 2010)
Random, Poly(L,D-lactide)	Neural cells	Different LN concentrations	(Ylä-Outinen et al. 2010)
Random and aligned, PCL	NPC	Thin and thick fibers, PORN/LN-coating	(Mahairaki et al. 2011)
Random, polyamide (Ultra-Web)	Neural cells	PORN/LN-coating	(Shahbazi et al. 2011)
Random, polyamide (Ultra-Web)	NPC	PORN/LN-coating	(Rahjouei et al. 2011)
Random and aligned, Tussah silk fibroin	NPC	Thin and thick fibers	(Wang et al. 2012a)
Random PES, CA, CS fibers	NPC		(Du et al. 2014)
Aligned, PCL	NPC		(Havasi et al. 2014)
Random and aligned, PCL	NPC	GDNF encapsulation into the fibers	(Mohtaram et al. 2015a)
Loop mesh and aligned, PCL	NPC	Thin and thick fibers, RA	(Mohtaram et al. 2015b)
Random, pDTEc	Induced neuronal cells	Thin and thick fibers, PDL/LN-coating	(Carlson et al. 2016)
Random, gelatin	Differentiation of motor neurons	LN-coating	(Tang et al. 2016)

Abbreviations: FGF2, fibroblast growth factor; EGF, epidermal growth factor; PORN, polyornithine; LN, laminin; PCL, poly(ϵ -caprolactone); CS, chitosan; CA, cellulose acetate; PES, polyethersulfone; GDNF, glial cell-derived neurotrophic factor; RA, retinoic acid; pDTEc, Poly(desaminotyrosyl tyrosine ethyl ester carbonate); NPC, neural precursor cell; PDL, poly-D-lysine

hPSC-derived NPCs and neurons have been reported to attach, remain viable, spread and differentiate efficiently on nanofiber platforms (Ylä-Outinen et al. 2010, Shahbazi et al. 2011, Havasi et al. 2014, Mohtaram et al. 2015a, Mohtaram et al. 2015b). Furthermore, aligned nanofibers have been shown to enhance neural differentiation and guide the cellular orientation *in vitro* (Lam et al. 2010, Mahairaki et al. 2011, Wang et al. 2012a). Thus far, studies on hPSC-derived astrocytes or oligodendrocytes on aligned nanofiber platform have not been published. However, the results gained with rat primary cells suggest that astrocytes attach and migrate on nanofiber platforms, while oligodendrocytes can even myelinate axon resembling nanofibers *in vitro* (Bauguera et al. 2010, Qu et al. 2013, Lee et al. 2012).

The most exploited material for nanofiber fabrication in studies investigating hPSC-derived neurons is poly(ϵ -caprolactone) (PCL). PCL is an easily fabricated and biocompatible material approved for clinical use by the Food and Drug Administration (FDA), and it has been used for fabrication of transplantable medical devices for decades (Woodruff and Hutmacher 2010). Nanofibers can be coated or functionalized with, for example, ECM molecules or growth factors in order to increase cell adhesion, survival, and guidance (Han and Cheung 2011, Low et al. 2015, Li et al. 2016b). Previously, at least laminin, EGF, FGF2, glial cell-derived neurotrophic factor (GDNF), and RA have been used for functionalization of the nanofibers with hPSC-derived neural cells (Lam et al. 2010, Mahairaki et al. 2011, Mohtaram et al. 2015a, Mohtaram et al. 2015b).

2.3.4 Guiding 3D culture platforms for hPSC-derived neural cells

A majority of *in vitro* cell culture experiments are performed under 2D culture conditions, which only vaguely resemble *in vivo* environments. Biomaterials have been used for creating 3D culture conditions for different cell types (Edmondson et al. 2014). Due to the substantially soft ECM structure in the CNS, hydrogels have been considered particularly suitable for neural cells. In addition to providing an excellent approach for modeling CNS conditions *in vitro*, hydrogels have been utilized for transplantation therapies in preclinical studies (Li et al. 2012). Previous *in vivo* studies with different CNS traumas have demonstrated that traditional cell transplantation strategies often result in low survival rate and viability of the transplanted cells (Hicks et al. 2009). Following trauma the cellular environment at the injury site is inhibitory due to various pathophysiological processes such as inflammatory and other immune responses, lack of trophic factors or supporting

ECM, and excitotoxicity (Li et al. 2012). The preventive effect towards the transplanted cells at the injury site could be relieved by seeding the cells with hydrogel, which creates supportive niche for the transplanted cells (Nisbet et al. 2008). Cell survival and differentiation within the hydrogel scaffolds, integration into the host tissue, and endogenous cell regeneration can be further enhanced by the incorporation of different components such as growth factors into the hydrogel (Li et al. 2014, Cook et al. 2016, Li et al. 2016a, Yasui et al. 2016). A variety of hydrogel materials have been used for 3D culturing of NPCs and neurons (Nisbet et al. 2008, Li et al. 2012).

Nanofibers, reviewed in a previous chapter, can also be fabricated into 3D structures (Carlson et al. 2016). However, nanofibers alone provide considerably stiffer 3D structure compared to CNS tissue *in vivo*. This might induce inhibitory reactions on the cells of the surrounding tissue via mechanotransduction (Koser et al. 2015). Furthermore, CNS trauma, especially SCI, also result in the formation of a cavity at the injury site. Filling the cavity with transplanted biomaterial would be beneficial, but it is challenging to achieve using nanofibers only (Rivet et al. 2015). Thus, a combination of hydrogels and nanofibers could provide a 3D structure, which mimics the mechanical properties of the CNS ECM but also guides cell migration and orientation to represent the anatomy of the spinal cord. In addition to incorporating nanofibers, other methods such as oriented channels or pores in the hydrogel can be used to guide cell migration and orientation (Sarig-Nadir et al. 2009, Kaneko et al. 2015).

Thus far, only a few studies have demonstrated the combination of hydrogel, nanofibers and human neural cells in 3D structures (McMurtrey 2014, Shelke et al. 2016). Human neuroblastoma -derived cells have been oriented in hyaluronic acid hydrogel using PCL nanofibers (McMurtrey 2014). hPSCs and mesenchymal stem cells (MSCs) have been cultured on semi-3D PCL nanofiber structure, coated with sodium alginate. These cells were directed to differentiate towards neurons but due to the lack of characterization of neural phenotype, no conclusion can be drawn about the neural behavior under these conditions. (Shelke et al. 2016) In conclusion, the combination of nanofibers, hydrogels, and neural cells has not been extensively studied.

2.4 Stem cell-based clinical applications for spinal cord injury repair

2.4.1 Spinal cord injury

The spinal cord is a cylindrical structure containing white and gray matter. The gray matter contains neuron and glial cell somas and is located in the interior part of the spinal cord, forming a clearly distinct region shaped like a butterfly. Gray matter is surrounded by the white matter, which is mainly composed of myelinated nerve fibers. Nerve fibers in the white matter form separate tracts responsible for transmitting information between the peripheral nervous system and the brain. (Pawlina and Ross 2015) Thus, cells and nerve fibers are highly oriented along the spinal cord (craniocaudal axis), especially in the white matter (Koser et al. 2015).

SCI is damage to the spinal cord that leads to the loss of muscle function, sensation, or autonomic functions to different extents. SCIs are classified into traumatic and non-traumatic injuries caused by mechanical damage and pathological conditions, respectively. (Sabapathy et al. 2015) Injuries are heterogeneous and cause varying degrees of impairment. SCI is followed by primary and secondary events, finally resulting in a chronic phase. The primary events include cell death and axonal sparing immediately after injury. The secondary events occur within hours to weeks after injury, causing widespread and prolonged tissue destruction mediated by excitotoxic, oxidative, inflammatory, and immune events. (Kramer et al. 2013) The loss of oligodendrocytes at the injury site is often accompanied by demyelination and unfeasible remyelination, leading to inefficient action potential transmission in the remaining axons (Nashmi and Fehlings 2001). Tissue destruction is followed by removal of cell debris by macrophages and microglia, resulting in the formation of a cavity at the injury site. Infiltrating macrophages, microglial cells, astrocytes, and OPCs form a glial scar to isolate the injury site from the surrounding healthy tissue. However, the glial scar also acts as a physical barrier and chemical inhibitor of axonal growth and regeneration. (Leal-Filho 2011) Rehabilitation exercises and physical therapy may have some effects on the recovery of motion and a number of different strategies for SCI repair have been and are currently studied. However, no efficient treatment for SCI exists thus far (Schwab et al. 2006, Rabchevsky et al. 2011, Ruff et al. 2012).

2.4.2 Stem cell-based clinical trials for spinal cord injury repair

Several clinical studies investigating stem cell transplantations in patients with SCI are ongoing (<https://clinicaltrials.gov>). However, most of these studies have utilized autologous mesenchymal stem cell (MSC) transplantation. The ongoing and recently completed clinical trials with human stem cell-derived neural cells for SCI treatment are listed in Table 2.

Table 2. Ongoing and recently completed clinical trials using human stem cell –derived neural cells.

Executor	Cell type	Aim	Number of patients	Initiated - Completion	ID
Federal Research Clinical Center of Federal Medical & Biological Agency, Russia, Novagenesis Foundation, Ophiuchus Technologies AG	Autologous NSCs	Feasibility and safety	30	2014 – 2018	NCT02326662
Chinese Academy of Sciences, Affiliated Hospital of Logistics University of CAPF, The First Affiliated Hospital of Soochow University, First Hospitals affiliated to the China PLA General Hospital	NeuroRegen scaffold with MSCs or NSCs	Safety and efficacy	30	2015 – 2017,	NCT02352077,
			30	2016 – 2017	NCT02688049
Asterias Biotherapeutics Inc.	AST-OPC1	Safety (dose escalation study)	35	2015 – 2018	NCT02302157
Neuralstem Inc.	Human spinal cord stem cells (NSI-566)	Safety	8	2014 – 2018	NCT01772810
StemCells Inc.	HuCNS-SC	Safety and efficacy	12	2011 – 2015,	NCT01321333,
			31	2014 – 2016,	NCT02163876,
			12	2012 – 2016	NCT01725880

Abbreviations: MSC, mesenchymal stem cell; NSC, neural stem cell; AST-OPC1, Asterias Biotherapeutics – oligodendrocyte precursor cells; HuCNS-SC, human central nervous system stem cells

Autologous NSCs derived from the patient's own bone marrow stem cells are being studied in patients with complete traumatic SCI (NCT02326662), but so far, no results from the ongoing trial have been reported (Sandquist 2016). Collagen fiber scaffolds (NeuroRegen) combined with MSCs or NSCs are currently under clinical trials executed by the Chinese research consortium. In 2016, results based on a one-year follow-up of 5 patients with NeuroRegen and autologous MSC transplantation were published (Xiao et al. 2016). In these trials, when scaffolds were transplanted, the scar tissue was surgically resected from the injury site. No adverse effect related to scar resection or NeuroRegen scaffold transplantation was reported. Furthermore, some improvements in functions related to autonomic nervous system and recovery of somatosensory evoked potentials from the lower limbs were detected. No results with human NSCs in NeuroRegen scaffolds have been reported, while the trial is still ongoing.

Asterias Biotherapeutics is studying hESC-derived OPCs, originally developed and initially taken to clinical trials by Geron Corporation (Priest et al. 2015). Asterias Biotherapeutics has reported positive safety and efficacy results with AST-OPC1s in models of thoracic and cervical SCI. Currently, phase 1/2 clinical trials are ongoing to study escalating doses of transplanted AST-OPC1s administered once between 14 and 30 days after injury. (<http://asteriasbiotherapeutics.com/AST-OPC1.php>)

Neuralstem Inc. is evaluating the safety and feasibility of using fetal spinal cord – derived NSCs (NSI-566) to repair chronic SCI. Transplantations were reported to be clinically safe and tolerable with thoracic SCI patients. Expansion of the clinical trial was announced based on positive safety and feasibility results acquired with a cohort of four patients, and new participants with cervical SCI are currently recruited. (<http://www.neuralstem.com/cell-therapy-for-sci>)

StemCells Inc. utilized fetal brain –derived NSCs (HuCNS-SC) for treatment of SCI. However, in 2016 StemCells Inc. announced termination of Phase II clinical trial due to lack of efficacy, resulting in closing out operations and winding down the company (http://investor.stemcellsinc.com/ phoenix.zhtml?c=86230&p=irol-newsArticle_print&ID=2173446). Preclinical studies in mouse and rat SCI models demonstrated the efficacy of HuCNS-SCs, but these studies were performed with research grade cells. After the termination of the clinical trial, comparison of research and clinical grade HuCNS-SCs revealed considerable difference in the efficacy of these cells and demonstrated no evidence of efficacy of the clinical grade cells in mouse model of SCI (Anderson et al. 2017). The cause of the difference is challenging to define as the manufacturing process of the clinical grade cells is not shared with the academic researchers.

Currently, a few clinical trials utilizing stem cell –derived neural cells are ongoing. The results from the safety studies are encouraging and no major adverse effects such as tumor formation have been reported. However, efficacy of these treatments have not yet been demonstrated. Thus far, only one trial utilizing transplantation of biomaterial scaffolds with stem cell-derived neural cells for SCI has been initiated.

3 Aims of the study

The focus of this thesis was to study various aspects, including the genetic background and chemical and mechanical inductions of hPSC-derived CNS cell differentiation and behavior *in vitro*. The results were aimed to be applicable for developing tissue engineering products for SCI repair. The specific aims of the studies are:

1. Comparing the neural differentiation potential of several hPSC lines and discover the presence of potential systematic differences between hESCs and hIPSCs (Study **I**).
2. Studying chemical induction for directing hPSC differentiation by developing differentiation protocol for hPSC-derived OPCs and oligodendrocytes (Study **II**).
3. Studying how defined ECM substrates influence the behavior of hPSC-derived CNS cells *in vitro* (Study **III, IV**).
4. Studying how mechanical alterations in the cell culture conditions affect hPSC-derived CNS cells *in vitro*, by culturing the cells in conditions mimicking the *in vivo* structure of the spinal cord (Study **IV**).

4 Materials and methods

4.1 hPSC culturing and differentiation

4.1.1 Ethical considerations

BioMediTech has permission from the National Authority for Medicolegal Affairs in Finland to conduct research with human embryos and derive hESC lines (1426/32/300/05). A supportive statement from the ethical committee of the Hospital District of Pirkanmaa allows the derivation, culturing, and differentiation of hESC lines (R05116) and hPSC lines (R08070). FES29, FiPS5-7, and A116 (all used in Study I) were generated at the University of Helsinki with the permissions of the Ethics Committee of the Helsinki University Central Hospital and the Coordinating Ethics Committee, Helsinki and Uusimaa Hospital District (143/E8/01; 423/13/00/08; and 54/2009).

4.1.2 hPSC lines and culture

The hPSC lines used in this thesis are listed in Table 3.

Table 3. Specifications of the used hPSC lines.

Cell line	Origin	Induction method	Established	Study
H7	Embryo	-	WiCell*	I
FES29	Embryo	-	University of Helsinki	I
Regea 06/040	Embryo	-	University of Tampere	II
Regea 08/023	Embryo	-	University of Tampere	I-V
Regea 11/013	Embryo	-	University of Tampere	IV
FiPS5-7	Foreskin fibroblast	Retrovirus	University of Helsinki	I
UTA.00112.hFF	Foreskin fibroblast	Retrovirus	University of Tampere	I
UTA.01006.WT	Adult skin fibroblast	Retrovirus	University of Tampere	I
UTA.04511.WT	Adult skin fibroblast	Sendai virus	University of Tampere	IV
A116	Adult skin fibroblast	Retrovirus	University of Helsinki	I, III
HEL24.3	Foreskin fibroblast	Sendai virus	University of Helsinki	I

*WiCell Research Institute, Madison, WI, USA. Cell line commercially available.

The maintenance of hPSC lines was performed as described earlier, with minor modifications (Rajala et al. 2007). Briefly, hPSCs were cultured on top of human feeder cell layers (CRL 2429, ATCC, Manassas, VA USA) and passaged mechanically or enzymatically once a week. The medium consisted of knockout Dulbecco's modified Eagle's medium (DMEM) supplemented with 20% knockout serum replacement, 2 mM GlutaMAX (all from Gibco, Thermo Fisher Scientific, Waltham, MA, USA), 1% nonessential amino acids, 50 U/ml penicillin/streptomycin (both from Lonza Group Ltd., Basel, Switzerland), 0.1 mM 2 mercaptoethanol (Gibco,

Thermo Fisher Scientific) and 8 ng/ml bFGF (R&D Systems Inc., Minneapolis, MN, USA).

The undifferentiated phenotype of the hPSCs were regularly monitored with gene and protein expression analyses of pluripotency markers (OCT-3/4, NANOG, tumor-related antigen (Tra) -1-81 and Tra-1-60 and EB formation assays. All cultures maintained normal karyotypes and were mycoplasma free.

4.1.3 Production of neurons and astrocytes

hPSCs were differentiated into neurons and astrocytes according to previously published protocol (Lappalainen et al. 2010). The hPSC colonies were mechanically dissected into small clusters and transferred into six-well ultralow attachment plates (Nunc, Thermo Fisher Scientific). Cells formed free-floating aggregates for neural differentiation in suspension culture. Neural differentiation medium (NDM) consisted of 1:1 DMEM/F-12:Neurobasal media supplemented with $1 \times B27$, $1 \times N2$, 2 mM GlutaMAX (all from Gibco, Thermo Fisher Scientific), 25 U/ml penicillin/streptomycin (Lonza Group Ltd.) and 20 ng/ml bFGF (R&D Systems Inc.). In Study **IV** neural differentiation was performed in the presence or absence of 0.1 μ M LDN193189 (Stemcell Technologies, Vancouver, Canada). The medium was changed three times per week, and the spheres were mechanically passaged once a week. After 8 to 12 weeks of differentiation in suspension cultures, the majority of the cells exhibited neuronal phenotype (Study **I**, **III**, **IV**). Prolonged differentiation in suspension culture changed the phenotype of the differentiating cells, resulting in astroglial-enriched population (Lappalainen et al. 2010). After 15 to 20 weeks of differentiation, astrocyte-enriched cultures were obtained (Study **III**, **IV**).

To analyze the differentiation, functionality, maturation and cell behavior under different culturing conditions, the cell aggregates were either dissociated into single cell suspension with TrypLE Select (Gibco, Thermo Fisher Scientific) or mechanically dissected into smaller aggregates. Predifferentiated cells were plated onto polystyrene, microelectrode array (MEA); nanofiber surface coated with mouse laminin (10-20 μ g/ml, Sigma-Aldrich, St. Louis, MO, USA) (Study **I**, **III**, **IV**), or non-coated nanofiber surface (Study **IV**). The cells were plated in neural differentiation medium lacking bFGF. For MEA measurements, the neural differentiation medium was supplemented with 4 ng/ml bFGF and 5 ng/ml BDNF (ProSpec -Tany TechnoGene Ltd., Rehovot, Israel) from one week of adherent culture onwards (Study **I**, **III**).

4.1.4 Production of oligodendrocytes

The differentiation method to produce hPSC-derived OPCs and oligodendrocytes was developed in Study II. hPSCs were differentiated towards OPCs using a protocol that included three phases. OPC differentiation was initiated in suspension culture as described with neural differentiation in Chapter 4.1.3.

The basal neural stem cell (NS) medium consisted of DMEM/F-12 supplemented with 1×N2, 2 mM GlutaMAX (all from Gibco, Thermo Fisher Scientific), 0.6% glucose, 5 mM HEPES, 2 µg/ml heparin (all from Sigma-Aldrich), and 25 U/ml penicillin/streptomycin (Lonza Group Ltd.). The xeno-free (XF) basal medium consisted of DMEM/F-12 with xeno-free neural stem cell (XF-NSC)-supplement StemPro (product under development; Invitrogen, Life Technologies, Carlsbad, CA, USA), 2 mM GlutaMAX (Gibco, Thermo Fisher Scientific), and 25 U/ml penicillin/streptomycin (Lonza Group Ltd.). Different combinations of additional growth factors in the basal media, listed in Tables 4 and 5, were studied for oligodendrocyte differentiation. The medium was changed three times per week and the spheres were mechanically passaged once a week.

Table 4. Supplements used in OPC differentiation media (Study II, IV)

Supplement	Concentration	Supplier
Epidermal growth factor, EGF	20 ng/ml	R&D Systems, Prospec*
Basic fibroblast growth factor, bFGF	20/10 ng/ml (stage 1/2)	R&D Systems
Ciliary neurotrophic factor, CNF	10 ng/ml	R&D Systems
Retinoic acid, RA	10 µM	Sigma-Aldrich
3,3',5-triiodo-L-thyronine, T3	40 ng/ml	Sigma-Aldrich
L-ascorbic acid 2-phosphate, AA	200 µM	Sigma-Aldrich
Insulin-like growth factor-1, IGF-1	100 ng/ml	Sigma-Aldrich, Prospec*
Platelet-derived growth factor- AA, PDGF-AA	20 ng/ml	Peprotech Inc., Prospec*
Human or mouse* laminin, LN	1 µg/ml	Sigma-Aldrich
Sonic hedgehog, SHH	100 ng/ml	R&D Systems
LDN193189*	0.1 µM	Stemcell Technologies
B27	1×	Gibco, Thermo Fisher Scientific

*Used in Study IV

Table 5. Differentiation media compositions used in Study II.

Stage	Tested media compositions
1. Neural induction 4 weeks*	NS1.1: EGF, bFGF, CNTF
	NS1.2: B27, RA*, T3, AA, EGF, bFGF, SHH#
	NS1.3: B27, RA*, T3, AA, EGF, bFGF, CNTF, SHH#
	XF1.1: EGF, bFGF, CNTF XF1.2: RA*, T3, AA, EGF, bFGF, SHH# XF1.3: RA*, T3, AA, EGF, bFGF, CNTF, SHH#
2. OPC production 3 weeks	NS2.1: EGF, bFGF, CNTF, IGF-1, PDGF-AA, LN
	NS2.2: B27, T3, AA, EGF, bFGF, IGF-1, PDGF-AA, LN, SHH
	NS2.3: B27, T3, AA, EGF, bFGF, CNTF, IGF-1, PDGF-AA, LN, SHH
	XF2.1: EGF, bFGF, CNTF, IGF-1, PDGF-AA, LN
	XF2.2: T3, AA, EGF, bFGF, IGF-1, PDGF-AA, LN, SHH XF2.3: T3, AA, EGF, bFGF, CNTF, IGF-1, PDGF-AA, LN, SHH
3. OPC maturation 2/4 weeks	NS3.1: T3, AA, CNTF
	NS3.2: B27, T3, AA, LN
	NS3.3: B27, T3, AA, CNTF, LN
	XF3.1: T3, AA, CNTF
	XF3.2: T3, AA, LN XF3.3: T3, AA, CNTF, LN

*RA used for the first three weeks in stage 1.

#SHH added after two weeks in stage 1.

Abbreviations: NS, neural stem cell medium; XF, xeno-free medium; OPC, oligodendrocyte precursor cell; see Table 4

The oligodendrocyte differentiation protocol developed in Study **II** was further modified and applied in Study **IV** (Hyysalo and Narkilahti 2015). Xenogenic conditions were applied and several components used for the differentiation media were acquired from different manufacturers. SHH was omitted from the protocol, and LDN193189 was added to the differentiation media in stages 1 and 2. Altogether, in Study **IV** OPCs were differentiated in the NS medium supplemented with B27, RA, T3, AA, EGF, bFGF, and LDN193189 in stage 1. In stage 2, the NS medium was supplemented with B27, T3, AA, EGF, bFGF, IGF-1, PDGF-AA, LN, and LDN193189. (Table 4) OPCs were cultured on nanofiber platform in stage 2 medium (Study **IV**).

The OPCs were plated down into adherent cultures for characterization during differentiation and analysis of cell behavior on nanofiber platforms. A mixture of

the ECM proteins laminin (10 $\mu\text{g}/\text{ml}$), collagen IV (10 $\mu\text{g}/\text{ml}$, both from Sigma-Aldrich), and nidogen 1 (1 $\mu\text{g}/\text{ml}$, R&D Systems) was used for coating surfaces for OPCs. (Study **II**, **IV**)

4.2 Recombinant human laminins

Recombinant human laminin isoforms were used as coating substrates for hPSC-derived neurons and astrocytes. Human recombinant laminin isoforms LN211, LN332, LN411, LN511, LN521 (10 $\mu\text{g}/\text{ml}$, 2 $\mu\text{g}/\text{cm}^2$, BioLamina, Sundbyberg, Sweden), and the LN511-E8 fragment (10 $\mu\text{g}/\text{ml}$, 1 $\mu\text{g}/\text{cm}^2$, Clontech, Takara Bio Inc., Shiga, Japan) were used for coating 2D polystyrene surfaces (Study **III**). Additionally, human recombinant laminin isoforms LN411, LN511, LN521 (10 $\mu\text{g}/\text{ml}$, 2 $\mu\text{g}/\text{cm}^2$), and the LN511-E8 fragment (10 $\mu\text{g}/\text{ml}$, 1 $\mu\text{g}/\text{cm}^2$) were used for coating nanofiber surfaces (Study **IV**).

4.3 Nanofiber platform

hPSC-derived neurons, astrocytes, and OPCs were cultured on commercial nanofiber surfaces (Study **IV**). NanoAligned™ 24-well plates and 24-well plate inserts (Nanofiber Solutions, Columbus, OH, USA) were used as the nanofiber platform. The nanofibers were fabricated from PCL, and products were xeno-free. The mean diameter of a single fiber was 700 nm, and fibers were plasma surface-treated to improve their hydrophilicity. (<http://www.nanofibersolutions.com/products.html>)

4.3.1 Nanofiber-hydrogel scaffolds

The hPSC-derived neurons were cultured on and encapsulated in 3D hydrogel-nanofiber constructs (Study **IV**). Commercial PuraMatrix™ hydrogel was used according to the manufacturer's instructions (Corning, Corning, NY, USA) and hydrogel scaffolds on top of nanofiber platforms were prepared according to previously published method, with minor modifications (Buxboim et al. 2010). The fabrication method of the hydrogel scaffolds is described in detail in the original publication (Study **IV**). Briefly, thin (15 μm) and thick (75 μm) hydrogel scaffolds were polymerized while sandwiched between a coverslip and a nanofiber platform.

Gel thickness was controlled by mixing the hydrogel with polystyrene microspheres of desired diameters. Excess hydrogel was removed prior to polymerization by placing a weight on top of the sandwiched structure. The coverslip was removed after polymerization, leaving the hydrogel attached to the nanofiber platform. The hPSC-derived neurons were either plated on top of a thin hydrogel or encapsulated within a thick hydrogel (Figure 6).

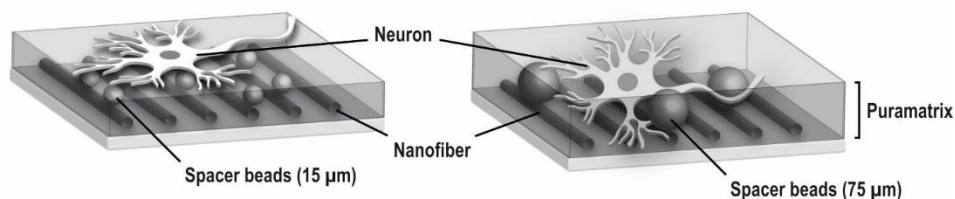


Figure 6. Culturing of hPSC-derived neurons on top of a thin hydrogel or within a thick hydrogel on nanofiber platforms. Illustrations are not to scale.

4.4 Characterization of differentiated neural cells

4.4.1 Morphology and time-lapse imaging

Cell morphology and growth were routinely observed during adherent culturing using Nikon T2000S microscope with a DS-Fi1 camera (Nikon Instruments, Amsterdam, Netherlands) (Study **I-IV**). More detailed analyses of morphology and cell behavior were performed with time-lapse imaging system (Cell-IQ®, Chip-Man Technologies Ltd, Tampere, Finland) (Study **I**). Automated imaging and cell-culturing platform enabled continuous monitoring of the cells with phase-contrast microscope optics (10×) and a CCD camera, as previously described (Narkilahti et al. 2007). After 4 and 8 weeks of differentiation in suspension cultures, the neurons were monitored continuously for 2 days in adherent cultures.

4.4.2 Cell viability

Viability of the cells was studied using a LIVE/DEAD® Viability/Cytotoxicity Kit for mammalian cells (Thermo Fisher Scientific) (Study **III, IV**). Briefly, the cells were incubated in culture medium supplemented with calcein AM (0.1 μM) and ethidium

homodimer-1 (0.5 μ M). The cells were imaged immediately after 30 minutes incubation at room temperature (RT) in a light-protected area.

Areas covered by calcein AM (live cells, emission 515 nm) and ethidium homodimer-1 (dead cells, emission 635 nm) in the cell cultures were quantified from immunofluorescence images using ImageJ-software (U.S. National Institutes of Health, Bethesda, MD, USA) (Study **III**).

4.4.3 Gene expression analysis

Reverse transcription-polymerase chain reaction (RT-PCR) and quantitative real time PCR (qPCR) were used to evaluate hPSC differentiation towards neural and glial lineages (Study **I**, **II**). Genes included in the analyses are listed in Table 6. RNA extraction, cDNA synthesis, PCR protocols, and primer sequences are described in detail in the original publications. Relative expression values were determined using the comparative $2^{-\Delta\Delta C_t}$ method (Livak and Schmittgen 2001). As opposed to the original publication, analysis of neural differentiation in Study **I** was performed for each cell line individually using undifferentiated samples as the calibrators.

Table 6. Genes used for RT-PCR and qPCR analyses

Gene	Expression	RT-PCR /qPCR	Study
<i>OCT3/4</i>	Pluripotent/Transgenic	RT-PCR/qPCR	I, II
<i>Musashi</i>	NPC	qPCR	I
<i>NF-68</i>	Neuron	qPCR	I
<i>GFAP</i>	Astrocyte	qPCR	I
<i>SOX2</i>	Transgenic	qPCR	I
<i>C-MYC</i>	Transgenic	qPCR	I
<i>KLF4</i>	Transgenic	qPCR	I
<i>NANOG</i>	Transgenic	qPCR	I
<i>LIN28</i>	Transgenic	qPCR	I
<i>Olig2</i>	OPC	RT-PCR/qPCR	II
<i>Nkx2.2</i>	OPC	RT-PCR/qPCR	II
<i>SHH</i>	Sonic Hedgehog-signaling	qPCR	II
<i>SOX10</i>	OPC	RT-PCR/qPCR	II
<i>PAX6</i>	Neuroepithelium	RT-PCR	II
<i>Nestin</i>	Neuroectoderm	RT-PCR	II
<i>PDGF-Ra</i>	OPC	RT-PCR	II
<i>NG2</i>	OPC	RT-PCR	II
<i>SOX9</i>	Glial precursor	RT-PCR	II
<i>Nkx6.2</i>	Oligodendrocyte	RT-PCR	II
<i>PLP</i>	Oligodendrocyte	RT-PCR	II
<i>OMG</i>	Oligodendrocyte	RT-PCR	II
<i>GAPDH</i>	Endogenous control gene	RT-PCR/qPCR	I, II

Abbreviations: OCT3/4, octamer-binding transcription factor 3/4; NF-68, neurofilament light chain; GFAP, glial fibrillary acidic protein; SOX2, SRY (Sex Determining Region Y)-Box 2; C-MYC, V-Myc avian myelocytomatosis viral oncogene homolog; KLF4, Kruppel-like factor 4; Olig2, oligodendrocyte transcription factor 2; Nkx2.2, NK2 homeobox 2; SHH, sonic hedgehog; SOX10, SRY-Box 10; PAX6, paired box 6; PDGF-R α , platelet-derived growth factor receptor α ; NG2, chondroitin sulphate proteoglycan 4; SOX9, SRY-Box 9; Nkx6.2, NK6 homeobox 2; PLP, proteolipid protein; OMG, oligodendrocyte myelin glycoprotein; GAPDH, glyceraldehyde 3-phosphate dehydrogenase; NPC, neural precursor cell; OPC, oligodendrocyte precursor cell

4.4.4 Protein expression analysis

Protein expression in differentiated neurons, astrocytes and OPCs was analyzed using immunocytochemistry (Study **I-IV**). The primary antibodies used for the analyses are listed in Table 7. For secondary antibody labelling, Alexa Fluor 488 and Alexa Fluor 568 dyes (both from Molecular Probes, Thermo Fisher Scientific) were used at 1:400 dilution. The staining protocol is described in detail in the original publications. In studies **II** and **IV**, staining with the oligodendrocyte marker O4 was performed for living cells. Live staining was performed by incubating cells in diluted antibody at 37°C for 30 minutes. The cells were subsequently either incubated with secondary antibody or fixed with 4% paraformaldehyde prior to secondary antibody incubation. Secondary incubation with Alexa Fluor 568 goat anti-mouse IgM was performed for 30 minutes at RT. Alternatively, O4 staining was performed for fixed cells as described above in Study **IV**. The stained samples were imaged using an Olympus IX51 fluorescence microscope (Olympus Corporation, Hamburg, Germany) or Zeiss LSM780 confocal microscope (Carl Zeiss, Oberkochen, Germany).

Table 7. Antibodies used for immunocytochemical analyses of protein expression

Antibody	Expression	Host	Dilution	Manufacturer	Study
OCT3/4	Pluripotent	Goat	1:200	R&D Systems	II
Tra 1-81	Pluripotent	Mouse	1:200	Santa Cruz Biotechnology	II
SOX2	Neural stem cell	Goat	1:200	Santa Cruz Biotechnology	II
SOX2	Neural stem cell	Mouse	1:200	R&D Systems	II
Nestin	Neuroectoderm	Mouse	1:1000	Merck Millipore	I, II, III
MAP-2	Neuron, dendritic	Rabbit	1:400	Merck Millipore	I-IV
β -tubulin _{III}	Neuron, axonal	Mouse	1:1000	Sigma-Aldrich	III, IV
β -tubulin _{III}	Neuron, axonal	Rabbit	1:2000	GenScript	III
GFAP	Astrocyte	Sheep	1:2000	R&D Systems	III
GFAP	Astrocyte	Chicken	1:4000	Abcam	III
S100 β	Astrocyte	Mouse	1:500	Abcam	IV
Olig2	OPC	Rabbit	1:200	Merck Millipore	II, IV
NG2	OPC	Rabbit	1:200	Merck Millipore	II, IV
GalC	OPC/ Oligodendrocyte	Mouse	1:200	Merck Millipore	II, IV
O4	OPC/ Oligodendrocyte	Mouse	1:100	R&D Systems	II, IV
MBP	Oligodendrocyte	Rabbit	1:200	Merck Millipore	II, IV
MBP	Oligodendrocyte	Rat	1:100	Abcam	IV

Abbreviations: OCT3/4, octamer-binding transcription factor 3/4; Tra 1-81, tumor-related antigen 1-81; SOX2, SRY (sex determining region Y)-box 2; MAP-2, microtubule-associated protein 2; GFAP, glial fibrillary acidic protein; Olig2, oligodendrocyte transcription factor 2; NG2, chondroitin sulphate proteoglycan 4; GalC, galactocerebroside; O4, oligodendrocyte marker O4; MBP, myelin basic protein; OPC, oligodendrocyte precursor cell

Visualization and analyses of the imaging data was performed using Adobe Photoshop (Adobe Systems Incorporated, San Jose, CA, USA), Huygens Essential (Scientific Volume Imaging B.V., Hilversum, Netherlands), Zeiss Microscope Software Zen (Carl Zeiss), and ImageJ (U.S. National Institutes of Health, Bethesda, MD, USA). The cell culture areas covered by microtubule-associated protein 2 (MAP-2)-positive cells were quantified using ImageJ (Study **I**), and cells positive for MAP-2/ β -tubulin_{III} (Study **III**) or GFAP were detected and counted automatically

using CellProfiler and CellProfiler Analyst (Carpenter et al. 2006, Jones et al. 2008). Distribution of cell orientation (Study **IV**) was analyzed using spectral analysis software CytoSpectre (Kartasalo et al. 2015).

4.4.5 Flow cytometry

The protein expression profiles of hPSC-derived OPCs were analyzed using flow cytometry (Study **II**). The detailed protocol for sample preparation is described in the original publication. The samples were analyzed using FACSARIA with FACS Diva software (BD Biosciences, Franklin Lakes, NJ, USA). Fluorochrome-conjugated cell surface markers used for the analysis are listed in Table 8. Additional antibodies used for flow cytometry analysis, including chondroitin sulphate proteoglycan 4 (NG2), O4, and Tra 1-81, are listed in Table 7. These antibodies lacking fluorochrome-conjugates were detected using phycoerythrin (PE)-conjugated goat anti-mouse IgM (Caltag Laboratories, Thermo Fisher Scientific) or donkey anti-mouse IgG Alexa Fluor 488 (Molecular Probes, Thermo Fisher Scientific).

Table 8. Antibodies used for analysis of cell surface markers with flow cytometry

Antibody	Full name	Conjugate	Manufacturer
A2B5	A2B5	APC	Miltenyi Biotec
CD44	H-CAM	PE	BD Biosciences
CD56	NCAM	PE	Immunotools
CD133	AC133, prominin-1	PE	Miltenyi Biotec
CD140a	PDGF-R α	PE	BD Biosciences
CD326	EpCAM	APC	Miltenyi Biotec

Abbreviations: H-CAM, homing cell adhesion molecule; NCAM, neural cell adhesion molecule; PDGF-R α , platelet-derived growth factor receptor α ; EpCAM, epithelial cell adhesion molecule; APC, allophycocyanin; PE, phycoerythrin

4.4.6 Scanning electron microscopy

The surface morphology and behavior of cell on nanofiber platforms were studied using a field emission scanning electron microscope (FESEM, ULTRApplus, Carl Zeiss) (Study **IV**). Samples were fixed with 5% glutaraldehyde for 1 hour at RT and

dehydrated in a graded ethanol series. The dehydrated samples were carbon glued onto the FESEM aluminum stubs followed by carbon coating (Turbo Carbon Coater, Agar Scientific, Stansted, UK). The samples were examined using an accelerating voltage of 3 kV and tilted $\sim 55^\circ$ to observe the 3D structures more easily.

4.4.7 Microelectrode array measurements

Spontaneous electrical activity of the neuronal networks was analyzed using MEA technology (Study **I**, **III**). The measurements were performed on standard or 6-well MEA-plates (Multichannel Systems [MCS], Reutlingen, Germany) coated with 0.05% w/v polyethyleneimine (PEI) and 20 $\mu\text{g}/\text{ml}$ mouse laminin (Study **I**) or standard 12-well plate MEAs (Axion Biosystems, Atlanta, GA, USA) coated with human recombinant laminin substrates (Study **III**). In MCS MEA-plates, the electrode areas were surrounded with in-house designed poly(dimethyl siloxane) (PDMS) structures (Kreutzer et al. 2012). Measurements were performed using MEA1060-Inv-BC-amplifier (Multichannel Systems) or Maestro MEA system (Axion Biosystems) and data were recorded with MC Rack (Multichannel Systems) or AxIS software (Axion Biosystems). Five minute recordings were performed twice a week (Study **I**) or ten minute recordings were performed once a week (Study **III**) for one to three weeks per experiment. A custom made MATLAB script was used for spike count and burst analysis, modified from (Kapucu et al. 2012) (Study **III**).

4.5 Statistical analyses

A non-parametric Kruskal-Wallis test (>2 groups) followed by Mann-Whitney test and Bonferroni correction were used due to the non-Gaussian distribution of the data (Study **I**, **III**). Statistical analyses were performed using SPSS Statistics (IBM Corp., Armonk, NY, USA) software. The results were considered significant if p-values were ≤ 0.05 .

5 Results

5.1 Differentiation capacities of individual hESC and hiPSC lines

Three hESC lines and four hiPSC lines were directed to differentiate towards hepatocytes, cardiomyocytes, neuronal- and retinal pigment epithelium (RPE) cells, which are derivatives of the endoderm, mesoderm, and ectoderm, respectively (Study I). The differentiation capacities of individual cell lines were evaluated using targeted differentiation methods and a wide range of characterization methods. A summary of cell line-specific differentiation propensities is presented in Table 9. The results of the directed neuronal differentiation are presented in more detail in this chapter.

Transgene expression in the hiPSC lines were studied prior to and at the end of differentiation experiments. Expression of *KLF4* was detected constantly prior to differentiation in the UTA.01006.WT cell line (Study I, Figure 1). This cell line also showed the weakest differentiation capacity with all differentiation methods used in this study (Table 9). No expression of transgenes was detected with the other hiPSC lines prior to differentiation. In addition, none of the hiPSC lines showed reactivation of the transgenes at the end of differentiation towards hepatocytes, cardiomyocytes, and neuronal cells. Upon long-term RPE differentiation, however, increased expression of transgenic *OCT3/4*, *NANOG*, and *LIN28* was detected (Study I, Supplementary Figure 2).

Table 9. Differentiation propensities of individual hESC and iPSC lines.

hPSC line	Endoderm	Mesoderm	Ectoderm	
	Hepatocyte	Cardiomyocyte	Neuron	RPE cell
hESC1, H7	++	+++	+	+
hESC2, FES29	++	++	++	++
hESC3, Regea 08/023	+++	+	+++	+++
iPSC1, FiPS5-7	++	+	++	+
iPSC2, UTA.00112.hFF	+++	++	++	+++
iPSC3, A116	++	++	+++	++
iPSC4, UTA.01006.WT	+	+	+	+

+ Low, ++ Average, +++ Excellent differentiation capacity

Abbreviations: RPE, retinal pigment epithelium

The neuronal differentiation efficiency was evaluated using morphological, gene expression, protein expression, and functional analyses. Expression of the pluripotency marker *OCT3/4* was downregulated in all cell lines as differentiation proceeded. The NPC marker *Musashi*, neuronal marker neurofilament light chain (*NF-68*), and astrocyte marker *GFAP* were all upregulated in all cell lines by the eight-week time point (Figure 7A). Comparison of combined gene expression data from all hESC and iPSC lines showed significantly higher downregulation of *OCT3/4* and upregulation of *NF-68* in hESC lines compared to those in iPSC lines at the eight-week time point (Figure 7B).

The amount of neurons produced by each cell line was evaluated by quantifying the area covered by MAP-2-positive cells in the cultures (Figure 7C). The highest coverage of MAP-2-positive cells was detected with 08/023. Other hESC lines, H7 and FES29, both produced considerably lower MAP-2-positive cell coverage. The iPSC line with the highest MAP-2-positive cell coverage was FiPS5-7. However, the purity of the differentiated neuronal population was higher for iPSC line A116 (Study I). The lowest MAP-2-positive cell coverage of all tested cell lines was detected with UTA.01006.WT. The comparison between combined data from hESC and iPSC lines revealed no difference in the MAP-2-positive cell coverage (Figure 7C). Spontaneous activity of the differentiated neurons was measured on MEA, and all cell lines were confirmed to produce functional neurons (Study I).

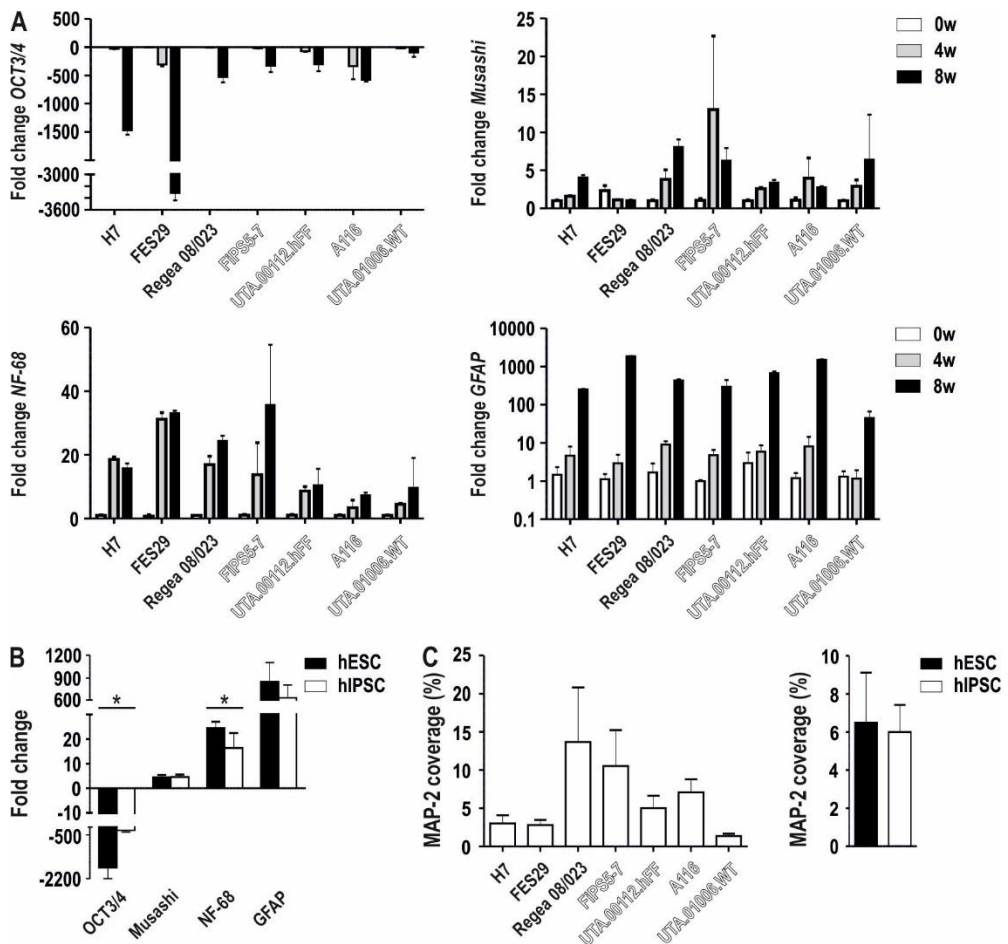


Figure 7. Neuronal differentiation capacity of individual hESC and hiPSC lines. (A) Changes in *OCT3/4*, *Musashi*, *NF-68*, and *GFAP* expression in hESC and hiPSC lines during neural differentiation. (B) Combined gene expression data from hESC and hiPSC lines at eight week time point. Mann-Whitney U-test (* $p \leq 0.05$). (C) Coverage of MAP-2 –positive cells in cultures at the eight-week time point, presented separately for each cell line and as combined data from hESC and hiPSC lines. Data presented as the mean with S.E.M. hESC and hiPSC lines presented with black and white legends or bars, respectively.

5.2 Differentiation of hPSC-derived oligodendrocytes and culturing of produced OPCs on nanofiber platforms

OPCs and oligodendrocytes were produced from hPSCs via directed differentiation (Study **II**, **IV**). Differentiation was chemically induced by administration of specific combinations of growth factors in the media. The differentiation protocol is divided into three phases; neural induction (stage 1), OPC production (stage 2), and OPC maturation (stage 3).

First, oligodendrocyte differentiation was studied under xeno-free and defined culture conditions (Study **II**). The xeno-free conditions XF1.2 – XF3.2 and corresponding control conditions NS1.2 – NS3.2 (see Table 5) were found to direct oligodendrocyte differentiation most efficiently, based on gene and protein expression analyses (Study **II**). Flow cytometric analysis (FACS) of the differentiating cells in stages 1, 2, and 3 revealed downregulation of glial precursor cell markers A2B5 and CD140a (Figure 8A). However, the expression of CD44 and chondroitin sulphate proteoglycan 4 (NG2), also expressed in glial precursor cells, were upregulated from stage 1 to stage 2, and remained relatively constant and highly expressed from stage 2 to stage 3. The expression of the neural precursor cell marker CD133 was downregulated during differentiation from stage 1 to stage 3 and that of the pluripotency marker Tra 1-81 remained at a constant low level during the differentiation process. (Figure 8A)

FACS analysis showed the upregulation of the developing oligodendrocyte marker O4 upon differentiation from stage 1 to stage 3, indicating maturation of the OPCs (Figure 8A). Expression of O4 was also studied with immunocytochemical (IC) analysis for a more detailed view of the cell morphology. However, higher variation and systematically lower proportions of O4-positive cells were detected by this method compared to FACS-results (Figure 8A-B). Maturation of the OPCs was also demonstrated with the upregulation of galactocerebroside (GalC) expression in the differentiating cells. At stage 3, the morphology of the GalC-positive cells was highly variable, ranging from immature bipolar OPCs to more ramified maturing oligodendrocytes (Study **II** Figure 7, Figure 8B). The results indicate efficient production of OPCs by stage 2, followed by heterogeneous oligodendrocyte maturation at stage 3.

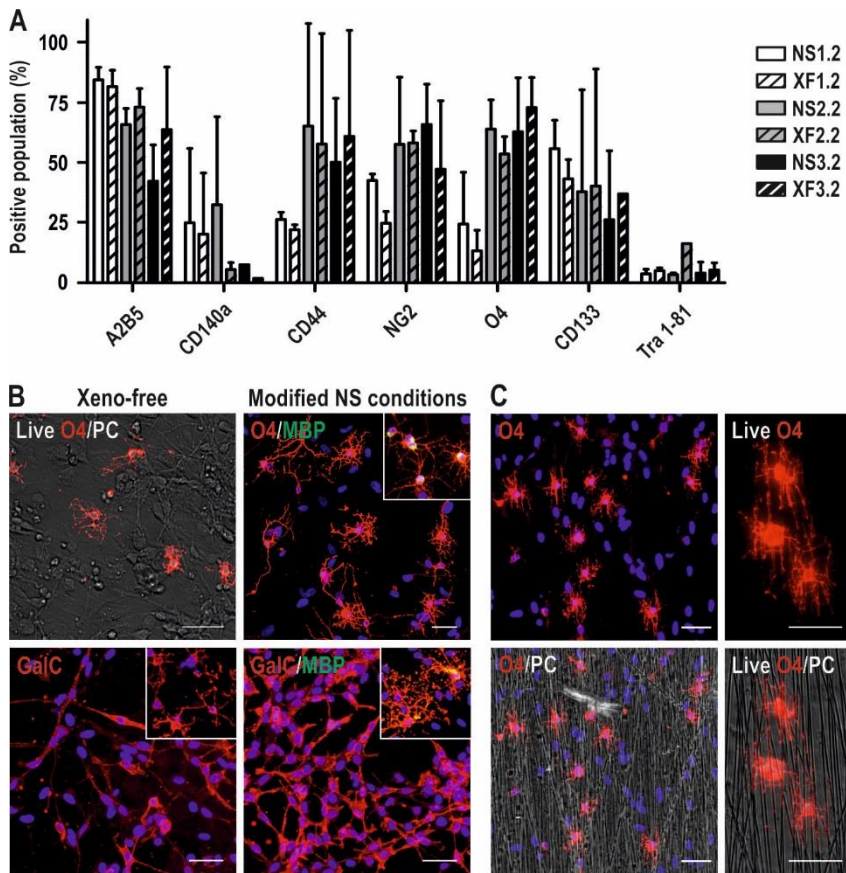


Figure 8. Characterization of hPSC-derived OPCs and oligodendrocytes. (A) Surface marker expression during oligodendrocyte differentiation in xeno-free (XF) and control (NS) conditions determined using flow cytometry. Data presented as the mean with S.E.M. (B) Representative images of O4, GalC, and MBP expressing OPCs and oligodendrocytes produced in xeno-free and modified NS conditions. Cells with more mature morphologies are presented within insets. Scale bar 50 μ m. (C) hPSC-derived OPCs cultured on PCL-nanofiber platforms. Scale bar 50 μ m. Abbreviations: Live O4, O4 staining performed for living cells; PC, Phase contrast

Xeno-free differentiation protocol is not required for production of OPCs and oligodendrocytes for research purposes. Production of the oligodendrocytes under these conditions is also considerably costly. Thus, further modifications for the differentiation protocol were performed in NS1.2 – NS3.2 control conditions to reduce the expenses of OPC production for non-clinical research applications (Study IV, Hyysalo and Narkilahti 2015). Maturation of the oligodendrocytes under modified NS conditions showed a similar trend as previously demonstrated with the xeno-free protocol. The expression of O4 and GalC were increased upon

differentiation, demonstrating maturation of the OPCs. The mature oligodendrocyte marker MBP was also detected in some O4- and GalC-positive cells with ramified morphologies (Figure 8B). However, the proportions of the cells expressing O4 displayed considerable variation between individual experiments and morphological heterogeneity within GalC-positive population was detected (Figure 8B, unpublished data).

The BMP signaling inhibitor LDN193189 was added to the modified xenogenic conditions at stage 1 and stage 2 in Study **IV** in order to reduce contaminating non-neural cells in the differentiating population. LDN193189 is generally used to increase hPSC differentiation into neural precursor lineage (Chambers et al. 2016). Addition of LDN193189 decreased the amount of non-neural cells producing cystic structures in the differentiating aggregates during suspension culture, whereas no effect on oligodendrocyte differentiation efficiency was detected (unpublished data).

The *in vitro* physical guidance of the cultured OPCs was studied on PCL nanofiber platforms (Study **IV**). The OPCs attached to the nanofibers and were detected to orientate according to the fiber alignment. The processes of maturing O4-positive cells aligned and followed single fibers (Figure 8C). Interestingly, the OPCs attached, migrated, and oriented on both bare and ECM protein-coated nanofibers with equal efficiencies (Study **IV**, Figure 1). No effect on oligodendrocyte differentiation or maturation was detected on nanofiber platform compared to control culture conditions (Study **IV**, Figure 1).

5.3 Specific laminin isoforms for *in vitro* culturing of hPSC-derived neurons and astrocytes

The effect of specific human laminin isoforms for *in vitro* culturing of hPSC-derived neurons and astrocytes was studied using human recombinant laminins LN211, LN332, LN411, and LN511. The attachment, viability and spreading of neurons and astrocytes on these substrates were compared with traditionally used mouse- and human-derived, undefined laminin substrates. (Study **III**, unpublished data) Both cell types attached and spread over the culture area most efficiently on the LN511-coated surface, forming dense networks of neurons and astrocytes (Figure 9A-B). Cell behavior on LN511 resembled mouse laminin-coated control cultures (Figure 9A-B). The second preferred coating material was LN211, where the cells formed considerably sparser networks. Cell spreading was modest on LN332 and very inefficient on LN411. The attached cells also peeled off easily from LN332- and

LN411-coated surfaces. Low cell attachment and spreading were also detected on human laminin substrate with both cell types (Figure 9A-B). Similar preference for laminin isoform substrates was detected with hPSC-derived neurons and astrocytes.

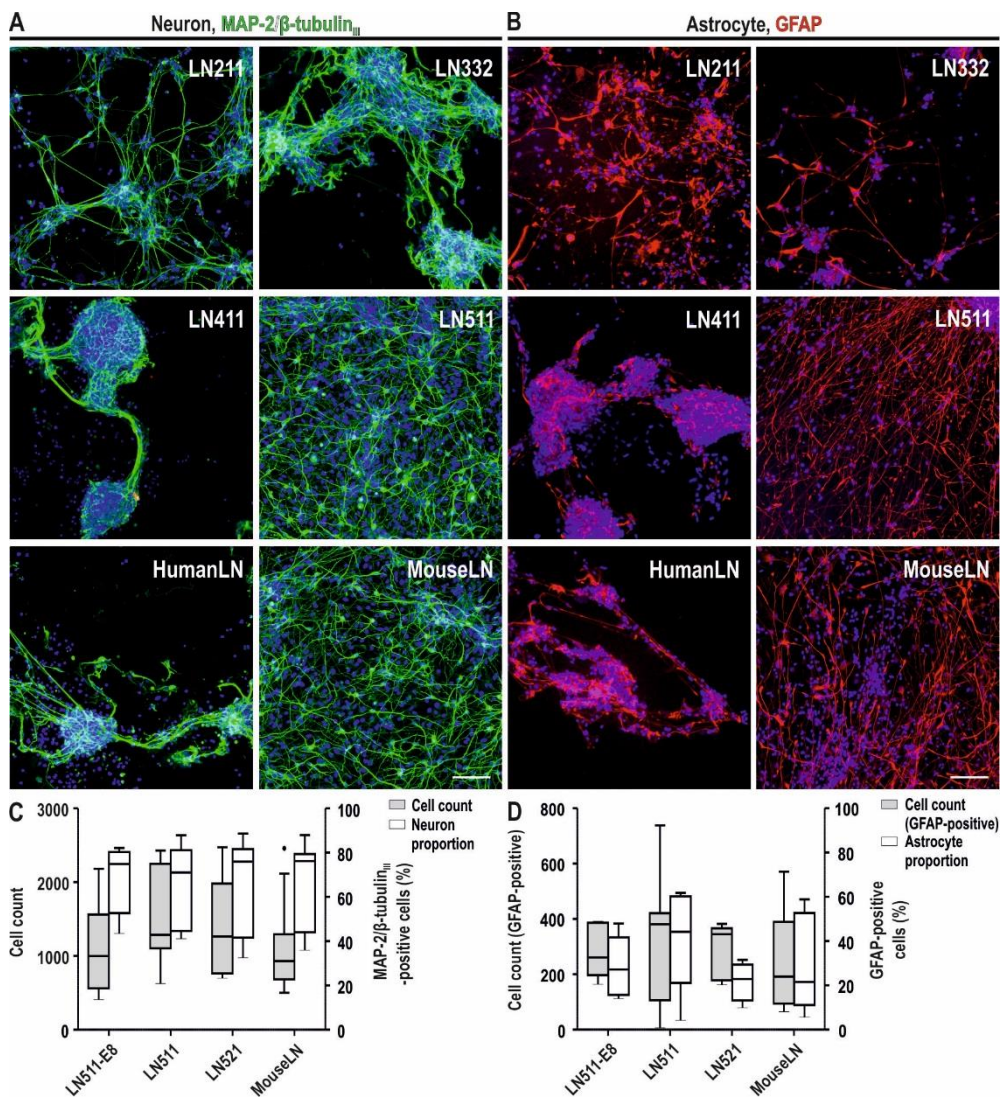


Figure 9. hPSC-derived neurons and astrocytes cultured on recombinant human laminin substrates. Representative images of neurons (A) and astrocytes (B) on LN211, LN332, LN411, LN511, human, and mouse laminin substrates. Cell count and proportion of neurons (C) and GFAP-positive cell count and proportion of astrocytes (D) on laminin $\alpha 5$ substrates and mouse laminin control substrate. No significant differences were found between different substrates. Mann-Whitney U-test ($p \leq 0.05$). Scale bar 100 μ m. Data presented as Tukey boxplots.

Furthermore, the most supporting laminin isoform, LN511, was compared with other structurally related substrates, LN521 and LN511 fragment E8. Hereafter, in this thesis, LN521, LN511, and LN511-E8 are referred to as laminin α 5 substrates. Cell counts, the proportions of MAP-2/ β -tubulin_{III}-positive neurons, and amount and proportion of GFAP-positive astrocytes were determined in the cultures. The median proportion of MAP-2/ β -tubulin_{III}-positive neurons on all laminin α 5 substrates was almost 80%, while the proportion of GFAP-positive astrocytes varied between 20 and 45%. All laminin α 5 substrates efficiently supported the attachment and growth of hPSC-derived neurons and astrocytes, and significant differences were not detected between cultures on these substrates or mouse laminin control (Figure 9B-C).

5.3.1 Functional development of hPSC-derived neuronal networks on different laminin substrates

The functional development of hPSC-derived neuronal networks on different laminin substrates was studied using MEA (Study **III**). The first signs of electrical activity in neuronal cultures are single spikes. Over the course of the maturation, the activity develops into spike trains and finally to bursts (Heikkilä et al. 2009). In this study, the proportions of electrodes detecting spike and burst activity were determined for each culture. The characteristics of network activity were studied by analyzing spike frequency, burst count, and burst duration on the active electrodes.

All laminin α 5 substrates supported the development of functional neuronal networks more efficiently than LN332, LN411, or human laminin control. This was detected as significantly higher levels of active electrodes in the cultures (Figure 10). The active electrode levels on LN211 and mouse laminin-coated cultures were also lower compared to cultures on laminin α 5 substrates, but the differences were significant only in the case of LN521. Furthermore, significantly higher proportions of burst detecting electrodes were observed in the cultures on LN521 compared to other laminin α 5 substrates (Figure 10B). Nevertheless, differences in the characteristics of neuronal activity were not found between the cultures on any coating substrates (Study **III**).

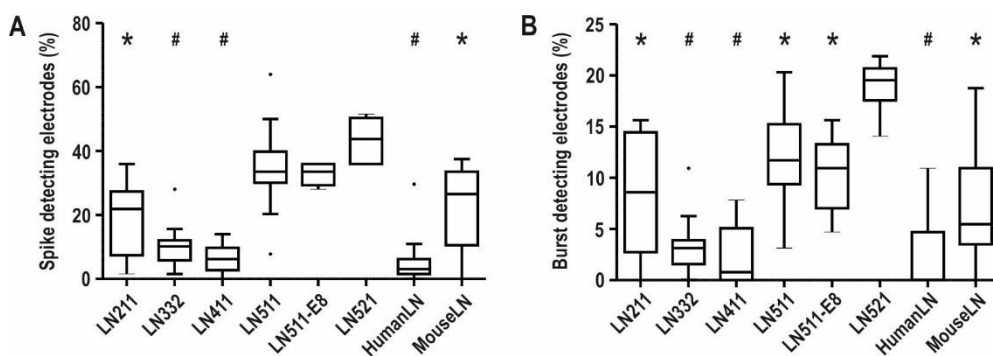


Figure 10. Active electrode proportions in the neuronal cultures on different laminin substrates. Proportions of spike (A) and burst (B) detecting electrodes per culture after three weeks of culturing on MEA. # Spike or burst detecting electrode level significantly differing from cultures on all laminin $\alpha 5$ substrates. * Spike or burst detecting electrode proportions significantly differing from cultures on LN521. Mann-Whitney U-test ($p \leq 0.05$). Data presented as Tukey boxplots.

5.4 Nanofiber platform for *in vitro* culturing of hPSC-derived neurons and astrocytes

5.4.1 hPSC-derived neurons and astrocytes on nanofiber platform

To study *in vitro* physical guidance of the cultured hPSC-derived neurons and astrocytes, commercially available aligned PCL nanofiber platforms were used (Study IV). Culturing of neither neurons nor astrocytes was successful on bare PCL nanofibers (Figure 11A-B). Aggregates of neurons and astrocytes attached to the bare nanofibers, but cell viability was low, and no cell migration was detected (Figure 11A-B). However, significantly enhanced growth was observed with both cell types when nanofibers were coated with ECM proteins.

Based on the results presented in Chapter 5.3, human recombinant laminin $\alpha 5$ substrates and LN411 were used for coating the nanofibers (Figure 11A-B; Study IV, Figure 1-2). Similar preferences for laminin $\alpha 5$ substrates was detected with hPSC-derived neurons and astrocytes on nanofiber platforms as previously presented with 2D polystyrene surfaces. LN411-coating on nanofibers resulted in modest improvement in cell spreading, whereas coating with laminin $\alpha 5$ substrates resulted in considerable improvements in both cell growth and migration (Figure 11A-B; Study IV, Figure 2).

Both neurons and astrocytes migrated along the fibers over the culture area and oriented according to the fiber alignment. Analysis of the mean orientation in the cultures demonstrated similar orientations for cells and fibers (Figure 11A-C). Scanning electron microscopy (SEM) revealed more details of nanofiber surface topography, cell attachment, and morphology of hPSC-derived neurons and astrocytes (Figure 11D). The cell somas were mostly attached to the nanofibers, and cell orientation could be detected. However, neuron and astrocyte processes were also clearly growing in an unoriented manner and crossing over the fibers, presumably as a result of uniform laminin-coating in the cultures.

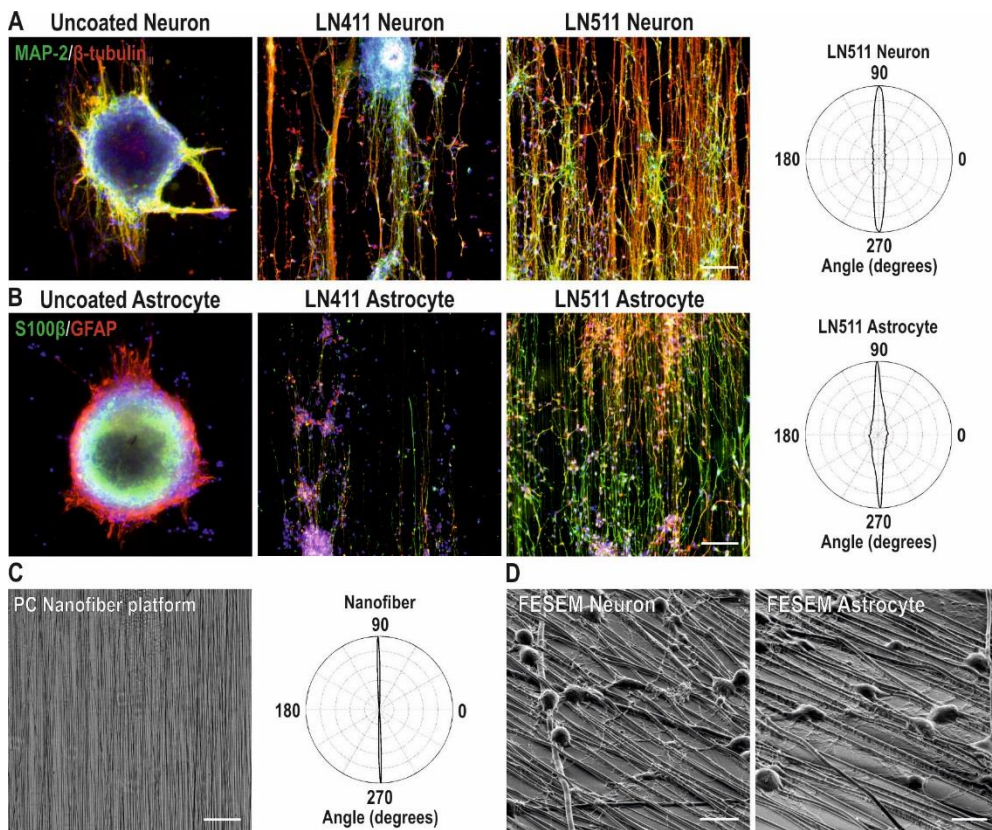


Figure 11. hPSC-derived neurons and astrocytes cultured on nanofiber platforms. Representative images of neurons (A) and astrocytes (B) on uncoated, LN411-coated, and LN511-coated nanofiber surfaces. Orientation distributions of cells on LN511-coated nanofiber surface are presented. (C) Representative image and orientation distribution of nanofiber platform. (D) Representative FESEM images of neurons and astrocytes attached to nanofiber surfaces. Scale bar 100 μ m (A-C), 10 μ m (D). Abbreviations: PC, Phase contrast; FESEM, Field emission scanning electron microscopy

5.4.2 hPSC-derived neurons on nanofiber-hydrogel scaffolds

PCL nanofibers were combined with commercial Puramatrix hydrogel in order to create a 3D environment on top of the nanofiber platform (Study **IV**). Previous work from our group has shown that a peptide-based Puramatrix hydrogel supports the growth of viable neural cells in 3D conditions (Ylä-Outinen et al. 2014). The hPSC-derived neurons were cultured either on top of 15 μm thick Puramatrix hydrogel or encapsulated within the 75 μm thick Puramatrix hydrogel on top of nanofiber surface.

Neurons plated on top of the nanofibers and the thin hydrogel scaffold spread in an unoriented manner on the hydrogel surface and inefficiently migrated into the hydrogel (Study **IV**, Figure 3). However, neurons encapsulated into the thick hydrogel gradually spread within the hydrogel. The neurons were plated within the hydrogel as small aggregates (diameter approximately 50 μm) and in a few days the cells were detected to spread out from these aggregates. Some neurons clearly attached to the fibers and adapted fiber orientation (arrows in Figure 12A) while others migrated in the hydrogel in an unoriented manner (arrowheads in Figure 12A). Further analysis with confocal imaging revealed that when the aggregate was initially placed in contact with the fiber surface at the bottom of the hydrogel scaffold, neurons that migrated out of the aggregates close (<10 μm) to the nanofiber surface followed the nanofiber alignment. In contrast, neurons migrating out from the aggregate farther (>10 μm) away from the nanofiber surface were not affected by the nanofibers' topography. (Figure 12B) Three-dimensional rendering of images with pseudo-colored depth coding demonstrate the distribution of the cells within the hydrogel (Figure 12C).

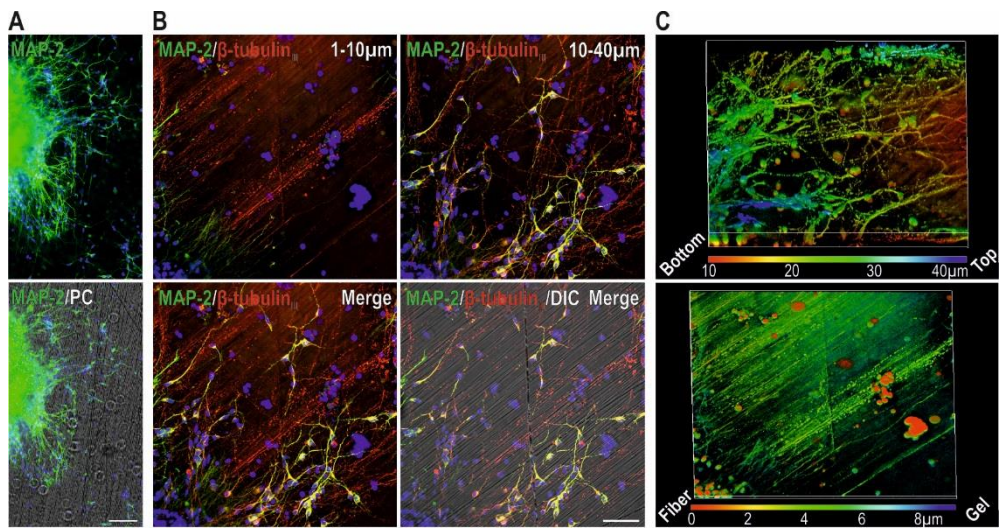


Figure 12. hPSC-derived neurons cultured in nanofiber-hydrogel scaffolds. (A) Neurons in nanofiber-hydrogel scaffolds imaged with fluorescence microscope. Scale bar 100 μ m. (B) hPSC-derived neurons in nanofiber-hydrogel scaffolds. Separate stacks from 1-10 μ m and 10-40 μ m distance from the bottom of the nanofiber platform are presented. Stacks are also merged together and presented with a DIC image of the nanofiber platform. Scale bar 50 μ m. (C) 3D rendering of images with pseudo colored depth coding of the same location presented in Figure 12B. Separate stacks from 1-10 μ m and 10-40 μ m distance from the bottom of the nanofiber platform are presented. Abbreviations: PC, Phase contrast; DIC, Differential interference contrast

6 Discussion

6.1 Differentiation propensity of individual hPSC lines

6.1.1 Comparison of hESC and hiPSC lines

The first aim of this thesis was to compare the neural differentiation potential of several hPSC lines in order to discover the presence of potential systematic differences between hESCs and hiPSCs (Study I). Differentiation efficiency was evaluated based on cell morphology, gene, and protein expression, and the functional development of the cells.

Significant differences were found in combined gene expression results between hESC and hiPSC lines. The expression of *OCT3/4* was significantly more downregulated and that of *NF-68* was significantly more upregulated in hESCs than hiPSCs. This would suggest more efficient neural differentiation among the hESC lines. However, line-specific gene expression results showed large variation within hESC and hiPSC lines. For example, the hESC line with lowest *OCT3/4* downregulation, Regea 08/023, was determined to differentiate most efficiently into neural lineage. On the other hand, the highest *NF-68* expression altogether was detected in the hiPSC line FIPS5-7. Thus, the significant differences between hESCs and hiPSCs could be due to the small number of cell lines in both groups.

Quantification of neural differentiation was initially performed based on morphology of the cells, but due to the confluency of the cultures, the amount of neurons could not be reliably determined (Study I). Thus MAP-2-positive cell coverage, relative to the amount and spreading of neurons in the cultures, was measured. The highest coverage was detected with the hESC line Regea 08/023 and the lowest with hiPSC line UTA.01006.WT. This was consistent with the qualitative immunocytochemical analyses. No difference in MAP-2-positive cell coverage was detected between hESC and hiPSC groups.

We concluded that although cell line-specific variations were detected, hESC and hiPSC lines show no systematic differences regarding their neural differentiation potential. Similar results were previously reported, indicating that cell line-specific

variation in neural differentiation potential cannot be explained by the origin of the cells (Kim et al. 2010, Boulting et al. 2011, Morizane et al. 2011, Falk et al. 2012). Both hESC and hiPSC lines have been demonstrated to have innate differentiation propensities towards specific germ layers or cell lineages, but the underlying molecular mechanisms remain partly unresolved (Boulting et al. 2011, Osafune et al. 2008).

In this study, neural differentiation method including spontaneous formation of neurospheres and differentiation in suspension cultures were used. Neural differentiation was not profusely induced in the culture system, and thus line-specific innate differentiation propensities could have a major effect on the neural differentiation efficiency. Although stronger chemical induction, such as dual-SMAD inhibition via media supplementation, has been reported to overcome the innate differentiation propensity, this is unlikely to standardize neural differentiation efficiency with all hiPSC lines (Chambers et al. 2009, Kim et al. 2010, Boulting et al. 2011). In conclusion, the origin of the cells does not define how a specific cell line can be utilized, but hiPSC lines should be carefully selected for specific research applications based on their intended use. Gene expression signature of undifferentiated hiPSCs, for example, currently enable predictive characterization of hiPSC lines, but additional methods such as proteomics or miRNA expression could also be utilized for evaluation of hiPSC lines in the future (Tsankov et al. 2015).

6.1.2 Transgene expression of hiPSC lines

In Study I, incomplete silencing of the *KLF4*-transgene in the hiPSC line UTA.01006.WT was detected. The cell line was derived using retroviral vectors and incomplete transgene silencing is a noted risk factor related to genomic integration of the transgenes (Hu 2014). UTA.01006.WT also showed inefficient differentiation towards all studied lineages, most likely due to the persistent expression of *KLF4*. Nevertheless, the correlation between incomplete transgene silencing and inefficient differentiation of hiPSCs is not necessarily as straightforward since Boulting and colleagues have reported efficient neural differentiation of hiPSCs despite having persistent expression of *KLF4* and *OCT3/4* transgenes (Boulting et al. 2011).

Moreover, transgene reactivation of *OCT3/4*, *NANOG*, and *LIN28* were detected during RPE differentiation in the retrovirally derived hiPSC lines. Reactivation of any of these transgenes was not detected with other differentiation protocols. The long and rather spontaneous differentiation towards RPE cells could

have caused transgene reactivation, as opposed to the shorter protocols for neural, cardiac, and hepatocyte differentiation. Since reactivation could also be related to genomic integration of the transgenes, an additional hPSC line HEL24.3, derived using Sendai-virus, was tested for RPE differentiation. Interestingly, transgene reactivation was not detected during differentiation of HEL24.3. In previous studies, the reactivation of reprogramming factors has been shown to cause dysplasia and tumor formation in mice (Hochedlinger et al. 2005, Markoulaki et al. 2009). The gene expression profiles of hPSC lines free of reprogramming factors have also been reported to be more closely related to hESCs than hPSCs carrying the transgenes (Soldner et al. 2009). Thus, generation of hPSC lines for future studies, especially for clinical applications, should be preferably performed using non-integrating or excisable vectors.

6.2 Differentiation of the central nervous system cells from hPSCs

6.2.1 Neurons and astrocytes

Neural differentiation was performed in our studies using a suspension culture method with FGF2-based neural induction (Study **I**, **III**, **IV**). The cells were cultured as spontaneously formed neurospheres, and prolonged culturing under these conditions led to the differentiation of astroglia-enriched populations. The majority of experiments were performed using Regea 08/023, as this hESC line demonstrated a high neural differentiation propensity (Study **I**). The proportion of neural cells in the differentiated populations was almost 80% on average (Study **III**). Our group had previously reported similar efficiencies with this differentiation method using other hESC lines (Lappalainen et al. 2010).

Astrocyte differentiation was not directly induced during the differentiation process, and the efficiency varied between batches of cells. The median proportion of GFAP-positive cells in the cultures was between 20 and 45% (unpublished data). However, astrocytes are a heterogeneous population; and although GFAP is a definitive astrocytic marker, it is not expressed by all astrocytes (Sofroniew and Vinters 2010). Thus, the proportion of astrocytes in our cultures are most likely higher than the numbers presented above. This was demonstrated in Study **IV**, when the astrocytes were double labeled with GFAP and S100 β . Although the

immunocytochemical staining was not quantified, high numbers of cells positive for S100 β but not for GFAP, were detected.

In conclusion, FGF2-induced neuronal differentiation in suspension cultures is generally efficient. However, the production of astrocytes could be enhanced by addition of growth factors directing the cell fate towards the astroglial lineage or by purification of the astrocytic population (Krencik et al. 2011, Holt and Olsen 2016).

6.2.2 OPCs and oligodendrocytes

The second aim of this thesis was to develop a differentiation protocol for hPSC-derived OPCs and oligodendrocytes (Study **II**). In previous studies, oligodendrocyte differentiation from hPSCs has been described in chemically defined culture conditions (Douvaras and Fossati 2015). Moreover, OPCs produced from hPSCs using animal-derived components have also been used in clinical trials with no reports of adverse effects (Lukovic et al. 2014). Preclinical data investigating the transplantation of these cells, however, revealed formation of small spinal cysts, which did not cause apparent clinical symptoms (Priest et al. 2015). Thus, further development of differentiation methods is needed to establish the production of OPCs and oligodendrocytes from hPSCs for clinical applications under Good Manufacturing Practice (GMP) standards.

In our study, the XF-NSC-supplement StemPro was used for xeno-free and defined culture media, and was compared to corresponding xenogeneic conditions including for example B27 supplement (Study **II**). The most efficient differentiation was induced by the administration of RA, SHH, EGF, bFGF, IGF-1, PDGF-AA, T3, AA, and LN in a temporally defined manner. As described in chapter 2.2.3, RA and SHH were used for regional and lineage specification; EGF and bFGF for neuralization and proliferation; PDGF-AA and IGF-1 for proliferation and oligodendrocyte fate decision; and finally, T3 in combination with mitogen withdrawal for OPC maturation. In addition, AA and LN were used to promote oligodendrocyte differentiation, survival, and myelination (Glaser et al. 2007, Relucio et al. 2009). All these components have been previously used for human oligodendrocyte differentiation (Nistor et al. 2005, Kang et al. 2007, Hu et al. 2009, Sundberg et al. 2010, Douvaras et al. 2014). Compared to the conditions with reduced growth factors (NS1.1-NS3.1 and XF1.1-XF3.1), enhanced NG2 and O4 expressions at stage 2 and stage 3, respectively, were detected with the addition of RA, T3, AA, and SHH. However, the effect of these growth factors was not studied

individually. Addition of CNTF with the above factors did not increase the efficiency of oligodendrocyte differentiation any further, although previous studies had demonstrated CNTF induced *Olig2* expression, survival and differentiation of OPCs (Talbot et al. 2007, Sundberg et al. 2010).

The production of hPSC-derived cells for clinical applications also requires the derivation and maintenance of hPSC lines under GMP-conditions (Tannenbaum et al. 2012). Furthermore, as discussed in Chapter 6.1. non-integrating methods for hPSC generation should be preferred for clinical applications. Recently, the efficient differentiation of OPCs from hPSCs generated using an episomal plasmid approach or Sendai-virus have been reported to circumvent the problems of genomic integration (All et al. 2015, Livesey et al. 2016).

While the production of OPCs and oligodendrocytes for research purposes would ideally be performed under the same defined and xeno-free conditions developed for clinical applications, this was restricted in our studies due to the high costs of xeno-free differentiation. Thus, xenogeneic compounds were used, and SHH was omitted from the differentiation media in Study **IV** (Hyysalo and Narkilahti 2015). Although importance of SHH signaling for OPC induction has previously been stated, removing SHH had no detectable effect on differentiation efficiency in our study (Lu et al. 2000, Hu et al. 2009). This could be explained by the fact that during *in vivo* development OPCs are generated in distinct stages and locations (Gallo and Deneen 2014). Studies in mouse models have shown that in addition to their origin in the ventral spinal cord, OPCs are generated in dorsal neural tube independently of SHH signaling (Cai et al. 2005, Vallstedt et al. 2005). Furthermore, neural stem cells isolated from murine dorsal spinal cord can generate oligodendrocytes *in vitro* in the absence of SHH (Chandran et al. 2003). In addition to cost-reducing modifications, LDN193189 was used to enhance differentiation into the neural precursor lineage in Study **IV** (Chambers et al. 2016). This approach, mostly in combination with SB431542, has previously been utilized for the initiation of oligodendrocyte differentiation (Douvaras et al. 2014, Piao et al. 2015, Livesey et al. 2016).

Our results demonstrate that efficient differentiation of OPCs was successful in both xeno-free and modified xenogeneic conditions. Maturation of the OPCs into oligodendrocytes, however, was induced at varying efficiencies. Additional growth factors and alterations to the modified xenogeneic differentiation protocol have been studied in order to stabilize the maturation stage, with no considerable effect (unpublished data). However, previous studies have demonstrated that OPCs transplanted into the shiverer model of dysmyelination can differentiate into

myelinating oligodendrocytes *in vivo* (Hu et al. 2009, Wang et al. 2013). Oligodendrocyte production *in vitro* has generally been a result of long-term differentiation (Hu et al. 2009, Sundberg et al. 2010, Stacpoole et al. 2013, Wang et al. 2013). This is consistent with *in vivo* development, since oligodendrocytes are the last major CNS cells to form and OPCs in the fetal human forebrain are not detected until gestational week 16 (Sim et al. 2011). Our protocols were substantially shorter, and this might have negatively influenced the maturation process of the oligodendrocytes. Previously published protocols have reported a wide range of differentiation efficiencies for the derivation of O4 and MBP-positive cells (Alsanie et al. 2013, Ogawa et al. 2011, Pouya et al. 2011, Stacpoole et al. 2013, Piao et al. 2015, Douvaras and Fossati 2015). However, since a majority of these protocols were used exclusively in one laboratory, the reproducibility of the methods is challenging to assess.

Purification of the differentiated OPC population has been performed by sorting with fluorescence- and magnetic-associated cell sorting (FACS and MACS, respectively) (Sundberg et al. 2010, Douvaras and Fossati 2015, All et al. 2015, Livesey et al. 2016). We have applied FACS for the purification of NG2-positive cells from OPC populations differentiated using xeno-free and further modified xenogeneic method (Study II, Hyysalo and Narkilahti 2015). Notably, NG2 is not a definitive marker of the oligodendrocytic lineage, and NG2-positive cells have the potential to further differentiate into other cell types in addition to myelinating oligodendrocytes (Richardson et al. 2011). Other markers that are generally used for the purification of the OPC population are A2B5 and platelet-derived growth factor receptor α (PDGF- α). Additionally, O4 can be applied for the purification of more lineage-restricted OPCs and oligodendrocytes, but the expansion capacity of these cells is more restricted (Goldman and Kuypers 2015).

In conclusion, OPCs can be efficiently produced from hPSCs under xeno-free and xenogeneic culture conditions, but further maturation of the cells into oligodendrocytes *in vitro* should be stabilized and enhanced. Recent development in the field of hPSC-derived oligodendrocyte production indicate increasing role for genetic modifications targeting hPSC differentiation in the future. Pawlowski and colleagues were the first to describe direct conversion or “forward programming” of hPSCs into oligodendrocytes by using genetic modification. Induced expression of Olig2 and SOX10 produced mature CNP/MBP -positive phenotype after 20 days of induction in oligodendrocyte differentiation medium (Pawlowski et al. 2017). Development of the induced cells is considerably faster and more efficient compared to differentiation based on chemically defined media alone, however, questions

concerning for example functionality of the produced cells *in vivo* remain to be resolved.

6.3 Effect of defined laminin substrates on *in vitro* culturing of hPSC-derived neural cells

6.3.1 Supporting growth of neurons and astrocytes with specific laminin substrates

The third aim of this thesis was to study how defined ECM substrates influence the behavior of hPSC-derived CNS cells *in vitro* (Study **III**, **IV**). For this, commercially available laminin isoforms were used for culturing hPSC-derived neurons and astrocytes. Previous studies investigating the growth of murine-derived neurons on different laminin isoforms showed that LN511 was most efficiently able to support neuronal growth *in vitro* (Plantman et al. 2008, Fusaoka-Nishioka et al. 2011). However, similar comparisons had not been performed with human cells or other CNS cell types. In our study LN211, LN332, LN411, and LN511 substrates were compared for culturing hPSC-derived neurons and astrocytes on a 2D polystyrene surface. The most efficient cell attachment, viability, spreading, and network formation was detected on LN511 with both cell types. These data were consistent with the previous results gained with murine cells (Plantman et al. 2008, Fusaoka-Nishioka et al. 2011).

In addition, the laminin isoform LN521, which structurally closely resembles LN511, and the E8 fragment of LN511 were studied. Although both substrates have been previously used for the production of hPSC-derived neurons, direct comparison in the same culture conditions had not been reported (Lu et al. 2014, Nakagawa et al. 2014, Doi et al. 2014, Nishimura et al. 2016). Systematic differences between cultures on LN511, LN521, and LN511-E8 were not detected with either cell type. Furthermore, similar result were obtained on PCL nanofiber platforms coated with these substrates. hPSC-derived neurons and astrocytes attached and oriented according to fiber alignment efficiently on all substrates. Our results thus indicate that $\alpha 5$ laminin substrates are equally supportive for culturing hPSC-derived neurons and astrocytes, and show that $\alpha 5$ laminin substrates can also be used in combination with PCL nanofibers.

Defined and xeno-free culturing substrates that enable efficient production and maintenance of human CNS cells facilitate the clinical applications of hPSC-derived neural cells. Our unpublished observations along with previous reports demonstrate that laminin $\alpha 5$ substrates can be used for the maintenance of hPSCs on feeder-free conditions (Rodin et al. 2010, Rodin et al. 2014b, Miyazaki et al. 2012, Nakagawa et al. 2014, Kele et al. 2016). Here, the effect of defined laminin substrates for attachment and growth of the differentiated neurons and astrocytes was studied, whereas in adherent differentiation conditions, selectively supportive laminin substrates can also be used to enhance neural differentiation from hPSCs (Kirkeby et al. 2017).

6.3.2 Functional development of neuronal networks

Since electrophysiological activity is a crucial feature for *in vitro* cultured neurons, the functional development of hPSC-derived neuronal networks on different laminin substrates was studied (Illes et al. 2007, Study III). We showed that the proportions of active electrodes were substantially higher in neuronal cultures on laminin $\alpha 5$ substrates than in cultures on other isoforms or control substrates. This is an indication of more efficiently distributed networks of electrophysiologically active neurons.

Interestingly, the proportion of burst detecting electrodes in cultures with LN521 was significantly higher compared to that in cultures with LN511 or LN511-E8. In general, the factors and mechanisms affecting the functionality of neuronal network are remotely characterized, and so it could not be concluded whether the detected difference in functional maturation was due to the normal heterogeneity of the hPSC-derived neuronal networks or actually caused by the culture substrate. We speculated that the specific laminin isoform could, via an undefined receptor, affect cell signaling and enhance the functional maturation of hPSC-derived neurons. Previously, alterations in neuronal culture conditions *in vitro*, such as cell density, have been shown to reflect neuronal network activity (Wagenaar et al. 2006, Biffi et al. 2013). Due to the lack of prior studies on the effect of defined laminin isoforms on neuronal functionality, additional experiments are needed to confirm the results and address these questions. Furthermore, enhancement of the functional development *in vitro* would be beneficial for the production of hPSC-derived neurons for applications in regenerative medicine.

6.4 Effect of mechanically altered environment on *in vitro* culturing of hPSC-derived neural cells

6.4.1 Guiding cell orientation with nanofibers in 2D culture conditions

The fourth aim of this thesis was to study how mechanical alterations of the culture conditions affect the behavior of hPSC-derived neurons, astrocytes and OPCs. The differentiated neural cells were cultured on commercially available aligned PCL-nanofiber platforms (Study IV). The neurons and astrocytes did not survive or spread well on bare nanofiber surfaces, but the cell viability and growth were rescued by ECM protein coating on nanofibers. Our results demonstrated that defined laminin substrates could be used to considerably enhance the growth of hPSC-derived neurons and astrocytes on PCL nanofibers. Importantly, neurons and astrocytes were clearly oriented according to the fiber alignment. Similar results have been reported with primary murine neurons and astrocytes and with hPSC-derived NPCs and neurons (Lam et al. 2010, Mahairaki et al. 2011, Qu et al. 2013, Bourke et al. 2014, Xia et al. 2014). Previously, ECM proteins, mainly laminin, have been used to enhance cell viability and migration on nanofiber surfaces (Han and Cheung 2011). However, laminin-coating is not beneficial with all fiber materials, and uniform laminin-coating on 2D nanofiber surface might even reduce the guiding effect of the nanofibers (Ylä-Outinen et al. 2010, McMurtrey 2014). Thus, ECM proteins or other molecules should already be incorporated onto the nanofibers at the fabrication stage to improve the functionalization of the fibers (Rivet et al. 2015).

Interestingly, the behavior of OPCs on nanofiber surfaces was not affected by ECM protein coating. However, OPCs were also detected to follow the fiber alignment, and O4-positive cells elongated their processes along single fibers. Some of these cells also expressed MBP. Primary rat OPCs have been shown to mature into oligodendrocytes and myelinate nanofibers *in vitro* (Lee et al. 2012). This aspect was studied in our cultures using immunocytochemistry as well as scanning and transmission electron microscopy, but no myelination was detected even after long-term (8-weeks) culturing (unpublished data). Myelination has previously been demonstrated to occur in both activity-dependent and activity-independent manners (Lundgaard et al. 2013). Myelination of synthetic nanofibers represents activity independent myelination, and this can be utilized for studying myelination mechanisms *in vitro* (Bechler et al. 2015). However, activity independent myelination of the nanofibers is not beneficial for clinical applications, as the oligodendrocytes

are intended to preferentially myelinate axons of the host tissue or co-transplanted neurons. PCL nanofiber platforms with graphene oxide coating have also been demonstrated to direct differentiation of oligodendrocytes from rat NPCs without chemical induction in the culture media (Shah et al. 2014). The use of nanofiber platforms for the enhancement of oligodendrocyte differentiation and maturation would be an appealing approach, but thus far such phenomenon has not been demonstrated with human cells.

In conclusion, our study showed that all hPSC-derived CNS cells were successfully cultured and oriented on the nanofiber platforms. These culture conditions mimic *in vivo* structures of the spinal cord and can be utilized for *in vitro* modeling and clinical applications aimed towards SCI repair.

6.4.2 Nanofiber guided neuronal orientation in 3D culture conditions

Nanofiber-induced orientation of hPSC-derived neurons was further studied in 3D conditions by combining PCL nanofibers with commercial Puramatrix hydrogel (Study IV). Our results showed that neurons encapsulated within the 3D hydrogel close ($<10\ \mu\text{m}$) to the nanofiber surface followed the fiber alignment. However, the neurons farther away from the nanofiber surface or on top of the hydrogel surface did not detect the nanofibers, resulting in random cellular orientation. Although previous studies investigating the behavior of neural cells on nanofiber-hydrogel scaffolds are very limited, our results are supported by the observations of McMurtrey, who demonstrated orientation of human neuroblastoma-derived cells on PCL nanofibers in hyaluronic acid hydrogel (McMurtrey 2014). Previously, successful culturing and orientation of murine primary astrocytes and OPCs was performed with nanofibers in type I collagen hydrogel (Weightman et al. 2014). However, in this study the survival, maturation and orientation of OPCs was dependent on co-culturing with astrocytes. Similar to the platform used in our experiments, these studies also utilized planar nanofiber mesh embedded into 3D hydrogel.

Structures with more uniform distribution of nanofibers within hydrogels have been achieved by combining fragmented nanofibers with hydrogel prior to polymerization (Hsieh et al. 2010). Primary rat NPCs were cultured in these scaffolds and survival, proliferation, and differentiation of the cells were demonstrated. However, this approach resulted in random alignment of the fiber fragments within the hydrogel. Shelke and colleagues used different approach by utilizing aligned

nanofiber lattice as a core of the scaffold (Shelke et al. 2016). The lattice was dipped in hydrogel solution and the cells were seeded to the surface of the scaffold after polymerization. hPSCs and hMSCs were cultured on these scaffolds in neural differentiation medium. Nevertheless, the neural differentiation and cell infiltration into the scaffolds were not extensively characterized.

In conclusion, our data demonstrated that hPSC-derived neurons can be oriented with nanofibers in a 3D hydrogel environment. The behavior of other human CNS cells in such conditions remains to be studied. Moreover, further development of the fabrication of feasible 3D nanofiber-hydrogel scaffolds is required.

6.5 Future perspectives

The field of stem cell research is still relatively new but rapid development during the recent years have already led into clinical trials with variety of patients suffering from previously incurable diseases (Trounson and DeWitt 2016). Ongoing clinical trials on stem cell transplantations for SCI repair are mostly based on autologous MSCs (<https://clinicaltrials.gov>). These cells are not directed towards the neural lineage, but they secrete trophic factors and support axonal regeneration (Ide and Kanekiyo 2016). Thus far, only few clinical trials with hESC- or fetal-derived neural stem cells are ongoing, aiming to replace the damaged tissue with exogenous neural cells. The important question of similarity between hESCs and hIPSCs also reflects to their clinical utilization. In this thesis, we studied differentiation propensity of several hESC and hIPSC lines and found no systematic difference between hPSC lines of different origins. Currently, no hIPSC-derived neural cells are included in clinical trials for SCI repair but patient-specific hIPSCs and their derivatives are increasingly gaining attention as they provide an opportunity for personalized medicine applications (Ferreira and Mostajo-Radji 2013). Although deriving and testing tailored cells individually for every patient is currently too expensive, slow, and uncertain, hIPSC-technology innovator Shinya Yamanaka is pioneering this field and aiming for establishing a hIPSC bank in Japan. Selection of hIPSC lines for clinical applications would enable more efficient production of transplantable cells and matching donors to recipients with human leukocyte antigens (HLAs) risk of immune rejection could be minimized. (Cyranoski 2012) Furthermore, clinical trial with hIPSC-derived RPE cells is already ongoing, but the trial protocol was revised after identification of several mutations in the patient's iPSCs (Garber 2015, <http://www.nature.com/news/japanese-man-is-first-to-receive-reprogrammed->

stem-cells-from-another-person-1.21730). Genetic abnormalities like mutations, incomplete transgene silencing, or transgene reactivation detected in our study (Study I) are related to reprogramming process. Thus, and as clinical utilization of hIPSCs is constantly increasing, the importance of thorough characterization of the pluripotent as well as differentiated cells is emphasized in order to minimize the adverse effects following transplantation.

As previously discussed, production of neural cells for transplantation purposes should be performed under xeno-free and defined culture conditions. Xenogenic contaminations, such as micro-organisms or non-human bioactive molecules, can result to infection or immune rejection after transplantation (Qian et al. 2013). Development of xeno-free culture protocols has been facilitated by availability of humanized and more defined cell culture media and chemical components, like B27 supplement, in addition to cell culture substrates such as recombinant human laminins used in this thesis. Thus far, production of GMP-grade hPSC-derived neurons have been published and in this thesis we have described hPSC-derived OPC differentiation under xeno-free conditions (Kirkeby et al. 2017, Study II).

Clinical trials utilizing stem cell-derived neural cells for SCI repair have shown positive results from safety studies (see Chapter 2.4.2). However, the efficacy of these transplantation therapies have not yet been reported. Previously, the integration of cells and biomaterial scaffolds have been used in preclinical studies to enhance cell viability and guide the functional development and integration into the host tissue following transplantation (Kumar et al. 2015). The scaffold materials can also be incorporated with immunosuppressants, anti-inflammatory substances, or growth factors to enhance cell survival and growth (Wang et al. 2012b, Cook et al. 2016, Yasui et al. 2016). Nevertheless, only one ongoing clinical trial combines neural cells with a supporting biomaterial scaffold (NCT02688049). In this thesis, hPSC-derived CNS cells were cultured on clinically relevant culture substrates and nanofiber platforms, resulting in a robust guiding effect on cell orientation *in vitro*. Furthermore, neuronal orientation was also induced by nanofibers in a 3D hydrogel environment.

Three-dimensional nanofiber-hydrogel scaffolds combine the permissive environment of a hydrogel with the cell guiding feature of nanofibers. Such scaffolds can be fully constructed *in vitro* by spinning a 3D lattice of nanofibers and then polymerizing hydrogel around the lattice (Shelke et al. 2016). Ideally, the cell suspension would be combined with the hydrogel prior to polymerization to ensure even distribution of the cells in the scaffold. This approach would require a surgical procedure for placing the scaffold at the injury site. Xiao and colleagues have also

reported scar tissue resection from the injury site when transplanting the scaffold in order to enhance integration of the transplanted cells (Xiao et al. 2016). However, such a procedure poses a risk of further damaging neural functions. Another option for transplantation would be to prepare injectable fibers and combine them with hydrogel in cell suspension (Rivet et al. 2015). Although placing the scaffold at the injury site would be less invasive in this way, it would also allow less control over the polymerization of the hydrogel. In addition, the alignment of the injectable fibers is challenging. In the future, substances such as shape-memory polymers or slidable, injectable, and gel-like (SLIDING) fibers could provide options for the alignment of injected nanofibers in the future (Meng and Li 2013, Lee et al. 2016).

Biomaterial scaffolds of nanofibers, hydrogels and combinations of hydrogel and guiding structures are being used for SCI repair also without the additional cell component (Kaneko et al. 2015, Rivet et al. 2015, Bozkurt et al. 2016, Cook et al. 2016, <https://clinicaltrials.gov; NCT02510365>). Preclinical studies in animal models have demonstrated neuronal regeneration and functional recovery in SCI models following transplantation of these scaffolds. However, thus far these results have not been translated into human SCI patients and due to the limited regeneration potential of adult CNS, addition of exogenous neural cells is considered to enhance regeneration and recovery (Subramanian et al. 2009).

In conclusion, several aspects need to be considered when designing tissue engineering products for clinical applications. The results presented in this thesis provide new insights and tools for developing functional cell grafts for SCI repair.

7 Conclusions

This thesis focused on studying various aspects, including the genetic background and chemical and mechanical induction of hPSC-derived CNS cell differentiation and behavior *in vitro*. Obtained knowledge was aimed to be applicable for developing tissue engineering products for SCI repair. Based on the results of this thesis, the following conclusions can be drawn:

1. hPSCs have cell line-specific capacities for neuronal differentiation, but the variation between individual hESC and hIPSC lines is greater than the variation between cell lines of different origins. Furthermore, the generation of hIPSC lines for future studies should be performed using non-integrating or excisable vectors to decrease transgenic instability.
2. Chemical induction can be used for differentiation of hPSC-derived OPCs and oligodendrocytes. Similar induction methods can be applied for oligodendrocyte differentiation in xenogeneic conditions for non-clinical studies and xeno-free and defined conditions for clinical grade applications. The efficient differentiation of OPCs was achieved with both protocols, while maturation of the cells into oligodendrocytes should be further stabilized and enhanced.
3. Xeno-free and defined $\alpha 5$ laminin ECM-components are supportive culture substrates for hPSC-derived neurons and astrocytes. These substrates can be used as platforms for efficient production of clinical grade neural cells from hPSCs, and can also be combined with PCL nanofibers to create more *in vivo*-like culture conditions for CNS cells.
4. hPSC-derived CNS cells can be cultured and oriented in nanofiber-based *in vitro* conditions mimicking the *in vivo* structure of the spinal cord. hPSC-derived neurons can also be oriented with nanofibers in a 3D hydrogel environment.

5. The novel combination of human-derived main CNS cell types, clinically relevant ECM substrates, the 3D environment of the hydrogel and guiding features of the nanofibers can be further applied for the development of functional cell grafts for SCI repair.

Acknowledgements

The research for this thesis was carried out at the Institute of Biosciences and Medical Technology (BioMediTech), University of Tampere. I wish to thank all those people who contributed to the experimental work and helped and advised me in my work during these years.

I would like to thank the Finnish Funding Agency for Technology and Innovation (Tekes), Tampere Graduate Programme in Biomedicine and Biotechnology (TGPBB), The Finnish Cultural Foundation (Central Foundation, as well as Satakunta and Pirkanmaa Regional Funds), The Finnish MS Foundation, Brain Research Society of Finland, European Science Foundation, and the City of Tampere for financially supporting my research and journeys to international conferences around the world.

I want to express my gratitude to my supervisor Docent Susanna Narkilahti. You gave me the opportunity to work in our research group and helped me to grow as a researcher but also as a person during these years. You are an exceptional person and boss who always fully believed and trusted me. I also wish to acknowledge the members of my follow-up group; Professor Karin Forsberg Nilsson and Associated Professor Heli Skottman for your valuable comments, support, and discussions at the annual meetings during these years. Furthermore, I owe my sincere gratitude to Professor Cecilia Sahlgren and Professor Meng Li for reviewing my thesis and providing critical comments and suggestions to improve the quality of this work.

I wish to thank all my co-authors; Sanna Toivonen, Marisa Ojala, Tanja Ilmarinen, Karolina Lundin, Jaan Palgi, Jere Weltner, Ras Trokovic, Kristiina Rajala, Mari Pekkanen-Mattila, Riikka Äänismaa, Olli Silvennoinen, Heli Skottman, Katriina Aalto-Setälä, Timo Otonkoski, Maria Sundberg, Soojung Shin, Mohan Vemuri, Riitta Suuronen, Mervi Ristola, Meeri Mäkinen, Sergei Häyrynen, Matti Nykter, Tiina Joki, Mari Honkanen, Minnamari Vippola. Without your contribution this work would not have been possible to accomplish.

From all my heart I want to thank the past and the present members of NeuroGroup. It has been a privilege to work with you and also share some non-work related experiences. I owe special thanks to Mervi Ristola, for working with me and guiding me during the last two projects in my thesis. You have taught me so

much from planning the experiments all the way to publishing the results. You were always there for me, regardless of the time or the crisis, and somehow you always made me feel better and keep going on. I also want to thank Laura Ylä-Outinen, for your scientific and mental support in all my projects, even though you were not responsible for my work. You are also always kind and cheerful, and turn me into good mood. Mervi and Laura, you both provided me invaluable support during the thesis writing. Thank you for reading and commenting on my text, it was extremely important for me. Riikka Äänismaa, you were my first supervisor in NeuroGroup and I have received your help, advises, and support ever since, all the way to my thesis writing even though you no longer work with us. Other PhD students in the NeuroGroup; Tanja Paavilainen, Tiina Joki, and Meeri Mäkinen, I would have been lost without your peer support, scientific expertise, and our countless discussions in order to improve the world. I have found amazing friends from all of you!

Maarit Patrikainen, Hanna Mäkelä, Eija Hannuksela, and Juha Heikkilä are warmly thanked for their technical guidance and assistance in the lab. You always had time for me and my questions or demands, and I truly appreciate that. In addition, Hanna you have also been literally holding my life in our hands countless times during these years! I would also like to acknowledge Hanna Pekkanen, Outi Melin, and Outi Heikkilä for all the pluripotent cells you have provided me during these years.

I wish to thank my coworkers in BioMediTech for all the “Super Fun Time Committee” activities and brilliant discussions over the coffee table. Furthermore, Heini Huhtala and Outi Paloheimo are acknowledged for valuable advice and instructions concerning statistical analyses and the outstanding artwork for my last publication and for my thesis, respectively.

I am grateful for all my friends and relatives, especially Toni, Tiru, Ilari, Minna, Kaisu, Kaisa, Tero, Tuomas, and Jenna for peer support and on the other hand healthy perspective for life. My family and the precious other halves Maria, Timo, Noora, Tuomas, Juho, and Ida are thanked for their endless support and trust in me. You all remind me that there is more to life than work and science.

Finally, I would like to thank Antti for everything you have done and enabled for me during these years. You have been my bedrock, and luckily understand the life of a scientist with the ultimate heights and depths.

Tampere, April 2017



References

All AH, Gharibani P, Gupta S et al (2015) Early intervention for spinal cord injury with human induced pluripotent stem cells oligodendrocyte progenitors. *PLoS One* 10(1):e0116933. doi:10.1371/journal.pone.0116933 [doi].

Alsanie WF, Niclis JC, Petratos S (2013) Human embryonic stem cell-derived oligodendrocytes: protocols and perspectives. *Stem Cells Dev* 22(18):2459-2476. doi:10.1089/scd.2012.0520 [doi].

American Spinal Injury Association. Available at: <http://asia-spinalinjury.org>. Accessed April 26 2017.

Anderson AJ, Piltti KM, Hooshmand MJ et al (2017) Preclinical Efficacy Failure of Human CNS-Derived Stem Cells for Use in the Pathway Study of Cervical Spinal Cord Injury. *Stem Cell Reports* 8(2):249-263. doi:S2213-6711(16)30308-3 [pii].

Armstrong RC, Dorn HH, Kufta CV et al (1992) Pre-oligodendrocytes from adult human CNS. *J Neurosci* 12(4):1538-1547.

Asterias Biotherapeutics. Available at: <http://asteriasbiotherapeutics.com/AST-OPC1.php>. Accessed April 26 2017.

Aumailley M, Bruckner-Tuderman L, Carter WG et al (2005) A simplified laminin nomenclature. *Matrix Biol* 24(5):326-332. doi:S0945-053X(05)00065-X [pii].

Baiguera S, Del Gaudio C, Fioravanzo L et al (2010) In vitro astrocyte and cerebral endothelial cell response to electrospun poly(epsilon-caprolactone) mats of different architecture. *J Mater Sci Mater Med* 21(4):1353-1362. doi:10.1007/s10856-009-3944-5 [doi].

Barateiro A, Fernandes A (2014) Temporal oligodendrocyte lineage progression: in vitro models of proliferation, differentiation and myelination. *Biochim Biophys Acta* 1843(9):1917-1929. doi:10.1016/j.bbamcr.2014.04.018 [doi].

Baxi EG, Schott JT, Fairchild AN et al (2014) A selective thyroid hormone beta receptor agonist enhances human and rodent oligodendrocyte differentiation. *Glia* 62(9):1513-1529. doi:10.1002/glia.22697 [doi].

Bechler ME, Byrne L, Ffrench-Constant C (2015) CNS Myelin Sheath Lengths Are an Intrinsic Property of Oligodendrocytes. *Curr Biol* 25(18):2411-2416. doi:10.1016/j.cub.2015.07.056 [doi].

Biffi E, Regalia G, Menegon A et al (2013) The influence of neuronal density and maturation on network activity of hippocampal cell cultures: a methodological study. *PLoS One* 8(12):e83899. doi:10.1371/journal.pone.0083899 [doi].

Bonneh-Barkay D, Wiley CA (2009) Brain extracellular matrix in neurodegeneration. *Brain Pathol* 19(4):573-585. doi:10.1111/j.1750-3639.2008.00195.x [doi].

Bosworth LA, Turner LA, Cartmell SH (2013) State of the art composites comprising electrospun fibres coupled with hydrogels: a review. *Nanomedicine* 9(3):322-335. doi:10.1016/j.nano.2012.10.008 [doi].

Boulting GL, Kiskinis E, Croft GF et al (2011) A functionally characterized test set of human induced pluripotent stem cells. *Nat Biotechnol* 29(3):279-286. doi:10.1038/nbt.1783 [doi].

Bourke JL, Coleman HA, Pham V et al (2014) Neuronal electrophysiological function and control of neurite outgrowth on electrospun polymer nanofibers are cell type dependent. *Tissue Eng Part A* 20(5-6):1089-1095. doi:10.1089/ten.TEA.2013.0295 [doi].

Bozkurt A, Boecker A, Tank J et al (2016) Efficient bridging of 20 mm rat sciatic nerve lesions with a longitudinally micro-structured collagen scaffold. *Biomaterials* 75:112-122. doi:10.1016/j.biomaterials.2015.10.009 [doi].

Burnside ER, Bradbury EJ (2014) Manipulating the extracellular matrix and its role in brain and spinal cord plasticity and repair. *NeuroPathol Appl Neurobiol* 40(1):26-59. doi:10.1111/nan.12114 [doi].

Buxboim A, Rajagopal K, Brown AE et al (2010) How deeply cells feel: methods for thin gels. *J Phys Condens Matter* 22(19):194116. doi:10.1088/0953-8984/22/19/194116 [doi].

Cai J, Qi Y, Hu X et al (2005) Generation of oligodendrocyte precursor cells from mouse dorsal spinal cord independent of Nkx6 regulation and Shh signaling. *Neuron* 45(1):41-53. doi:S0896627304008335 [pii].

Cao H, Liu T, Chew SY (2009) The application of nanofibrous scaffolds in neural tissue engineering. *Adv Drug Deliv Rev* 61(12):1055-1064. doi:10.1016/j.addr.2009.07.009 [doi].

Carlson AL, Bennett NK, Francis NL et al (2016) Generation and transplantation of reprogrammed human neurons in the brain using 3D microtopographic scaffolds. *Nat Commun* 7:10862. doi:10.1038/ncomms10862 [doi].

Carpenter AE, Jones TR, Lamprecht MR et al (2006) CellProfiler: image analysis software for identifying and quantifying cell phenotypes. *Genome Biol* 7(10):R100. doi:gb-2006-7-10-r100 [pii].

Carpenter MK, Inokuma MS, Denham J et al (2001) Enrichment of neurons and neural precursors from human embryonic stem cells. *Exp Neurol* 172(2):383-397. doi:10.1006/exnr.2001.7832 [doi].

Cefalo RC, Berghmans RL, Hall SP (1994) The bioethics of human fetal tissue research and therapy: moral decision making of professionals. *Am J Obstet Gynecol* 170(1 Pt 1):12-19. doi:S0002937894004114 [pii].

Chambers SM, Fasano CA, Papapetrou EP et al (2009) Highly efficient neural conversion of human ES and iPS cells by dual inhibition of SMAD signaling. *Nat Biotechnol* 27(3):275-280. doi:10.1038/nbt.1529 [doi].

Chambers SM, Mica Y, Lee G et al (2016) Dual-SMAD Inhibition/WNT Activation-Based Methods to Induce Neural Crest and Derivatives from Human Pluripotent Stem Cells. *Methods Mol Biol* 1307:329-343. doi:10.1007/7651_2013_59 [doi].

Chandran S, Kato H, Gerreli D et al (2003) FGF-dependent generation of oligodendrocytes by a hedgehog-independent pathway. *Development* 130(26):6599-6609. doi:10.1242/dev.00871 [doi].

Chandrasekaran A, Avci HX, Leist M et al (2016) Astrocyte Differentiation of Human Pluripotent Stem Cells: New Tools for Neurological Disorder Research. *Front Cell Neurosci* 10:215. doi:10.3389/fncel.2016.00215 [doi].

Chen G, Gulbranson DR, Hou Z et al (2011) Chemically defined conditions for human iPSC derivation and culture. *Nat Methods* 8(5):424-429. doi:10.1038/nmeth.1593 [doi].

Chun SJ, Rasband MN, Sidman RL et al (2003) Integrin-linked kinase is required for laminin-2-induced oligodendrocyte cell spreading and CNS myelination. *J Cell Biol* 163(2):397-408. doi:10.1083/jcb.200304154 [doi].

Cook DJ, Nguyen C, Chun HN et al (2016) Hydrogel-delivered brain-derived neurotrophic factor promotes tissue repair and recovery after stroke. *J Cereb Blood Flow Metab*. doi:0271678X16649964 [pii].

Cui QL, Fragoso G, Miron VE et al (2010) Response of human oligodendrocyte progenitors to growth factors and axon signals. *J Neuropathol Exp Neurol* 69(9):930-944. doi:10.1097/NEN.0b013e3181ef3be4 [doi].

Cyranoski D (2012) Stem-cell pioneer banks on future therapies. *Nature* 488(7410):139. doi:10.1038/488139a [doi].

Database of clinical trials conducted around the world. Available at: <https://clinicaltrials.gov>. Accessed April 26 2017.

Dhara SK, Stice SL (2008) Neural differentiation of human embryonic stem cells. *J Cell Biochem* 105(3):633-640. doi:10.1002/jcb.21891 [doi].

Doi D, Samata B, Katsukawa M et al (2014) Isolation of human induced pluripotent stem cell-derived dopaminergic progenitors by cell sorting for successful transplantation. *Stem Cell Reports* 2(3):337-350. doi:10.1016/j.stemcr.2014.01.013 [doi].

Domogatskaya A, Rodin S, Tryggvason K (2012) Functional diversity of laminins. *Annu Rev Cell Dev Biol* 28:523-553. doi:10.1146/annurev-cellbio-101011-155750 [doi].

Douvaras P, Fossati V (2015) Generation and isolation of oligodendrocyte progenitor cells from human pluripotent stem cells. *Nat Protoc* 10(8):1143-1154. doi:10.1038/nprot.2015.075 [doi].

Douvaras P, Wang J, Zimmer M et al (2014) Efficient generation of myelinating oligodendrocytes from primary progressive multiple sclerosis patients by induced pluripotent stem cells. *Stem Cell Reports* 3(2):250-259. doi:10.1016/j.stemcr.2014.06.012 [doi].

Du J, Tan E, Kim HJ et al (2014) Comparative evaluation of chitosan, cellulose acetate, and polyethersulfone nanofiber scaffolds for neural differentiation. *Carbohydr Polym* 99:483-490. doi:10.1016/j.carbpol.2013.08.050 [doi].

Edmondson R, Broglie JJ, Adcock AF et al (2014) Three-dimensional cell culture systems and their applications in drug discovery and cell-based biosensors. *Assay Drug Dev Technol* 12(4):207-218. doi:10.1089/adt.2014.573 [doi].

Engelhardt B (2003) Development of the blood-brain barrier. *Cell Tissue Res* 314(1):119-129. doi:10.1007/s00441-003-0751-z [doi].

Erceg S, Ronaghi M, Stojkovic M (2009) Human embryonic stem cell differentiation toward regional specific neural precursors. *Stem Cells* 27(1):78-87. doi:10.1634/stemcells.2008-0543 [doi].

Falk A, Koch P, Kesavan J et al (2012) Capture of neuroepithelial-like stem cells from pluripotent stem cells provides a versatile system for in vitro production of human neurons. *PLoS One* 7(1):e29597. doi:10.1371/journal.pone.0029597 [doi].

Ferreira LM, Mostajo-Radji MA (2013) How induced pluripotent stem cells are redefining personalized medicine. *Gene* 520(1):1-6. doi:10.1016/j.gene.2013.02.037 [doi].

Fortier LA (2005) Stem cells: classifications, controversies, and clinical applications. *Vet Surg* 34(5):415-423. doi:VSU00063 [pii].

Franze K, Janmey PA, Guck J (2013) Mechanics in neuronal development and repair. *Annu Rev Biomed Eng* 15:227-251. doi:10.1146/annurev-bioeng-071811-150045 [doi].

Fusaki N, Ban H, Nishiyama A et al (2009) Efficient induction of transgene-free human pluripotent stem cells using a vector based on Sendai virus, an RNA virus that does not integrate into the host genome. *Proc Jpn Acad Ser B Phys Biol Sci* 85(8):348-362. doi:JST.JSTAGE/pjab/85.348 [pii].

Fusaoka-Nishioka E, Shimono C, Taniguchi Y et al (2011) Differential effects of laminin isoforms on axon and dendrite development in hippocampal neurons. *Neurosci Res* 71(4):421-426. doi:10.1016/j.neures.2011.08.012 [doi].

Gallo V, Deneen B (2014) Glial development: the crossroads of regeneration and repair in the CNS. *Neuron* 83(2):283-308. doi:10.1016/j.neuron.2014.06.010 [doi].

Garber K (2015) RIKEN suspends first clinical trial involving induced pluripotent stem cells. *Nat Biotechnol* 33(9):890-891. doi:10.1038/nbt0915-890 [doi].

Genethliou N, Panayiotou E, Panayi H et al (2009) SOX1 links the function of neural patterning and Notch signalling in the ventral spinal cord during the neuron-glial fate switch. *Biochem Biophys Res Commun* 390(4):1114-1120. doi:10.1016/j.bbrc.2009.08.154 [doi].

Glaser T, Pollard SM, Smith A et al (2007) Tripotential differentiation of adherently expandable neural stem (NS) cells. *PLoS One* 2(3):e298. doi:10.1371/journal.pone.0000298 [doi].

Goldman SA, Kuypers NJ (2015) How to make an oligodendrocyte. *Development* 142(23):3983-3995. doi:10.1242/dev.126409 [doi].

Gonzalez F, Barragan Monasterio M, Tiscornia G et al (2009) Generation of mouse-induced pluripotent stem cells by transient expression of a single nonviral polycistronic

vector. *Proc Natl Acad Sci U S A* 106(22):8918-8922. doi:10.1073/pnas.0901471106 [doi].

Gopalakrishnan S, Hor P, Ichida JK (2015) New approaches for direct conversion of patient fibroblasts into neural cells. *Brain Res.* doi:S0006-8993(15)00749-0 [pii].

Gordon J, Amini S, White MK (2013) General overview of neuronal cell culture. *Methods Mol Biol* 1078:1-8. doi:10.1007/978-1-62703-640-5_1 [doi].

Haggerty AE, Marlow MM, Oudega M (2016) Extracellular matrix components as therapeutics for spinal cord injury. *Neurosci Lett.* doi:S0304-3940(16)30736-4 [pii].

Halfter W, Dong S, Yip YP et al (2002) A critical function of the pial basement membrane in cortical histogenesis. *J Neurosci* 22(14):6029-6040. doi:20026580 [doi].

Han D, Cheung KC (2011) Biodegradable Cell-Seeded Nanofiber Scaffolds for Neural Repair. *Polymers* 3:1684-1733. doi:10.3390/polym3041684.

Havasi P, Soleimani M, Morovvati H et al (2014) The proliferation study of hips cell-derived neuronal progenitors on poly-caprolactone scaffold. *Basic Clin Neurosci* 5(2):117-123.

Heikkilä TJ, Ylä-Outinen L, Tanskanen JM et al (2009) Human embryonic stem cell-derived neuronal cells form spontaneously active neuronal networks in vitro. *Exp Neurol* 218(1):109-116. doi:10.1016/j.expneurol.2009.04.011 [doi].

Hicks AU, Lappalainen RS, Narkilahti S et al (2009) Transplantation of human embryonic stem cell-derived neural precursor cells and enriched environment after cortical stroke in rats: cell survival and functional recovery. *Eur J Neurosci* 29(3):562-574. doi:10.1111/j.1460-9568.2008.06599.x [doi].

Hochedlinger K, Yamada Y, Beard C et al (2005) Ectopic expression of Oct-4 blocks progenitor-cell differentiation and causes dysplasia in epithelial tissues. *Cell* 121(3):465-477. doi:S0092-8674(05)00163-7 [pii].

Holt LM, Olsen ML (2016) Novel Applications of Magnetic Cell Sorting to Analyze Cell-Type Specific Gene and Protein Expression in the Central Nervous System. *PLoS One* 11(2):e0150290. doi:10.1371/journal.pone.0150290 [doi].

Hsieh A, Zahir T, Lapitsky Y et al (2010) Hydrogel/electrospun fiber composites influence neural stem/progenitor cell fate. *Soft Matter* 6:2227-2237. doi:10.1039/b924349f.

Hsieh J, Aimone JB, Kaspar BK et al (2004) IGF-I instructs multipotent adult neural progenitor cells to become oligodendrocytes. *J Cell Biol* 164(1):111-122. doi:10.1083/jcb.200308101 [doi].

Hu BY, Du ZW, Li XJ et al (2009) Human oligodendrocytes from embryonic stem cells: conserved SHH signaling networks and divergent FGF effects. *Development* 136(9):1443-1452. doi:10.1242/dev.029447 [doi].

Hu BY, Weick JP, Yu J et al (2010) Neural differentiation of human induced pluripotent stem cells follows developmental principles but with variable potency. *Proc Natl Acad Sci U S A* 107(9):4335-4340. doi:10.1073/pnas.0910012107 [doi].

Hu K (2014) All roads lead to induced pluripotent stem cells: the technologies of iPSC generation. *Stem Cells Dev* 23(12):1285-1300. doi:10.1089/scd.2013.0620 [doi].

Hu X, Jin L, Feng L (2004) Erk1/2 but not PI3K pathway is required for neurotrophin 3-induced oligodendrocyte differentiation of post-natal neural stem cells. *J Neurochem* 90(6):1339-1347. doi:10.1111/j.1471-4159.2004.02594.x [doi].

Hyysalo A, Narkilahti S (2015) Directed Differentiation of Human PSC into Oligodendrocytes. In: Kaur N, Vemuri M (eds) *Neural Stem Cell Assays*, 1st edn. John Wiley & Sons, Inc., Hoboken, NJ, USA., p 111-118.

Ide C, Kanekiyo K (2016) Points regarding cell transplantation for the treatment of spinal cord injury. *Neural Regen Res* 11(7):1046-1049. doi:10.4103/1673-5374.187021 [doi].

Illes S, Fleischer W, Siebler M et al (2007) Development and pharmacological modulation of embryonic stem cell-derived neuronal network activity. *Exp Neurol* 207(1):171-176. doi:S0014-4886(07)00218-X [pii].

Itsykson P, Ilouz N, Turetsky T et al (2005) Derivation of neural precursors from human embryonic stem cells in the presence of noggin. *Mol Cell Neurosci* 30(1):24-36. doi:S1044-7431(05)00111-9 [pii].

Izrael M, Zhang P, Kaufman R et al (2007) Human oligodendrocytes derived from embryonic stem cells: Effect of noggin on phenotypic differentiation in vitro and on myelination in vivo. *Mol Cell Neurosci* 34(3):310-323. doi:S1044-7431(06)00260-0 [pii].

Johnson MA, Weick JP, Pearce RA et al (2007) Functional neural development from human embryonic stem cells: accelerated synaptic activity via astrocyte coculture. *J Neurosci* 27(12):3069-3077. doi:27/12/3069 [pii].

Jones TR, Kang IH, Wheeler DB et al (2008) CellProfiler Analyst: data exploration and analysis software for complex image-based screens. *BMC Bioinformatics* 9:482-2105-9-482. doi:10.1186/1471-2105-9-482 [doi].

Kaneko A, Matsushita A, Sankai Y (2015) A 3D nanofibrous hydrogel and collagen sponge scaffold promotes locomotor functional recovery, spinal repair, and neuronal regeneration after complete transection of the spinal cord in adult rats. *Biomed Mater* 10(1):015008-6041/10/1/015008. doi:10.1088/1748-6041/10/1/015008 [doi].

Kang SM, Cho MS, Seo H et al (2007) Efficient induction of oligodendrocytes from human embryonic stem cells. *Stem Cells* 25(2):419-424. doi:2005-0482 [pii].

Kapucu FE, Tanskanen JM, Mikkonen JE et al (2012) Burst analysis tool for developing neuronal networks exhibiting highly varying action potential dynamics. *Front Comput Neurosci* 6:38. doi:10.3389/fncom.2012.00038 [doi].

Kartasalo K, Polonen RP, Ojala M et al (2015) CytoSpectre: a tool for spectral analysis of oriented structures on cellular and subcellular levels. *BMC Bioinformatics* 16:344-015-0782-y. doi:10.1186/s12859-015-0782-y [doi].

Kele M, Day K, Ronnholm H et al (2016) Generation of human iPS cell line CTL07-II from human fibroblasts, under defined and xeno-free conditions. *Stem Cell Res* 17(3):474-478. doi:S1873-5061(16)30143-X [pii].

Kim DS, Lee JS, Leem JW et al (2010) Robust enhancement of neural differentiation from human ES and iPS cells regardless of their innate difference in differentiation propensity. *Stem Cell Rev* 6(2):270-281. doi:10.1007/s12015-010-9138-1 [doi].

Kim SY, Kim MJ, Jung H et al (2012) Comparative proteomic analysis of human somatic cells, induced pluripotent stem cells, and embryonic stem cells. *Stem Cells Dev* 21(8):1272-1286. doi:10.1089/scd.2011.0243 [doi].

Kirkeby A, Grealish S, Wolf DA et al (2012) Generation of regionally specified neural progenitors and functional neurons from human embryonic stem cells under defined conditions. *Cell Rep* 1(6):703-714. doi:10.1016/j.celrep.2012.04.009 [doi].

Kirkeby A, Nelander J, Parmar M (2013) Generating regionalized neuronal cells from pluripotency, a step-by-step protocol. *Front Cell Neurosci* 6:64. doi:10.3389/fncel.2012.00064 [doi].

Kirkeby A, Nolbrant S, Tiklova K et al (2017) Predictive Markers Guide Differentiation to Improve Graft Outcome in Clinical Translation of hESC-Based Therapy for Parkinson's Disease. *Cell Stem Cell* 20(1):135-148. doi:S1934-5909(16)30298-3 [pii].

- Kolind K, Leong KW, Besenbacher F et al (2012) Guidance of stem cell fate on 2D patterned surfaces. *Biomaterials* 33(28):6626-6633. doi:10.1016/j.biomaterials.2012.05.070 [doi].
- Koser DE, Moeendarbary E, Hanne J et al (2015) CNS cell distribution and axon orientation determine local spinal cord mechanical properties. *Biophys J* 108(9):2137-2147. doi:10.1016/j.bpj.2015.03.039 [doi].
- Kramer AS, Harvey AR, Plant GW et al (2013) Systematic review of induced pluripotent stem cell technology as a potential clinical therapy for spinal cord injury. *Cell Transplant* 22(4):571-617. doi:10.3727/096368912X655208 [doi].
- Krencik R, Weick JP, Liu Y et al (2011) Specification of transplantable astroglial subtypes from human pluripotent stem cells. *Nat Biotechnol* 29(6):528-534. doi:10.1038/nbt.1877 [doi].
- Kreutzer J, Ylä-Outinen L, Kärnä P et al (2012) Structured PDMS Chambers for Enhanced Human Neuronal Cell Activity on MEA Platforms. *Journal of Bionic Engineering* 9(1):1-10. doi:http://dx.doi.org/10.1016/S1672-6529(11)60091-7.
- Kshitiz, Park J, Kim P et al (2012) Control of stem cell fate and function by engineering physical microenvironments. *Integr Biol (Camb)* 4(9):1008-1018.
- Kumar P, Choonara YE, Modi G et al (2015) Multifunctional therapeutic delivery strategies for effective neuro-regeneration following traumatic spinal cord injury. *Curr Pharm Des* 21(12):1517-1528. doi:CPD-EPUB-64572 [pii].
- Kyttälä A, Moraghebi R, Valensisi C et al (2016) Genetic Variability Overrides the Impact of Parental Cell Type and Determines iPSC Differentiation Potential. *Stem Cell Reports* 6(2):200-212. doi:10.1016/j.stemcr.2015.12.009 [doi].
- Lam HJ, Patel S, Wang A et al (2010) In vitro regulation of neural differentiation and axon growth by growth factors and bioactive nanofibers. *Tissue Eng Part A* 16(8):2641-2648. doi:10.1089/ten.TEA.2009.0414 [doi].
- Lappalainen RS, Salomaki M, Ylä-Outinen L et al (2010) Similarly derived and cultured hESC lines show variation in their developmental potential towards neuronal cells in long-term culture. *Regen Med* 5(5):749-762. doi:10.2217/rme.10.58 [doi].
- Lau LW, Cua R, Keough MB et al (2013) Pathophysiology of the brain extracellular matrix: a new target for remyelination. *Nat Rev Neurosci* 14(10):722-729. doi:10.1038/nrn3550 [doi].

Leal-Filho MB (2011) Spinal cord injury: From inflammation to glial scar. *Surg Neurol Int* 2:112-7806.83732. Epub 2011 Aug 13. doi:10.4103/2152-7806.83732 [doi].

Lee S, Leach MK, Redmond SA et al (2012) A culture system to study oligodendrocyte myelination processes using engineered nanofibers. *Nat Methods* 9(9):917-922. doi:10.1038/nmeth.2105 [doi].

Lee S, Yun S, Park KI et al (2016) Sliding Fibers: Slidable, Injectable, and Gel-like Electrospun Nanofibers as Versatile Cell Carriers. *ACS Nano* 10(3):3282-3294. doi:10.1021/acsnano.5b06605 [doi].

Li H, Ham TR, Neill N. et al (2016a) A Hydrogel Bridge Incorporating Immobilized Growth Factors and Neural Stem/Progenitor Cells to Treat Spinal Cord Injury. *Advanced Healthcare Materials* 5(7):802-812. doi:10.1002/adhm.201500810.

Li H, Koenig AM, Sloan P et al (2014) In vivo assessment of guided neural stem cell differentiation in growth factor immobilized chitosan-based hydrogel scaffolds. *Biomaterials* 35(33):9049-9057. doi:http://dx.doi.org/10.1016/j.biomaterials.2014.07.038.

Li N, Leung GK (2015) Oligodendrocyte Precursor Cells in Spinal Cord Injury: A Review and Update. *Biomed Res Int* 2015:235195. doi:10.1155/2015/235195 [doi].

Li X, Li M, Sun J et al (2016b) Radially Aligned Electrospun Fibers with Continuous Gradient of SDF1 α for the Guidance of Neural Stem Cells. *Small* 12(36):5009-5018. doi:10.1002/sml.201601285 [doi].

Li X, Katsanevakis E, Liu X et al (2012) Engineering neural stem cell fates with hydrogel design for central nervous system regeneration. *Progress in Polymer Science* 37(8):1105-1129. doi:http://dx.doi.org/10.1016/j.progpolymsci.2012.02.004.

Lippmann ES, Estevez-Silva MC, Ashton RS (2014) Defined human pluripotent stem cell culture enables highly efficient neuroepithelium derivation without small molecule inhibitors. *Stem Cells* 32(4):1032-1042. doi:10.1002/stem.1622 [doi].

Livak KJ, Schmittgen TD (2001) Analysis of relative gene expression data using real-time quantitative PCR and the 2⁻($\Delta\Delta C_T$) Method. *Methods* 25(4):402-408. doi:10.1006/meth.2001.1262 [doi].

Livesey MR, Magnani D, Cleary EM et al (2016) Maturation and electrophysiological properties of human pluripotent stem cell-derived oligodendrocytes. *Stem Cells* 34(4):1040-1053. doi:10.1002/stem.2273 [doi].

Low WC, Rujitanaroj PO, Wang F et al (2015) Nanofiber-mediated release of retinoic acid and brain-derived neurotrophic factor for enhanced neuronal differentiation of neural progenitor cells. *Drug Deliv Transl Res* 5(2):89-100. doi:10.1007/s13346-013-0131-5 [doi].

Lu HF, Chai C, Lim TC et al (2014) A defined xeno-free and feeder-free culture system for the derivation, expansion and direct differentiation of transgene-free patient-specific induced pluripotent stem cells. *Biomaterials* 35(9):2816-2826. doi:10.1016/j.biomaterials.2013.12.050 [doi].

Lu QR, Yuk D, Alberta JA et al (2000) Sonic hedgehog--regulated oligodendrocyte lineage genes encoding bHLH proteins in the mammalian central nervous system. *Neuron* 25(2):317-329. doi:S0896-6273(00)80897-1 [pii].

Lukovic D, Stojkovic M, Moreno-Manzano V et al (2014) Perspectives and future directions of human pluripotent stem cell-based therapies: lessons from Geron's clinical trial for spinal cord injury. *Stem Cells Dev* 23(1):1-4. doi:10.1089/scd.2013.0266 [doi].

Lundgaard I, Luzhynskaya A, Stockley JH et al (2013) Neuregulin and BDNF induce a switch to NMDA receptor-dependent myelination by oligodendrocytes. *PLoS Biol* 11(12):e1001743. doi:10.1371/journal.pbio.1001743 [doi].

Ma W, Tavakoli T, Derby E et al (2008) Cell-extracellular matrix interactions regulate neural differentiation of human embryonic stem cells. *BMC Dev Biol* 8:90-213X-8-90. doi:10.1186/1471-213X-8-90 [doi].

Mahairaki V, Lim SH, Christopherson GT et al (2011) Nanofiber matrices promote the neuronal differentiation of human embryonic stem cell-derived neural precursors in vitro. *Tissue Eng Part A* 17(5-6):855-863. doi:10.1089/ten.TEA.2010.0377 [doi].

Markoulaki S, Hanna J, Beard C et al (2009) Transgenic mice with defined combinations of drug-inducible reprogramming factors. *Nat Biotechnol* 27(2):169-171. doi:10.1038/nbt.1520 [doi].

Martynoga B, Drechsel D, Guillemot F (2012) Molecular control of neurogenesis: a view from the mammalian cerebral cortex. *Cold Spring Harb Perspect Biol* 4(10):10.1101/cshperspect.a008359. doi:10.1101/cshperspect.a008359 [doi].

Mason I (2007) Initiation to end point: the multiple roles of fibroblast growth factors in neural development. *Nat Rev Neurosci* 8(8):583-596. doi:nrn2189 [pii].

McMorris FA, Dubois-Dalcq M (1988) Insulin-like growth factor I promotes cell proliferation and oligodendroglial commitment in rat glial progenitor cells developing in vitro. *J Neurosci Res* 21(2-4):199-209. doi:10.1002/jnr.490210212 [doi].

McMurtrey RJ (2014) Patterned and functionalized nanofiber scaffolds in three-dimensional hydrogel constructs enhance neurite outgrowth and directional control. *J Neural Eng* 11(6):066009-2560/11/6/066009. Epub 2014 Oct 31. doi:10.1088/1741-2560/11/6/066009 [doi].

Melkounian Z, Weber JL, Weber DM et al (2010) Synthetic peptide-acrylate surfaces for long-term self-renewal and cardiomyocyte differentiation of human embryonic stem cells. *Nat Biotechnol* 28(6):606-610. doi:10.1038/nbt.1629 [doi].

Meng H, Li G (2013) A review of stimuli-responsive shape memory polymer composites. *Polymer* 54(9):2199-2221. doi:http://dx.doi.org/10.1016/j.polymer.2013.02.023.

Mertens J, Marchetto MC, Bardy C et al (2016) Evaluating cell reprogramming, differentiation and conversion technologies in neuroscience. *Nat Rev Neurosci* 17(7):424-437. doi:10.1038/nrn.2016.46 [doi].

Miner JH, Cunningham J, Sanes JR (1998) Roles for laminin in embryogenesis: exencephaly, syndactyly, and placentopathy in mice lacking the laminin alpha5 chain. *J Cell Biol* 143(6):1713-1723.

Miyazaki T, Futaki S, Suemori H et al (2012) Laminin E8 fragments support efficient adhesion and expansion of dissociated human pluripotent stem cells. *Nat Commun* 3:1236. doi:10.1038/ncomms2231 [doi].

Mohtaram NK, Ko J, Agbay A et al (2015a) Development of a glial cell-derived neurotrophic factor-releasing artificial dura for neural tissue engineering applications. *J Mater Chem B* 3(40):7974-7985. doi:10.1039/C5TB00871A.

Mohtaram NK, Ko J, King C et al (2015b) Electrospun biomaterial scaffolds with varied topographies for neuronal differentiation of human-induced pluripotent stem cells. *J Biomed Mater Res A* 103(8):2591-2601. doi:10.1002/jbm.a.35392 [doi].

Monaco G, van Dam S, Casal Novo Ribeiro JL et al (2015) A comparison of human and mouse gene co-expression networks reveals conservation and divergence at the tissue, pathway and disease levels. *BMC Evol Biol* 15:259-015-0534-7. doi:10.1186/s12862-015-0534-7 [doi].

Morizane A, Doi D, Kikuchi T et al (2011) Small-molecule inhibitors of bone morphogenic protein and activin/nodal signals promote highly efficient neural induction from human pluripotent stem cells. *J Neurosci Res* 89(2):117-126. doi:10.1002/jnr.22547 [doi].

Muguruma K, Nishiyama A, Kawakami H et al (2015) Self-organization of polarized cerebellar tissue in 3D culture of human pluripotent stem cells. *Cell Rep* 10(4):537-550. doi:10.1016/j.celrep.2014.12.051 [doi].

Munoz-Sanjuan I, Brivanlou AH (2002) Neural induction, the default model and embryonic stem cells. *Nat Rev Neurosci* 3(4):271-280. doi:10.1038/nrn786 [doi].

Muratore CR, Srikanth P, Callahan DG et al (2014) Comparison and optimization of hiPSC forebrain cortical differentiation protocols. *PLoS One* 9(8):e105807. doi:10.1371/journal.pone.0105807 [doi].

Nakagawa M, Koyanagi M, Tanabe K et al (2008) Generation of induced pluripotent stem cells without Myc from mouse and human fibroblasts. *Nat Biotechnol* 26(1):101-106. doi:nbt1374 [pii].

Nakagawa M, Taniguchi Y, Senda S et al (2014) A novel efficient feeder-free culture system for the derivation of human induced pluripotent stem cells. *Sci Rep* 4:3594. doi:10.1038/srep03594 [doi].

Nanofiber Solutions. Available at: <http://www.nanofibersolutions.com/products.html>. Accessed April 26 2017.

Narkilahti S, Rajala K, Pihlajamäki H et al (2007) Monitoring and analysis of dynamic growth of human embryonic stem cells: comparison of automated instrumentation and conventional culturing methods. *BioMedical Engineering OnLine* 6(11). doi:10.1186/1475-925X-6-11.

Narsinh KH, Plews J, Wu JC (2011) Comparison of human induced pluripotent and embryonic stem cells: fraternal or identical twins?. *Mol Ther* 19(4):635-638. doi:10.1038/mt.2011.41 [doi].

Nashmi R, Fehlings MG (2001) Mechanisms of axonal dysfunction after spinal cord injury: with an emphasis on the role of voltage-gated potassium channels. *Brain Res Brain Res Rev* 38(1-2):165-191. doi:S0165017301001345 [pii].

Nat R, Nilbratt M, Narkilahti S et al (2007) Neurogenic neuroepithelial and radial glial cells generated from six human embryonic stem cell lines in serum-free suspension and adherent cultures. *Glia* 55(4):385-399. doi:10.1002/glia.20463 [doi].

Nature News. Available at: <http://www.nature.com/news/japanese-man-is-first-to-receive-reprogrammed-stem-cells-from-another-person-1.21730>. doi:10.1038/nature.2017.21730. Accessed April 26 2017.

Nedergaard M, Ransom B, Goldman SA (2003) New roles for astrocytes: redefining the functional architecture of the brain. *Trends Neurosci* 26(10):523-530. doi:S0166-2236(03)00266-2 [pii].

Neuralstem Inc. Available at: <http://www.neuralstem.com/cell-therapy-for-sci>. Accessed April 26 2017.

Nisbet DR, Crompton KE, Horne MK et al (2008) Neural tissue engineering of the CNS using hydrogels. *J Biomed Mater Res B Appl Biomater* 87(1):251-263. doi:10.1002/jbm.b.31000 [doi].

Nishimura K, Doi D, Samata B et al (2016) Estradiol Facilitates Functional Integration of iPSC-Derived Dopaminergic Neurons into Striatal Neuronal Circuits via Activation of Integrin $\alpha 5\beta 1$. *Stem Cell Reports* 6(4):511-524. doi:10.1016/j.stemcr.2016.02.008 [doi].

Nistor GI, Totoiu MO, Haque N et al (2005) Human embryonic stem cells differentiate into oligodendrocytes in high purity and myelinate after spinal cord transplantation. *Glia* 49(3):385-396. doi:10.1002/glia.20127 [doi].

Ogawa S, Tokumoto Y, Miyake J et al (2011) Induction of oligodendrocyte differentiation from adult human fibroblast-derived induced pluripotent stem cells. *In Vitro Cell Dev Biol Anim* 47(7):464-469. doi:10.1007/s11626-011-9435-2 [doi].

Oh S, Huang X, Chiang C (2005) Specific requirements of sonic hedgehog signaling during oligodendrocyte development. *Dev Dyn* 234(3):489-496. doi:10.1002/dvdy.20422 [doi].

Osafune K, Caron L, Borowiak M et al (2008) Marked differences in differentiation propensity among human embryonic stem cell lines. *Nat Biotechnol* 26(3):313-315. doi:10.1038/nbt1383 [doi].

Park HJ, Shin J, Kim J et al (2014) Nonviral delivery for reprogramming to pluripotency and differentiation. *Arch Pharm Res* 37(1):107-119. doi:10.1007/s12272-013-0287-z [doi].

Pasca AM, Sloan SA, Clarke LE et al (2015) Functional cortical neurons and astrocytes from human pluripotent stem cells in 3D culture. *Nat Methods* 12(7):671-678. doi:10.1038/nmeth.3415 [doi].

Patani R, Hollins AJ, Wishart TM et al (2011) Retinoid-independent motor neurogenesis from human embryonic stem cells reveals a medial columnar ground state. *Nat Commun* 2:214. doi:10.1038/ncomms1216 [doi].

Pawlina W, Ross M (2015) Nerve tissue. In: Taylor C, Nicholl G (eds) *Histology: A Text and Atlas*, 7th edition edn. Lippincott Williams and Wilkins, p 356-391.

Pawlowski M, Ortmann D, Bertero A et al (2017) Inducible and Deterministic Forward Programming of Human Pluripotent Stem Cells into Neurons, Skeletal Myocytes, and Oligodendrocytes. *Stem Cell Reports*. doi:S2213-6711(17)30083-8 [pii].

Piao J, Major T, Auyeung G et al (2015) Human embryonic stem cell-derived oligodendrocyte progenitors remyelinate the brain and rescue behavioral deficits following radiation. *Cell Stem Cell* 16(2):198-210. doi:10.1016/j.stem.2015.01.004 [doi].

Plantman S, Patarroyo M, Fried K et al (2008) Integrin-laminin interactions controlling neurite outgrowth from adult DRG neurons in vitro. *Mol Cell Neurosci* 39(1):50-62. doi:10.1016/j.mcn.2008.05.015 [doi].

Pouya A, Satarian L, Kiani S et al (2011) Human induced pluripotent stem cells differentiation into oligodendrocyte progenitors and transplantation in a rat model of optic chiasm demyelination. *PLoS One* 6(11):e27925. doi:10.1371/journal.pone.0027925 [doi].

Priest CA, Manley NC, Denham J et al (2015) Preclinical safety of human embryonic stem cell-derived oligodendrocyte progenitors supporting clinical trials in spinal cord injury. *Regen Med* 10(8):939-958. doi:10.2217/rme.15.57 [doi].

Qian X, Villa-Diaz LG, Krebsbach PH (2013) Advances in culture and manipulation of human pluripotent stem cells. *J Dent Res* 92(11):956-962. doi:10.1177/0022034513501286 [doi].

Qu J, Wang D, Wang H et al (2013) Electrospun silk fibroin nanofibers in different diameters support neurite outgrowth and promote astrocyte migration. *J Biomed Mater Res A* 101(9):2667-2678. doi:10.1002/jbm.a.34551 [doi].

Quadrato G, Brown J, Arlotta P (2016) The promises and challenges of human brain organoids as models of neuropsychiatric disease. *Nat Med* 22(11):1220-1228. doi:10.1038/nm.4214 [doi].

Rabchevsky AG, Patel SP, Springer JE (2011) Pharmacological interventions for spinal cord injury: where do we stand? How might we step forward?. *Pharmacol Ther* 132(1):15-29. doi:10.1016/j.pharmthera.2011.05.001 [doi].

Rahjouei A, Kiani S, Zahabi A et al (2011) Interactions of human embryonic stem cell-derived neural progenitors with an electrospun nanofibrillar surface in vitro. *Int J Artif Organs* 34(7):559-570. doi:10.5301/IJAO.2011.8511 [doi].

Rajala K, Hakala H, Panula S et al (2007) Testing of nine different xeno-free culture media for human embryonic stem cell cultures. *Hum Reprod* 22(5):1231-1238. doi:del523 [pii].

Relucio J, Tzvetanova ID, Ao W et al (2009) Laminin alters fyn regulatory mechanisms and promotes oligodendrocyte development. *J Neurosci* 29(38):11794-11806. doi:10.1523/JNEUROSCI.0888-09.2009 [doi].

Reubinoff BE, Itsykson P, Turetsky T et al (2001) Neural progenitors from human embryonic stem cells. *Nat Biotechnol* 19(12):1134-1140. doi:10.1038/nbt1201-1134 [doi].

Richardson WD, Young KM, Tripathi RB et al (2011) NG2-glia as multipotent neural stem cells: fact or fantasy?. *Neuron* 70(4):661-673. doi:10.1016/j.neuron.2011.05.013 [doi].

Rivet CJ, Zhou K, Gilbert RJ et al (2015) Cell infiltration into a 3D electrospun fiber and hydrogel hybrid scaffold implanted in the brain. *Biomatter* 5:e1005527. doi:10.1080/21592535.2015.1005527 [doi].

Robinton DA, Daley GQ (2012) The promise of induced pluripotent stem cells in research and therapy. *Nature* 481(7381):295-305. doi:10.1038/nature10761 [doi].

Rodin S, Antonsson L, Hovatta O et al (2014a) Monolayer culturing and cloning of human pluripotent stem cells on laminin-521-based matrices under xeno-free and chemically defined conditions. *Nat Protoc* 9(10):2354-2368. doi:10.1038/nprot.2014.159 [doi].

Rodin S, Antonsson L, Niaudet C et al (2014b) Clonal culturing of human embryonic stem cells on laminin-521/E-cadherin matrix in defined and xeno-free environment. *Nat Commun* 5:3195. doi:10.1038/ncomms4195 [doi].

Rodin S, Domogatskaya A, Strom S et al (2010) Long-term self-renewal of human pluripotent stem cells on human recombinant laminin-511. *Nat Biotechnol* 28(6):611-615. doi:10.1038/nbt.1620 [doi].

Rowitch DH (2004) Glial specification in the vertebrate neural tube. *Nat Rev Neurosci* 5(5):409-419. doi:10.1038/nrn1389 [doi].

Ruff CA, Wilcox JT, Fehlings MG (2012) Cell-based transplantation strategies to promote plasticity following spinal cord injury. *Exp Neurol* 235(1):78-90. doi:10.1016/j.expneurol.2011.02.010 [doi].

Sabapathy V, Tharion G, Kumar S (2015) Cell Therapy Augments Functional Recovery Subsequent to Spinal Cord Injury under Experimental Conditions. *Stem Cells Int* 2015:132172. doi:10.1155/2015/132172 [doi].

Sandquist EJ (2016) 2.4 Stem Cell-Based Approaches Coupled with Bioengineering for Translational Applications. In: Zhang LG, Kaplan DL (eds) *Neural Engineering: From Advanced Biomaterials to 3D Fabrication Techniques*, 1 edn. Springer International Publishing, Springer International Publishing Switzerland, p 64.

Sarig-Nadir O, Livnat N, Zajdman R et al (2009) Laser photoablation of guidance microchannels into hydrogels directs cell growth in three dimensions. *Biophys J* 96(11):4743-4752. doi:10.1016/j.bpj.2009.03.019 [doi].

Schwab JM, Brechtel K, Mueller CA et al (2006) Experimental strategies to promote spinal cord regeneration--an integrative perspective. *Prog Neurobiol* 78(2):91-116. doi:S0301-0082(05)00196-6 [pii].

Servier Medical Art. Available at: <http://servier.com/Powerpoint-image-bank>. Accessed April 26 2017.

Shah S, Yin PT, Uehara TM et al (2014) Guiding stem cell differentiation into oligodendrocytes using graphene-nanofiber hybrid scaffolds. *Adv Mater* 26(22):3673-3680. doi:10.1002/adma.201400523 [doi].

Shahbazi E, Kiani S, Gourabi H et al (2011) Electrospun nanofibrillar surfaces promote neuronal differentiation and function from human embryonic stem cells. *Tissue Eng Part A* 17(23-24):3021-3031. doi:10.1089/ten.TEA.2011.0121 [doi].

Shelke N, Leed P, Anderson M et al (2016) Neural tissue engineering: nanofiber-hydrogel based composite scaffolds. *Polymers for Advanced Technologies* 27(1):42-51. doi:DOI: 10.1002/pat.3594.

Shi Y, Kirwan P, Smith J et al (2012) Human cerebral cortex development from pluripotent stem cells to functional excitatory synapses. *Nat Neurosci* 15(3):477-86, S1. doi:10.1038/nn.3041 [doi].

Sim FJ, McClain CR, Schanz SJ et al (2011) CD140a identifies a population of highly myelinogenic, migration-competent and efficiently engrafting human oligodendrocyte progenitor cells. *Nat Biotechnol* 29(10):934-941. doi:10.1038/nbt.1972 [doi].

Singh P, Schwarzbauer JE (2012) Fibronectin and stem cell differentiation - lessons from chondrogenesis. *J Cell Sci* 125(Pt 16):3703-3712. doi:10.1242/jcs.095786 [doi].

Skottman H (2010) Derivation and characterization of three new human embryonic stem cell lines in Finland. *In Vitro Cell Dev Biol Anim* 46(3-4):206-209. doi:10.1007/s11626-010-9286-2 [doi].

Sofroniew MV, Vinters HV (2010) Astrocytes: biology and pathology. *Acta Neuropathol* 119(1):7-35. doi:10.1007/s00401-009-0619-8 [doi].

Soldner F, Hockemeyer D, Beard C et al (2009) Parkinson's disease patient-derived induced pluripotent stem cells free of viral reprogramming factors. *Cell* 136(5):964-977. doi:10.1016/j.cell.2009.02.013 [doi].

Stacpoole SR, Spitzer S, Bilican B et al (2013) High yields of oligodendrocyte lineage cells from human embryonic stem cells at physiological oxygen tensions for evaluation of translational biology. *Stem Cell Reports* 1(5):437-450. doi:10.1016/j.stemcr.2013.09.006 [doi].

Stadtfeld M, Nagaya M, Utikal J et al (2008) Induced pluripotent stem cells generated without viral integration. *Science* 322(5903):945-949. doi:10.1126/science.1162494 [doi].

StemCells Inc. Available at: http://investor.stemcellsinc.com/phoenix.zhtml?c=86230&p=irol-newsArticle_print&ID=2173446. Accessed April 26 2017.

Straley KS, Foo CW, Heilshorn SC (2010) Biomaterial design strategies for the treatment of spinal cord injuries. *J Neurotrauma* 27(1):1-19. doi:10.1089/neu.2009.0948 [doi].

Subramanian A, Krishnan UM, Sethuraman S (2009) Development of biomaterial scaffold for nerve tissue engineering: Biomaterial mediated neural regeneration. *J Biomed Sci* 16:108-0127-16-108. doi:10.1186/1423-0127-16-108 [doi].

Sundberg M, Skottman H, Suuronen R et al (2010) Production and isolation of NG2+ oligodendrocyte precursors from human embryonic stem cells in defined serum-free medium. *Stem Cell Res* 5(2):91-103. doi:10.1016/j.scr.2010.04.005 [doi].

Suzuki IK, Vanderhaeghen P (2015) Is this a brain which I see before me? Modeling human neural development with pluripotent stem cells. *Development* 142(18):3138-3150. doi:10.1242/dev.120568 [doi].

Takahashi K, Tanabe K, Ohnuki M et al (2007) Induction of pluripotent stem cells from adult human fibroblasts by defined factors. *Cell* 131(5):861-872. doi:S0092-8674(07)01471-7 [pii].

Talbott JF, Cao Q, Bertram J et al (2007) CNTF promotes the survival and differentiation of adult spinal cord-derived oligodendrocyte precursor cells in vitro but

fails to promote remyelination in vivo. *Exp Neurol* 204(1):485-489. doi:S0014-4886(06)00637-6 [pii].

Tang Y, Liu L, Li J et al (2016) Effective motor neuron differentiation of hiPSCs on a patch made of crosslinked monolayer gelatin nanofibers. *J Mater Chem B* 4(19):3305-3312. doi:10.1039/C6TB00351F.

Tannenbaum SE, Turetsky TT, Singer O et al (2012) Derivation of xeno-free and GMP-grade human embryonic stem cells--platforms for future clinical applications. *PLoS One* 7(6):e35325. doi:10.1371/journal.pone.0035325 [doi].

Trounson A, DeWitt ND (2016) Pluripotent stem cells progressing to the clinic. *Nat Rev Mol Cell Biol* 17(3):194-200. doi:10.1038/nrm.2016.10 [doi].

Tsai Y, Cutts J, Kimura A et al (2015) A chemically defined substrate for the expansion and neuronal differentiation of human pluripotent stem cell-derived neural progenitor cells. *Stem Cell Res* 15(1):75-87. doi:10.1016/j.scr.2015.05.002 [doi].

Tsankov AM, Akopian V, Pop R et al (2015) A qPCR ScoreCard quantifies the differentiation potential of human pluripotent stem cells. *Nat Biotechnol* 33(11):1182-1192. doi:10.1038/nbt.3387 [doi].

Vallstedt A, Klos JM, Ericson J (2005) Multiple dorsoventral origins of oligodendrocyte generation in the spinal cord and hindbrain. *Neuron* 45(1):55-67. doi:S0896627304008426 [pii].

Velasco I, Salazar P, Giorgetti A et al (2014) Concise review: Generation of neurons from somatic cells of healthy individuals and neurological patients through induced pluripotency or direct conversion. *Stem Cells* 32(11):2811-2817. doi:10.1002/stem.1782 [doi].

Villa-Diaz LG, Nandivada H, Ding J et al (2010) Synthetic polymer coatings for long-term growth of human embryonic stem cells. *Nat Biotechnol* 28(6):581-583. doi:10.1038/nbt.1631 [doi].

Wagenaar DA, Pine J, Potter SM (2006) An extremely rich repertoire of bursting patterns during the development of cortical cultures. *BMC Neurosci* 7:11. doi:1471-2202-7-11 [pii].

Wang J, Ye R, Wei Y et al (2012a) The effects of electrospun TSF nanofiber diameter and alignment on neuronal differentiation of human embryonic stem cells. *J Biomed Mater Res A* 100(3):632-645. doi:10.1002/jbm.a.33291 [doi].

Wang LC, Almazan G (2016) Role of Sonic Hedgehog Signaling in Oligodendrocyte Differentiation. *Neurochem Res* 41(12):3289-3299. doi:10.1007/s11064-016-2061-3 [doi].

Wang S, Bates J, Li X et al (2013) Human iPSC-derived oligodendrocyte progenitor cells can myelinate and rescue a mouse model of congenital hypomyelination. *Cell Stem Cell* 12(2):252-264. doi:10.1016/j.stem.2012.12.002 [doi].

Wang W, Deng L, Liu S et al (2012b) Adjustable degradation and drug release of a thermosensitive hydrogel based on a pendant cyclic ether modified poly(epsilon-caprolactone) and poly(ethylene glycol)co-polymer. *Acta Biomater* 8(11):3963-3973. doi:10.1016/j.actbio.2012.07.021 [doi].

Weightman A, Jenkins S, Pickard M et al (2014) Alignment of multiple glial cell populations in 3D nanofiber scaffolds: toward the development of multicellular implantable scaffolds for repair of neural injury. *Nanomedicine* 10(2):291-295. doi:10.1016/j.nano.2013.09.001 [doi].

Wilson HC, Onischke C, Raine CS (2003) Human oligodendrocyte precursor cells in vitro: phenotypic analysis and differential response to growth factors. *Glia* 44(2):153-165. doi:10.1002/glia.10280 [doi].

Wilson PA, Hemmati-Brivanlou A (1995) Induction of epidermis and inhibition of neural fate by Bmp-4. *Nature* 376(6538):331-333. doi:10.1038/376331a0 [doi].

Wobus AM, Boheler KR (2005) Embryonic stem cells: prospects for developmental biology and cell therapy. *Physiol Rev* 85(2):635-678. doi:85/2/635 [pii].

Woodruff MA, Hutmacher DW (2010) The return of a forgotten polymer—Polycaprolactone in the 21st century. *Progress in Polymer Science* 35(10):1217-1256. doi:http://dx.doi.org/10.1016/j.progpolymsci.2010.04.002.

Xia H, Liu D, Zhong D et al (2014) Impact of topographic features of electrospun polymethylmethacrylate nanofibers on growth pattern of rat primary astrocytes. *Nan Fang Yi Ke Da Xue Xue Bao* 34(11):1569-1573.

Xiao Z, Tang F, Tang J et al (2016) One-year clinical study of NeuroRegen scaffold implantation following scar resection in complete chronic spinal cord injury patients. *Sci China Life Sci* 59(7):647-655. doi:10.1007/s11427-016-5080-z [doi].

Xie J, Willerth SM, Li X et al (2009) The differentiation of embryonic stem cells seeded on electrospun nanofibers into neural lineages. *Biomaterials* 30(3):354-362. doi:10.1016/j.biomaterials.2008.09.046 [doi].

Yamanaka S (2012) Induced pluripotent stem cells: past, present, and future. *Cell Stem Cell* 10(6):678-684. doi:10.1016/j.stem.2012.05.005 [doi].

Yang K, Jung H, Lee HR et al (2014) Multiscale, hierarchically patterned topography for directing human neural stem cells into functional neurons. *ACS Nano* 8(8):7809-7822. doi:10.1021/nn501182f [doi].

Yang Y, Higashimori H, Morel L (2013) Developmental maturation of astrocytes and pathogenesis of neurodevelopmental disorders. *J Neurodev Disord* 5(1):22-1955-5-22. doi:10.1186/1866-1955-5-22 [doi].

Yap MS, Nathan KR, Yeo Y et al (2015) Neural Differentiation of Human Pluripotent Stem Cells for Nontherapeutic Applications: Toxicology, Pharmacology, and In Vitro Disease Modeling. *Stem Cells Int* 2015:105172. doi:10.1155/2015/105172 [doi].

Yasui G, Yamamoto Y, Shichinohe R et al (2016) Neuregulin-1 released by biodegradable gelatin hydrogels can accelerate facial nerve regeneration and functional recovery of traumatic facial nerve palsy. *J Plast Reconstr Aesthet Surg* 69(3):328-334. doi:10.1016/j.bjps.2015.10.037 [doi].

Ylä-Outinen L, Mariani C, Skottman H et al (2010) Electrospun Poly(L,D-lactide) Scaffolds Support the Growth of Human Embryonic Stem Cell-derived Neuronal Cells. *The Open Tissue Engineering and Regenerative Medicine Journal* 3:1-9.

Ylä-Outinen L, Joki T, Varjola M et al (2014) Three-dimensional growth matrix for human embryonic stem cell-derived neuronal cells. *J Tissue Eng Regen Med* 8(3):186-194. doi:10.1002/term.1512 [doi].

Yu J, Vodyanik MA, Smuga-Otto K et al (2007) Induced pluripotent stem cell lines derived from human somatic cells. *Science* 318(5858):1917-1920. doi:1151526 [pii].

Yu WY, He DW (2015) Current trends in spinal cord injury repair. *Eur Rev Med Pharmacol Sci* 19(18):3340-3344. doi:9499 [pii].

Yuan F, Fang KH, Cao SY et al (2015) Efficient generation of region-specific forebrain neurons from human pluripotent stem cells under highly defined condition. *Sci Rep* 5:18550. doi:10.1038/srep18550 [doi].

Zhang J, Jiao J (2015) Molecular Biomarkers for Embryonic and Adult Neural Stem Cell and Neurogenesis. *Biomed Res Int* 2015:727542. doi:10.1155/2015/727542 [doi].

Zhang SC, Ge B, Duncan ID (2000) Tracing human oligodendroglial development in vitro. *J Neurosci Res* 59(3):421-429. doi:10.1002/(SICI)1097-4547(20000201)59:33.0.CO;2-C [pii].

Zhang SC, Wernig M, Duncan ID et al (2001) In vitro differentiation of transplantable neural precursors from human embryonic stem cells. *Nat Biotechnol* 19(12):1129-1133. doi:10.1038/nbt1201-1129 [doi].

Zhou S, Ochalek A, Szczesna K et al (2016) The positional identity of iPSC-derived neural progenitor cells along the anterior-posterior axis is controlled in a dosage-dependent manner by bFGF and EGF. *Differentiation*. doi:S0301-4681(15)30053-0 [pii].

Zhou W, Freed CR (2009) Adenoviral gene delivery can reprogram human fibroblasts to induced pluripotent stem cells. *Stem Cells* 27(11):2667-2674. doi:10.1002/stem.201 [doi].

Zirra A, Wiethoff S, Patani R (2016) Neural Conversion and Patterning of Human Pluripotent Stem Cells: A Developmental Perspective. *Stem Cells Int* 2016:8291260. doi:10.1155/2016/8291260 [doi].

Original publications



Comparative Analysis of Targeted Differentiation of Human Induced Pluripotent Stem Cells (hiPSCs) and Human Embryonic Stem Cells Reveals Variability Associated With Incomplete Transgene Silencing in Retrovirally Derived hiPSC Lines

SANNA TOIVONEN,^{a,*} MARISA OJALA,^{b,c,*} ANU HYYSALO,^{b,c,*} TANJA ILMARINEN,^{b,c}
KRISTIINA RAJALA,^{b,c} MARI PEKKANEN-MATTILA,^{b,c} RIIKKA ÄÄNISMAA,^{b,c} KAROLINA LUNDIN,^a
JAAN PALGI,^a JERE WELTNER,^a RAS TROKOVIC,^a OLLI SILVENNOINEN,^{b,c} HELI SKOTTMAN,^{b,c}
SUSANNA NARKILAHTI,^{b,c} KATRIINA AALTO-SETÄLÄ^{b,c,d} TIMO OTONKOSKI^{a,e}

Key Words. Embryonic stem cells • Pluripotent stem cells • Hepatocyte differentiation • Cardiac • Neural differentiation • Retinal pigmented epithelium • Differentiation

ABSTRACT

Functional hepatocytes, cardiomyocytes, neurons, and retinal pigment epithelial (RPE) cells derived from human embryonic stem cells (hESCs) or human induced pluripotent stem cells (hiPSCs) could provide a defined and renewable source of human cells relevant for cell replacement therapies, drug discovery, toxicology testing, and disease modeling. In this study, we investigated the differences between the differentiation potentials of three hESC lines, four retrovirally derived hiPSC lines, and one hiPSC line derived with the nonintegrating Sendai virus technology. Four independent protocols were used for hepatocyte, cardiomyocyte, neuronal, and RPE cell differentiation. Overall, cells differentiated from hESCs and hiPSCs showed functional similarities and similar expression of genes characteristic of specific cell types, and differences between individual cell lines were also detected. Reactivation of transgenic *OCT4* was detected specifically during RPE differentiation in the retrovirally derived lines, which may have affected the outcome of differentiation with these hiPSCs. One of the hiPSC lines was inferior in all directions, and it failed to produce hepatocytes. Exogenous *KLF4* was incompletely silenced in this cell line. No transgene expression was detected in the Sendai virus-derived hiPSC line. These findings highlight the problems related to transgene expression in retrovirally derived hiPSC lines. *STEM CELLS TRANSLATIONAL MEDICINE* 2013;2:83–93

INTRODUCTION

Human embryonic stem cells (hESCs) and human induced pluripotent stem cells (hiPSCs), collectively termed human pluripotent stem cells (hPSCs), are considered a renewable source of cells for regenerative medicine because of their potential to differentiate into all cell types found in the adult human body [1]. hESCs are derived from the inner cell mass of developing embryos [2], whereas hiPSCs are reprogrammed from somatic cells [3, 4]. hiPSCs share several characteristics with hESCs, including similar morphology, expression of pluripotency markers, and the ability to differentiate into definitive cell lineages [5–8]. Initial studies have suggested that fully reprogrammed iPSCs are indistinguishable from ESCs [3, 4, 9]. More comprehensive studies have revealed that particularly early passage iPSCs show differences in their gene expression profile, but continued propagation tends

to increase the similarity between hESCs and iPSCs [10, 11].

Recent studies have revealed that iPSCs maintain differential DNA methylation patterns as a sign of incomplete reprogramming [12, 13]. The possible consequences of this “epigenetic memory” still remain unknown. Some recent studies indicate that the origin of iPSCs is relevant for their differentiation capacity. iPSCs derived from retinal pigment epithelial (RPE) cells have a high tendency for pigmentation [14], and reprogramming of cardiac fibroblasts produces more cardiomyocytes than fibroblasts from other sources [15]. Although hiPSCs in general seem to differentiate into specific lineages as efficiently as hESCs, there are several examples of incomplete pluripotent differentiation capacity, possibly reflecting their epigenetic barriers [11, 16].

Most studies comparing the properties of hESCs and hiPSCs have focused on their undif-

^aResearch Programs Unit, Molecular Neurology, Biomedicum Stem Cell Center, University of Helsinki, Helsinki, Finland;

^bInstitute of Biomedical Technology and

^cBioMediTech, University of Tampere, Tampere, Finland;

^dHeart Center, Tampere University Hospital, Tampere, Finland;

^eChildren’s Hospital, Helsinki University Central Hospital, Helsinki, Finland

*Contributed equally as first authors.

Correspondence: Timo Otonkoski, M.D., Ph.D., Biomedicum Helsinki, Room C507b, P.O. Box 63, 00014 University of Helsinki, Helsinki, Finland. Telephone: 358-9-191-25692; Fax: 358-9-191-25610; E-Mail: timo.otonkoski@helsinki.fi

Received May 2, 2012; accepted for publication October 26, 2012; first published online in *SCTM EXPRESS* January 22, 2013.

©AlphaMed Press
1066-5099/2013/\$20.00/0

<http://dx.doi.org/10.5966/sctm.2012-0047>

differentiated phenotype, their uncontrolled differentiation capacity in embryoid bodies or teratomas, or their differentiation toward a single specific lineage [6, 17–19]. However, many extended protocols have been developed for the differentiation of specific derivatives of all germ lines, such as hepatocytes (endoderm), cardiomyocytes (mesoderm), or neurons and retinal cells (ectoderm). The rationale of our study was to systematically compare the capability of the same hiPSC and hESC lines to develop into functional cell types following the protocols optimized by researchers dedicated to their respective line of differentiation. We studied four hiPSC and three hESC lines for their ability to differentiate into functional hepatocyte-like cells (HLCs), beating cardiomyocytes, neurons forming active neuronal networks, and highly pigmented mature RPE cells. Cell lines hiPSC1 to hiPSC4 were derived in two different laboratories, from neonatal and adult fibroblasts using retroviral vectors. One of the cell lines was derived using *NANOG*, *OCT4*, *SOX2*, and *LIN28*, whereas the other cell lines were derived by overexpressing *OCT4*, *SOX2*, *KLF4*, and *c-MYC*. In addition, the hiPSC5 line was derived with an integration-free Sendai-viral system. All of the cell lines were adapted in the same culture conditions prior to each differentiation protocol to avoid variation caused by different culture environments. Our results did not point to a systematic difference in the differentiation efficiency between hiPSC and hESC lines, except for one cell line with incomplete transgene silencing. Re-activation of transgenes was occasionally observed, especially with a long RPE differentiation protocol. These observations raise concerns related to the use of integrating reprogramming methods.

MATERIALS AND METHODS

Ethical Issues

The Institute of Biomedical Technology has an approval of National Authority for Medicolegal Affairs Finland to study human embryos (Dnro1426/32/300/05), as well as the support of the Ethical Committee of Pirkanmaa Hospital District to derive, culture, and differentiate hESC lines from surplus human embryos (R05116) and to produce new hiPSC lines (R08070). The generation of hiPSC lines in Biomedicum Stem Cells Center Helsinki was approved by the Coordinating Ethics Committee of the Helsinki and Uusimaa Hospital District (Nro 423/13/03/00/08).

Cell Lines and Cell Culture

Three hESC lines (H7 [hESC1; WiCell Research Institute, Madison, WI, <http://www.wicell.org>], FES29 [hESC2] [20], and Regea 08/023 [hESC3] [21]) and five hiPSC lines (FiPS5-7 [hiPSC1] [22], UTA.00112.hFF [hiPSC2] [23], A116 [hiPSC3] [supplemental online Fig. 1], UTA.01006.WT [hiPSC4] [23], and Hel24.3 [hiPSC5] [supplemental online Fig. 1]) were used in this study. The hiPSC lines FiPS5-7 and UTA.00112.hFF were derived from human foreskin fibroblasts (hFFs) (CRL-2429; American Type Culture Collection, Manassas, VA, <http://www.atcc.org>), and the hiPSC lines A116, UTA.01006.WT, and Hel24.3 were derived from adult skin fibroblasts. FiPS5-7 (hiPSC1) was reprogrammed with *NANOG*, *OCT4*, *SOX2*, and *LIN28* and the other hiPSC lines with *OCT4*, *SOX2*, *KLF4*, and *c-MYC*. The cell lines used in this study are presented in supplemental online Table 1. Details of hiPSC reprogramming conditions are provided in the supplemental online Materials and Methods.

Differentiation Protocols

Pluripotent stem cell lines were differentiated into hepatocyte-like cells, cardiomyocytes, neural cells, and RPE cells. Detailed methods of differentiation and characterization are provided in the supplemental online Materials and Methods.

The efficiency of hepatic differentiation was evaluated by studying the expression of *OCT4*, *SOX17*, *FOXA2*, *AFP*, and *Albumin* at day (d) 7, d14, and d21 by quantitative polymerase chain reaction (qPCR) analysis and by studying the expression of OCT4, FOXA2, SOX17, AFP, and albumin with immunocytochemistry. The definitive endoderm induction was analyzed at d7 by flow cytometry for CXCR4+ cells, and the functionality of the differentiated hepatocyte-like cells was studied by albumin secretion measured with an enzyme-linked immunosorbent assay.

Cardiac differentiation was characterized by studying the expression of *Nanog*, *OCT4*, *SOX17*, *Brachyury T*, and *NKX2.5* at time points d0, d3, d6, d13, and d30 by qPCR and by studying the expression of α -actinin, Troponin T, connexin-43, and ventricular myosin heavy chain (MHC) with immunocytochemistry. The efficiency of cardiac differentiation was evaluated by immunocytochemical analysis of cytospin samples on day 20 and counting the number of beating areas in the end of differentiation on day 30. The functionality of the cardiomyocytes was analyzed using the microelectrode array (MEA) platform.

Neural differentiation was evaluated at the 4- and 8-week time points by studying the expression of *OCT4*, *Musashi*, *Neurofilament-68 (NF-68)*, and *glial fibrillary acidic protein (GFAP)* by qPCR and by studying the expression of OCT4, EpCAM, Nestin, microtubule-associated protein 2 (MAP-2), GFAP, brain lipid-binding protein (BLBP), chondroitin sulfate proteoglycan (NG2), and galactocerebroside (GalC) by immunocytochemistry. The morphological analysis was performed with time-lapse imaging. The spontaneous functionality of developing neuronal networks was characterized using MEA.

To evaluate putative RPE cell differentiation, the appearance of the first pigmented cells was followed daily and recorded. The percentage of pigment-containing cell aggregates from the total amount of aggregates was counted on day 28 ± 1 of the differentiation. The expression of *OCT4*, *MITF*, *BEST1*, and *RLBP1* was analyzed by qPCR from d0, d28, d52, and d82 of RPE differentiation. The expression of OCT4, MITF and bestrophin-1 proteins was quantified with cytospin analysis on day 82 or on day 116.

Statistical Analysis

Statistical analysis between two groups was performed with the unpaired Student's *t* test or Mann-Whitney *U* test according to the sample set. In the case of multiple groups, one-way analysis of variance and the Tukey post hoc test were used. A *p* value of $<.05$ was considered statistically significant.

RESULTS

Transgene Silencing

hiPSC lines hiPSC1 [22], hiPSC2 [23], and hiPSC4 [23] were independently established by retroviral infection (*OCT4*, *SOX2*, *c-MYC*, and *KLF4* or *OCT4*, *SOX2*, *NANOG*, and *LIN28*) and characterized as described previously [22, 23]. hiPSC3 and hiPSC5 (supplemental online Fig. 1) lines were separately characterized

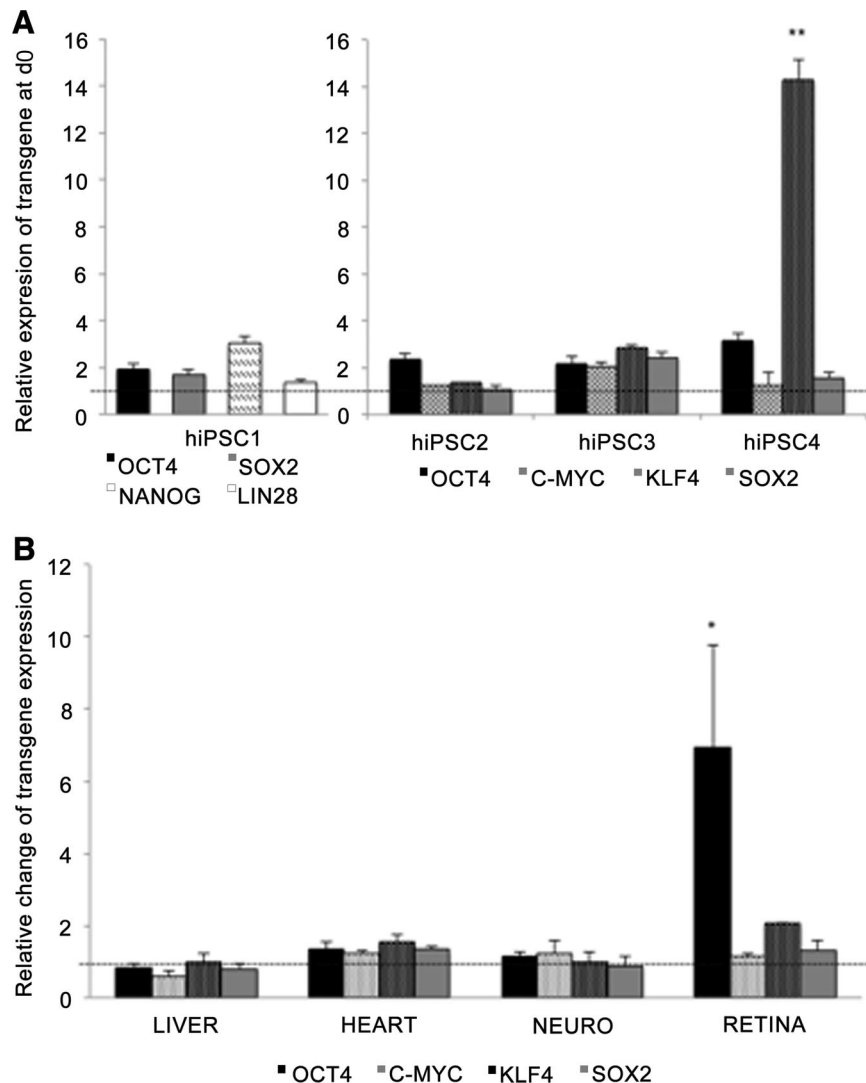


Figure 1. Transgene silencing. **(A):** Quantitative polymerase chain reaction (qPCR) analysis for expression of the transgenes *OCT4*, *SOX2*, *NANOG*, *LIN28*, *c-MYC*, and *KLF4* at the onset of differentiation (d0). The data are shown as the average (\pm SEM) relative value from four independent experiments. The value 1 indicates total silencing of transgenes. One-way analysis of variance with Tukey post hoc test was used for statistical analysis. **, $p < .01$. **(B):** qPCR analysis for activation of transgene expression during each differentiation protocol. The value 1 indicates no change in transgene expression. *, $p < .05$. Abbreviations: d, day; hiPSC, human induced pluripotent stem cell; NEURO, neural differentiation.

for this study. Relative transcriptional levels of the transgenes were studied by qPCR before and at the end of each differentiation protocol in lines hiPSC1–hiPSC4. The results revealed constant expression of exogenous *KLF4* in hiPSC4 at d0, whereas transgenes in other cell lines were silenced (Fig. 1A; supplemental online Fig. 2A). Transgene expression in general was not significantly induced by the differentiation protocols, with one remarkable exception. Levels of exogenous *OCT4* mRNA were systematically increased at the end of the long-term RPE differentiation protocol in all retrovirally derived hiPSC lines (Fig. 1B; supplemental online Fig. 2B), and *OCT4*⁺ cells could be detected by immunocytochemistry after 82 days of RPE differentiation (supplemental online Fig. 3B). In addition, exogenous *LIN28* and *NANOG* mRNA levels were markedly increased during the RPE differentiation in hiPSC1, the only cell line derived by overexpression of these factors (supplemental online Fig. 2B). When the Sendai-virally derived hiPSC5 line was differentiated into RPE

cells, no reactivation of transgene expression was detected (supplemental online Fig. 3A, 3B).

Definitive Endoderm Differentiation

Hepatocyte differentiation protocol consists of three stages, slightly modified from that described by Hay et al. [24] (Fig. 2A). The first stage directs the cells from pluripotent cells into committed definitive endoderm (DE) cells. In this stage, after 7 days from the onset of induction, all the cell lines had lost their embryonic stem-like small, round, and dense morphology and the cells were growing as homogeneous monolayers. qPCR analysis showed marked upregulation of the anterior definitive endoderm genes *SOX17* and *Hhex* in all lines at day 7 (Fig. 2B; supplemental online Fig. 4A). During differentiation, the expression of *OCT4* decreased in all cell lines and became undetectable by day 14. The process was somewhat slower in hiPSCs than hESCs (Fig. 2D). There was no change in

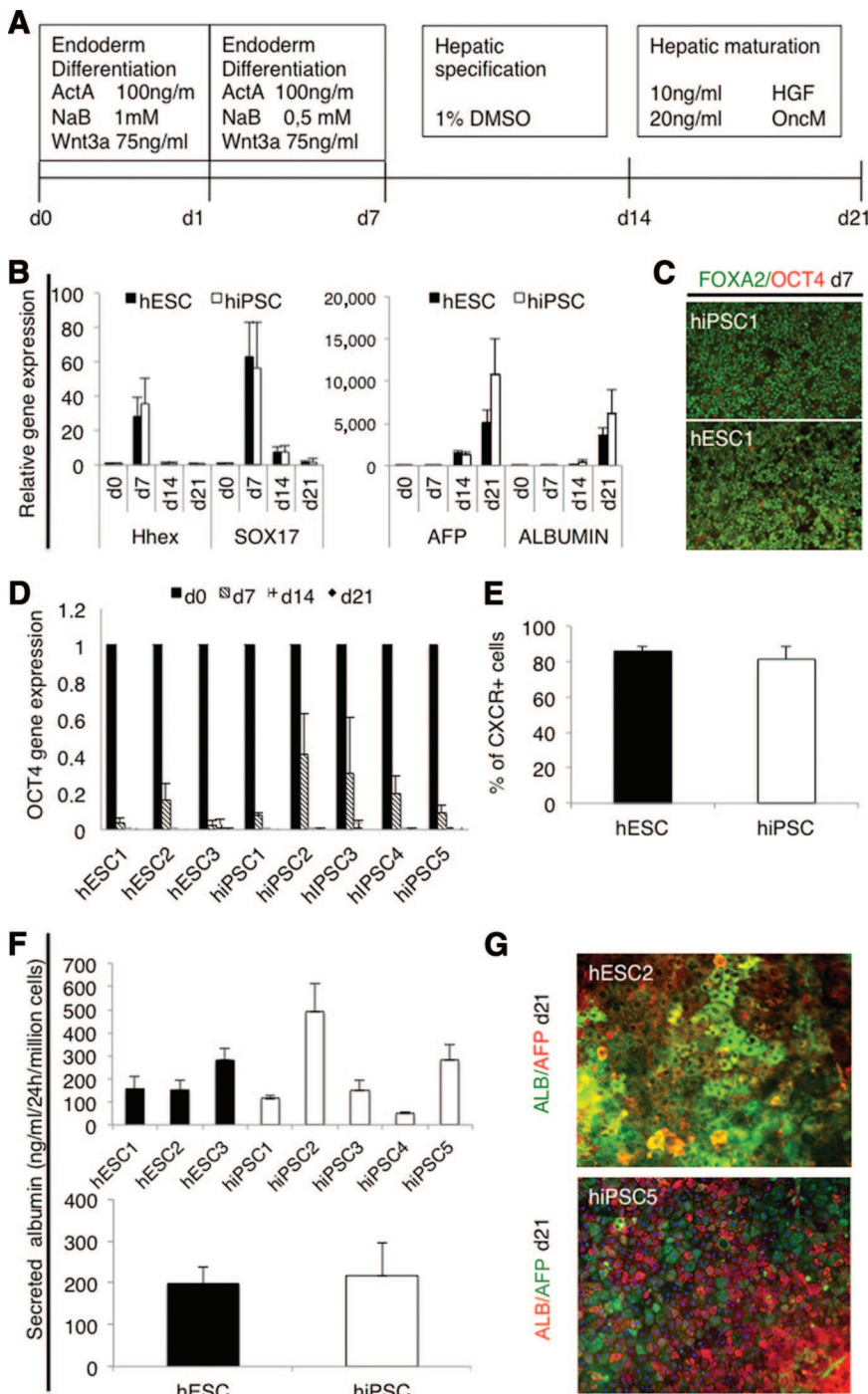


Figure 2. Hepatocyte differentiation. **(A):** Schematic presentation of the protocol used to differentiate human pluripotent stem cells into hepatocyte-like cells. **(B):** Quantitative polymerase chain reaction (qPCR) analysis for expression of the genes marking key stages of differentiation, first into definitive endoderm cells (*SOX17*, *Hhex*) and then into hepatocyte-like cells (*AFP*, *Albumin*). The columns show the average fold change from at least two independent experiments \pm SEM for each line. **(C):** Representative immunostaining after 7 days of differentiation, demonstrating that almost all cells expressed nuclear FOXA2 as a sign of definitive endoderm differentiation and very few cells still expressed the pluripotency marker OCT4. **(D):** qPCR analysis for expression of the pluripotency gene *OCT4* at d0, d7, d14, and d21. The columns show the average fold change from at least two independent experiments \pm SEM, demonstrating the rapid downregulation in both hESC and hiPSC lines. **(E):** Fluorescence-activated cell sorting analysis of cells expressing the endoderm marker CXCR4 at d7. Columns represent the average for hESCs ($n = 6$) and hiPSCs ($n = 8$). **(F):** Albumin secretion into the medium by the differentiated cells. In the upper graph, each cell line is presented separately (two or three repeated experiments). Lower graph shows the comparison between iPSCs ($n = 10$) and hESCs ($n = 6$). **(G):** Representative immunostaining after 21 days of differentiation of hESC2 and hiPSC5. Hepatocyte markers ALB and AFP are shown. Magnification, $\times 20$. Abbreviations: AFP, α -fetoprotein; ALB, albumin; d, day; DMSO, dimethyl sulfoxide; hESC, human embryonic stem cell; HGF, hepatocyte growth factor; hiPSC, human induced pluripotent stem cell.

the expression level of the extraembryonic endoderm gene *SOX7* (data not shown). In immunocytochemical analysis more than 90% of the cells were positive for definitive endoderm marker FOXA2, and very few if any OCT4⁺ cells could be found (Fig. 2C; supplemental online Fig. 5A). The percentage of CXCR4⁺ cells as analyzed by flow cytometry varied between 65% and 96% between all the lines (supplemental online Fig. 5B), and there were no significant difference between hESC ($n = 3$) and hiPSC ($n = 4$) lines in group comparison (Fig. 2E). These results suggest that the hESC and hiPSC lines used in this study differentiated into definitive endoderm stage with equal efficiency.

Hepatocyte Differentiation

The resulting DE cells were then differentiated into HLCs by 7-day culture in medium supplemented with 1% dimethyl sulfoxide (stage 2) and by a final maturation step in medium supplemented with hepatocyte growth factor and Oncostatin M for a further 7 days [24] (Fig. 2A). During this time the cells displayed morphological changes from a spiky shape to a polygonal shape. On day 21, the cultures contained foci exhibiting features of human hepatocytes, including a typical polygonal shape with distinct round nuclei, and many of the cells were binuclear (supplemental online Fig. 5C). Only hiPSC4-derived cells failed to develop a

distinct hepatocyte-like morphology (supplemental online Fig. 5C). In qPCR analysis, *AFP* was highly upregulated at day 14 and *Albumin* at day 21 (Fig. 2B; supplemental online Fig. 4A).

The HLCs derived from hiPSC2 expressed the highest levels of *AFP* and *Albumin*, whereas the expression of these hepatocyte-specific markers was nearly undetectable with hiPSC4-derived cells. Variation in the differentiation efficiency, as measured by albumin expression, was detected between hESCs and iPSCs, but the differences were not statistically significant in a group comparison. The hepatocyte-specific functionality of the differentiated cells was analyzed by albumin secretion assay. The results correlated well with qPCR data; there was no overall difference in albumin secretion rate between the hESC1–hESC3 lines and the hiPSC1–hiPSC5 lines in a group comparison, although there was variation between the individual cell lines (Fig. 2F), particularly because hiPSC4 failed to develop into albumin-secreting cells. Taken together, both the highest and the lowest levels of differentiation were observed in the hiPSC lines, whereas there was less variation among the hESC lines.

Cardiomyocyte Differentiation

hiPSC lines were differentiated into cardiomyocytes using the END-2 coculture method [25]. The progression of cardiac differentiation was monitored and cells analyzed as shown in Figure 3A. All four hiPSC and three hESC lines differentiated into beating cardiomyocytes, but the differentiation efficiency was variable. In addition, the cardiac differentiation efficiency varied between separate differentiation experiments within the same cell line. All cell lines formed compact structures in END-2 coculture except hiPSC4, which tended to form more cystic structures than the other cell lines. Cardiomyocytes derived from the cell lines expressed α -actinin, Troponin T, connexin-43, and MHC in immunocytochemical stainings (Fig. 3B). The electrical activity of cardiomyocytes was monitored with MEA measurements. The normal beating rate of the cell clusters was measured and the beating rate was increased by adding the β -adrenergic agonist isoprenaline to MEA chambers. All hESC- and hiPSC-derived cardiomyocytes beat and gave a signal on MEA and thus can be considered functional cardiomyocytes (Fig. 3C).

Quantitative immunocytochemical analysis was performed on cells cultured in END-2 cocultures on day 20, and beating areas were counted at the end of differentiation on day 30. The number of beating areas was highly variable between separate differentiation experiments within the same cell line. As a group, hESCs formed more beating areas than hiPSCs ($p < .001$, Fig. 3D). hESC1 had the most efficient cardiac differentiation efficiency, whereas hiPSC1 and hiPSC4 had the least efficient cardiac differentiation and the lowest number of beating areas (Fig. 3D). The results from the quantitative immunocytochemical analysis detecting cardiac Troponin T-positive cells were in accordance with the number of beating areas (Fig. 3E). In the hESC1 line, the beating areas were smaller than in other cell lines, but there were more beating areas. This may explain the difference between quantitative immunocytochemical results and the number of beating areas detected.

The expression of pluripotency markers *NANOG* and *OCT4* was highest on day 0 and descended during cardiac differentiation (supplemental online Fig. 6A, 6B). The expression of endodermal *SOX17* was the highest on day 3 in all hiPSC and hESC lines (supplemental online Fig. 6C). The expression of *Brachyury T* was also the highest on day 3 with the hESC lines (Fig. 3F). Interest-

ingly, with hiPSC lines the highest expression of *Brachyury T* was detected on day 6, and it was significantly higher in hiPSC lines than in hESC lines ($p = .003$), suggesting a slower tempo of cardiac differentiation. The expression of *Nkx2.5* ascended evenly during differentiation in all hiPSC and hESC lines.

Neural Differentiation

The neural differentiation protocol and the analyses used in this study are summarized in Figure 4A. Cell lines displayed clear differences when differentiated and cultured as neurospheres in neural differentiation medium. Neurospheres usually develop into firm cell aggregates within 2 weeks. The hiPSC3-derived neurospheres, however, showed persistent growth of unwanted cystic structures up to 4 weeks of differentiation (supplemental online Fig. 7). When the cysts were repeatedly manually removed from the cultures, the cyst formation declined. In addition to hiPSC3, the hiPSC2 line produced relatively fast-growing and less firm neurospheres. The growth of hiPSC4-derived neurospheres was weaker than that in the other lines. Neurospheres derived from hESC lines showed less variation during differentiation and culture.

According to qPCR analysis, the expression of *OCT4* was strongly downregulated within every cell line during the neural differentiation at 8 weeks (Fig. 4B). The downregulation was, however, significantly stronger in neurospheres derived from hESC than from hiPSC lines ($p < .01$). The expression of neural precursor cell marker *Musashi* and neural marker *NF-68* increased during differentiation, and both were significantly higher in neurospheres derived from hESCs than from hiPSC lines (*Musashi* week 8, $p = .034$; *NF-68* weeks 4 and 8, $p = .002$ and $p = .01$, respectively) (Fig. 4B). Expression of glial marker *GFAP* was undetectable in 0 and 4 weeks, and it was expressed at a low level in every cell line after 8 weeks of differentiation. Line-specific expression of *OCT4*, *Musashi*, and *NF-68* is shown in supplemental online Figure 4.

The cells were monitored with time-lapse imaging at 4 and 8 weeks during the neural differentiation. Quantitative analysis of time-lapse imaging data was performed by Cell-IQ analysis software (Chip-Man Technologies Ltd., Tampere, Finland) [26], but the accurate neuronal cell number could not be reliably determined because of confluence of the cultures (supplemental online Fig. 7). Qualitative analysis of the imaged data showed that hESC3 and hiPSC3 produced very pure neuronal populations in 8 weeks, whereas hiPSC4 was clearly the weakest cell line for neural differentiation, producing a lot of flat epithelial-like cells (Fig. 4C). The cells in hiPSC1-derived cultures were also mostly neuronal, but more cells with non-neuronal morphology were detected compared with hESC3- and hiPSC3-derived cultures.

Immunocytochemical staining supported the results of the time-lapse imaging analysis (Fig. 4D). The highest levels of MAP-2-positive cells were detected within hESC3- and hiPSC3-derived cultures. In hiPSC4-derived cultures only single cells positive for MAP-2 could be detected. The number of Nestin-positive cells decreased in all lines from 4 weeks to 8 weeks. No *OCT4*, *CD326*, *GFAP*, or *BLBP* was detected in any cell lines, indicating that no undifferentiated cells, astrocytes, or radial glial cells were present in the cultures. Only single cells positive for *NG2* or *GalC* could be detected at 8 weeks, indicating the presence of few oligodendrocyte precursor cells in the cultures (supplemental online Fig. 7).

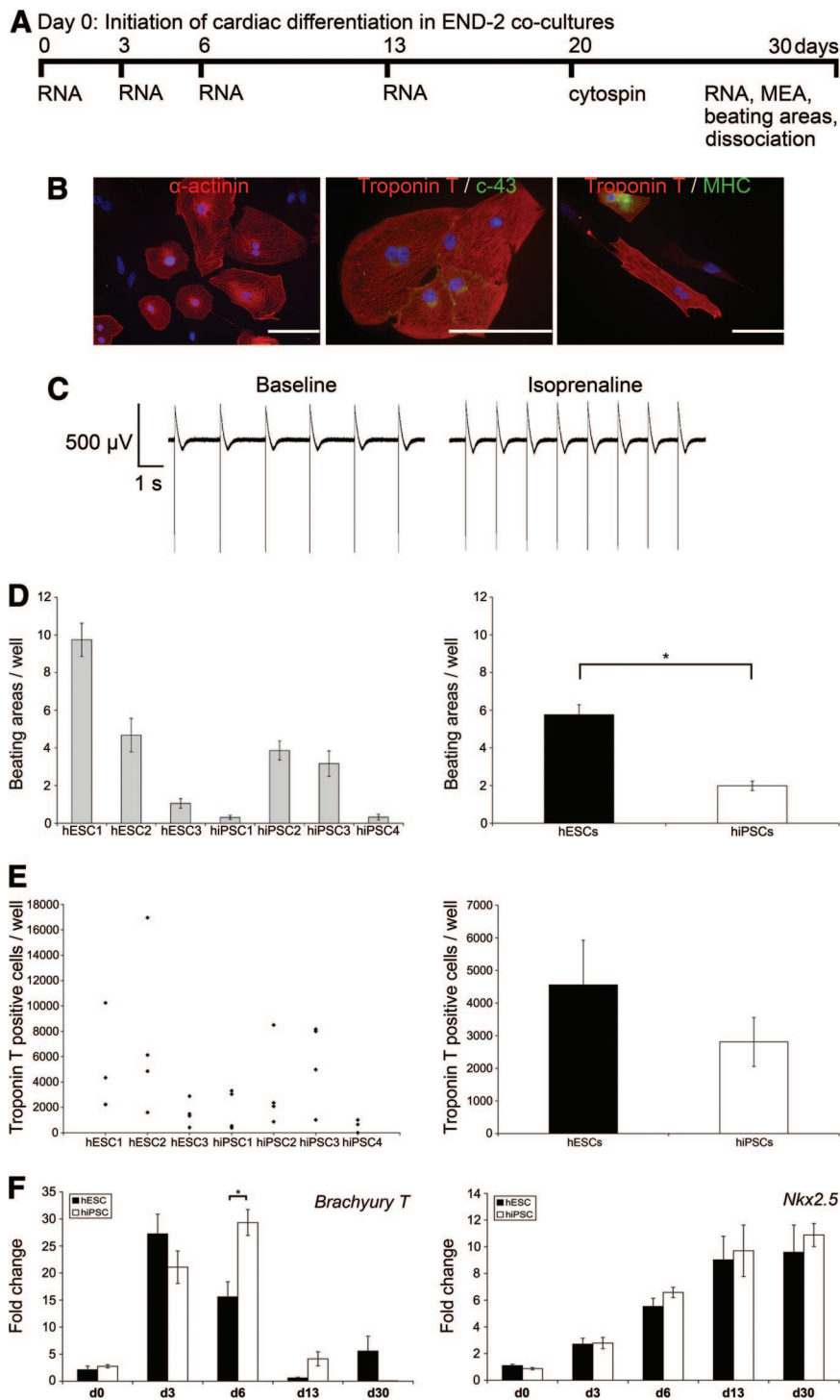


Figure 3. Cardiomyocyte differentiation. **(A):** Schematic presentation of the cardiac differentiation protocol and experimental design. **(B):** Cardiomyocytes derived from all human pluripotent stem cell (hPSC) lines expressed α -actinin, connexin-43, and ventricular myosin heavy chain proteins. Representative images of hiPSC2 line. Scale bars = 100 μ m. **(C):** All hPSC lines gave a signal on the MEA platform, and the beating rate was increased by isoprenaline (80 nM). Shown are representative images of the hiPSC3 line. **(D):** The number of beating areas in one well with each hPSC line (left) and in hESC and hiPSC groups (right). Error bars show the SEM. *, $p < .001$. **(E):** Scatter plots (left) show the number of Troponin T-positive cells in one well, and the columns (right) show the Troponin T-positive cells found in the hESC and hiPSC groups. Error bars show the SEM. **(F):** Results of the gene expression analysis on *Brachyury T* and *Nkx2.5* genes at the d0, d3, d6, d13, and d30 time points during cardiac differentiation. The expression of genes was compared between hESC and hiPSC lines. In hiPSC lines the highest expression of *Brachyury T* was detected on day 6, and it was significantly higher in hiPSC lines than in hESC lines (*, $p < .003$). Error bars show the SEM. Abbreviations: c-43, connexin-43; d, day; hESC, human embryonic stem cell; hiPSC, human induced pluripotent stem cell; MEA, microelectrode array; MHC, myosin heavy chain; RNA, quantitative polymerase chain reaction samples.

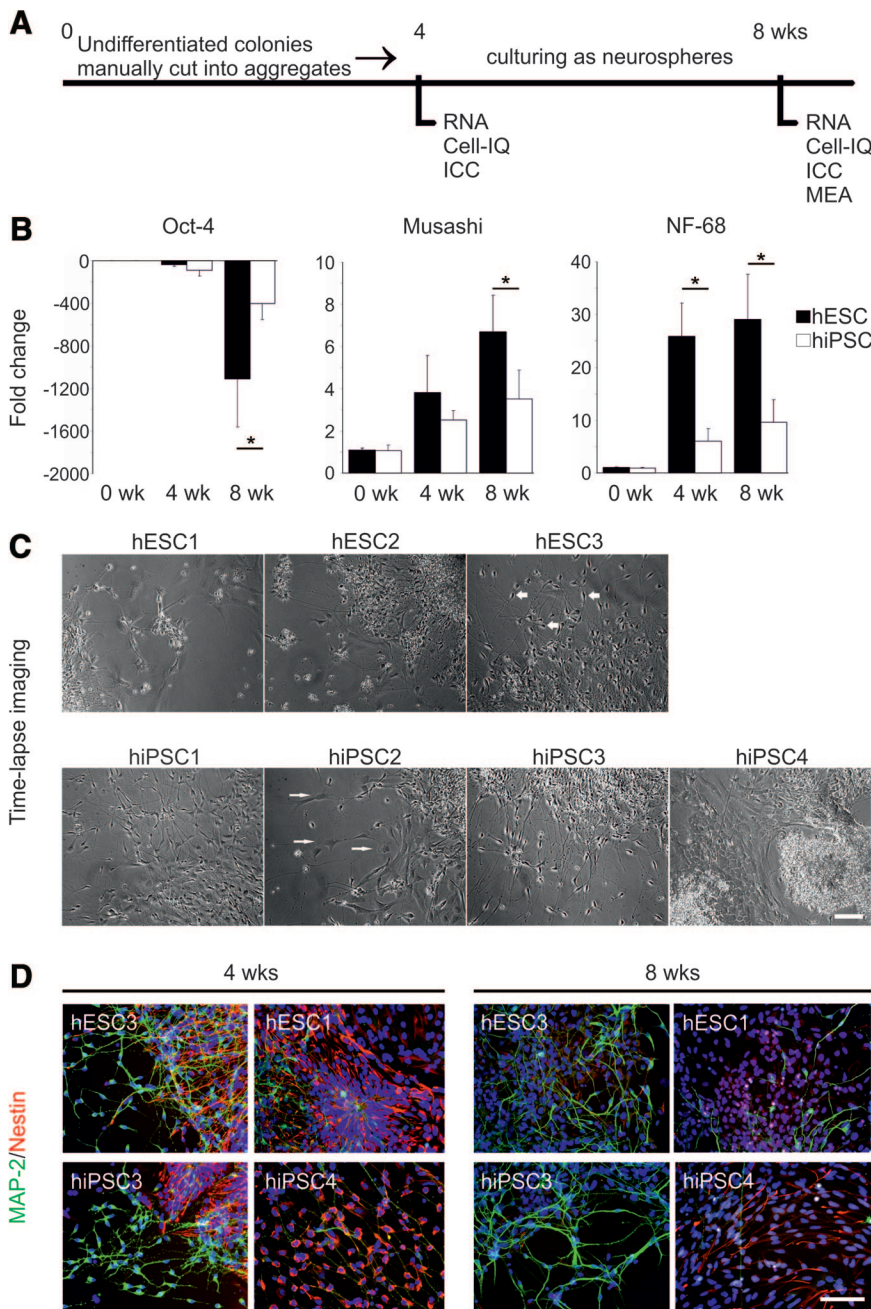


Figure 4. Neuronal differentiation. **(A):** Schematic presentation of the neural differentiation protocol and experimental design. **(B):** Results of the gene expression analysis of *OCT4*, *Musashi*, and *NF-68* at the 0-, 4-, and 8-week time points. The expressions of the genes were compared between hESC and hiPSC lines. Columns represent an average of hESC ($n = 3$) and hiPSC ($n = 4$) lines \pm SEM. *Musashi* week 8, $p = .034$; *NF-68* weeks 4 and 8, $p = .002$ and $p = .01$, respectively. *, $p < .05$, Mann-Whitney U test. **(C):** Morphologies of the cells derived from different cell lines at the 8-week time point. hESC3-, hiPSC1-, and hiPSC3-derived cells displayed mostly neuronal morphology (thick arrows), whereas other cell lines produced cells with flat epithelial cell-like morphology (thin arrows). Scale bar = 100 μ m. **(D):** Immunocytochemical characteristics of the differentiated cells. Neural precursor cell marker Nestin (red) and neural marker MAP-2 (green) were both detected in all the populations derived from hESC and hiPSC lines. Cell cultures derived from hESC3 and hiPSC3 lines were detected with high amounts of MAP-2-positive cells at both time points, whereas clearly fewer MAP-2-positive cells could be detected from the cultures of hESC1 and hiPSC4. The number of Nestin-positive cells decreased within all the cell lines from 4 to 8 weeks. Scale bar = 100 μ m. Abbreviations: Cell-IQ, time-lapse imaging; hESC, human embryonic stem cell; hiPSC, human induced pluripotent stem cell; ICC, immunocytochemistry; MAP-2, microtubule-associated protein 2; MEA, microelectrode array; NF-68, Neurofilament-68; RNA, quantitative polymerase chain reaction samples; wk, week.

Downloaded from stemcellstm.alphaamedpress.org by MARISA OJALA on February 21, 2013

Electrophysiological Properties of Neuronal Networks

As previously described [27], the first form of electrical activity detected from the neuronal networks was single spikes, whereas the mature neuronal networks displayed bursts containing multiple spikes simultaneously on several electrodes (supplemental online Fig. 8). The cell lines with the highest neural differentiation efficiencies based on morphological and immunocytochemical characterizations (hESC3 and hiPSC3) displayed burst-activity within 3 weeks in MEA culture. The spontaneously active bursting neuronal networks were routinely recorded from hESC3- and hiPSC3-derived cultures. The neuronal networks formed by the other cell lines displayed activities varying from single spikes to bursts.

RPE Differentiation

The hESC and hiPSC1–hiPSC5 lines were differentiated into RPE cells according to a previously reported protocol, which is based on spontaneous differentiation in EB-like cultures [8]. The differentiation protocol and analyses are summarized in Figure 5A. The RPE differentiation potential of the cell lines was studied by monitoring the appearance of the first pigmented cells emerging in the cultures. In addition, the percentage of cell clusters containing pigmented cells was counted on day 28 after initiation of differentiation.

All the examined cell lines produced pigmented cells on average within 22 days after initiation of differentiation (Fig. 5B). hESC lines produced pigmented cells on average 2 days earlier than hiPSC lines. The first pigmented cells were detected on day

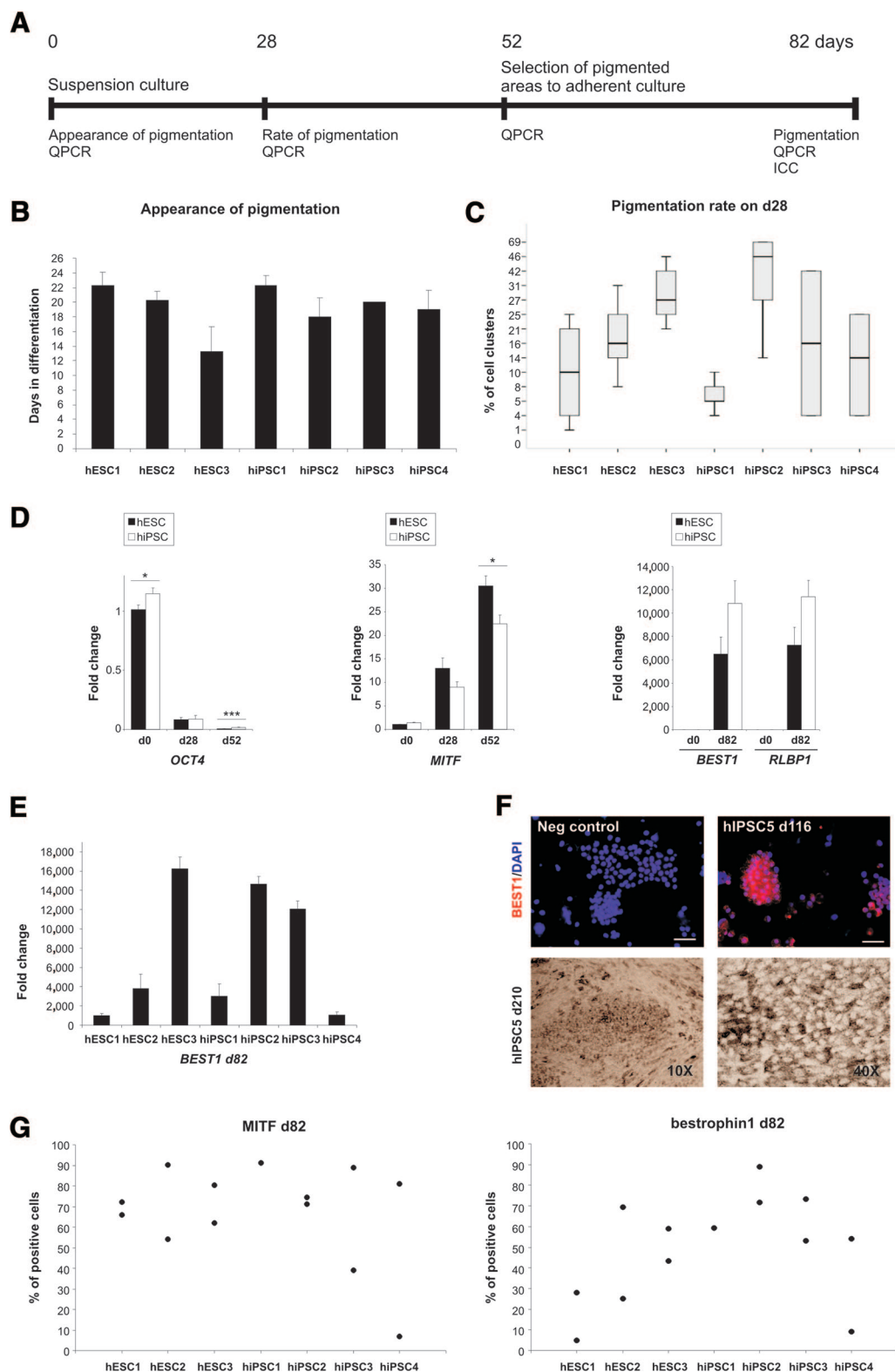


Figure 5. Retinal pigment epithelial (RPE) differentiation. **(A):** Schematic representation of the RPE differentiation protocol and experimental design. **(B):** Appearance of the first pigmented cells in the cultures at the beginning of RPE differentiation. Columns are representing an average of two to four independent experiments (n) \pm SEM. Shown are hESC1 ($n = 4$), hESC2 ($n = 4$), hESC3 ($n = 3$), hiPSC1 ($n = 4$), hiPSC2 ($n = 3$), hiPSC3 ($n = 2$), and hiPSC4 ($n = 3$). **(C):** Rate of pigmentation on differentiation day 28. Box plots show the sample minimum, lower quartile, median, upper quartile, and sample maximum of two to four independent experiments. The number of experiments/total number of cell clusters counted were as follows: hESC1, 4/674; hESC2, 3/448; hESC3, 3/339; hiPSC1, 3/656; hiPSC2, 3/427; hiPSC3, 2/445; and hiPSC4, 2/704. **(D):** QPCR analysis for expression of genes marking key stages of human pluripotent stem cell differentiation (*OCT4*) into pigment-producing cells (*MITF*) and subsequently into RPE-like cells (*BEST1* and *RLBP1*). The columns show the average fold change from at least two

Table 1. Differentiation potential of individual human pluripotent stem cell lines

Cell line	Endodermal lineage: hepatocyte	Mesodermal lineage: cardiac	Ectodermal lineage	
			Neuronal	RPE
hESC1	++	+++	+	+
hESC2	++	++	++	++
hESC3	+++	+	+++	+++
hiPSC1	++	+	++	+
hiPSC2	+++	++	++	+++
hiPSC3	++	++	+++	++
hiPSC4	+	+	+	+
hiPSC5	+++	+	+	+++

Shown is the differentiation efficiency of the cell lines based on the rate of albumin secretion (hepatocyte), number of beating cardiomyocytes (cardiac), morphological and immunocytochemical criteria (neural), and rate of pigmentation (retinal pigment epithelial). + indicates lower differentiation potential than average, ++ indicates average differentiation capacity, and +++ indicates excellent differentiation capacity.

Abbreviations: hESC, human embryonic stem cell; hiPSC, human induced pluripotent stem cell; RPE, retinal pigment epithelial.

13 (hESC3). On day 28, the highest proportion of pigmented cell clusters in hESC lines was detected in hESC3 (31%) and the lowest in hESC1 (11%) (Fig. 5C). Of the hiPSC lines, the best performer was hiPSC2 (43%) and the weakest hiPSC1 (6%) (Fig. 5C). In a groupwise comparison, none of the differences between the hESC and hiPSC lines were statistically significant.

During differentiation, the expression of endogenous *OCT4* decreased in all cell lines. However, it was higher in the hiPSC than in the hESC lines on day 0 ($p = .03$) and day 52 ($p < .001$) (Fig. 5D). Expression of the selected differentiation markers *MITF*, *BEST1*, and *RLBP1* increased in all cell lines during differentiation. In a comparison of hESC and hiPSC lines, the pigment cell marker *MITF* was higher in hESC on day 52 ($p = .011$) (Fig. 5D). The more RPE-specific markers *BEST1* and *RLBP1* appeared higher on d82 in the hiPSC lines, but the differences were not statistically significant (Fig. 5D). The Sendai-virally derived hiPSC5 line was characterized only partially, but it also differentiated into pigmented epithelium with cobblestone morphology and bestrophin-1 immunoreactivity (Fig. 5F). At the protein level, all cell lines expressed *MITF* and bestrophin-1 proteins. The highest proportion of *MITF*-positive cells in hESC lines was detected in hESC2 (72%) and the lowest in hESC1 (69%). The results were less reproducible in the hiPSC lines (Fig. 5G). Bestrophin-1-positive cells tended to be more abundant in the hiPSC than the hESC lines (Fig. 5G), and the results correlated with *BEST1* gene expression and also with the rate of pigmentation.

When analyzed comprehensively, it appears that the hESC lines (particularly hESC1 and hESC3) displayed variable propensities for mesodermal versus ectodermal differentiation. The same cell lines differentiated consistently more efficiently in the ectodermal (neuronal and RPE) directions or mesodermal (cardiac) direction. However, none of the induced pluripotent stem cell (iPSC) lines showed such preferential differentiation capacity (Table 1).

DISCUSSION

We studied the differentiation capacity of three hESC and five hiPSC lines. The four retrovirally derived hiPSC lines were characterized in detail using four well-established differentiation protocols and specific functional assays. Through this approach, we hope to elucidate the true variability between human pluripotent stem cell lines with respect to their most important characteristic: the ability to develop into physiologically functional cell types.

To our knowledge, our study is the first to use four separate extended differentiation protocols into derivatives of all germ layers in a systematic comparison of hPSC lines. In this study most of the cell lines showed no differentiation preference toward any specific cell lineages but rather showed more or less differentiation potential toward all different cell types produced. Only two of the cell lines (hESC1 and hESC3) had consistently more differentiation potential toward specific lineages. hESC1 differentiated well into beating cardiomyocytes and poorly into ectodermal lineages, and hESC3 had the best ectodermal differentiation capacity but produced few beating areas in cardiomyocyte differentiation. One reason for these differences may be the fact that the cardiac (END2 coculture) and neuronal (EB formation) protocols in this study are based more on the spontaneous differentiation of the cells than the hepatocyte protocol, which is based on guidance by specific growth factors. It is likely that the genetic background of the cells plays a more crucial role in the former than the latter situation.

Analysis of transgene expression showed that *KLF4* was incompletely silenced in hiPSC4 (Fig. 1A; supplemental online Fig. 2A), suggesting that this cell line was only partially reprogrammed. The retroviral transgenes are usually silenced as a late event of the reprogramming process [28] because of the activation of DNA [29] and histone methyltransferases [12]. This process, however, is often incomplete, resulting in partially reprogrammed cell lines [9, 30, 31]. This residual activity of viral transgenes in hiPSC-derived cells can affect their developmental potential [9]. Partially incomplete reprogramming may explain the poor differentiation capacity of hiPSC4, which was observed throughout this study.

All of the hESC and hiPSC lines differentiated efficiently into early DE progenitors. However, when the DE cells were further induced into HLCs some variability became evident. Although all the hESC lines differentiated with approximately equal efficiency, the iPSC lines were much more variable, ranging from very poor (hiPSC4) to excellent (hiPSC2). This variation was not correlated with the method used for hiPSC induction, and it is unlikely that it would be due to the different donor age (neonatal vs. adult). It has also been noted by others that there are differences in the timing of onset of expression of hepatocyte-specific genes between different cell lines [7].

The cardiomyocyte differentiation protocol used in this study produced beating areas from all the cell lines with variable efficiency. Overall, cardiac differentiation on END-2 cocultures is rather unspecific, and many other cell types besides cardiomyocytes are also induced [32]. Normally, the highest peak of

independent experiments \pm SEM. *, $p < .05$; ***, $p < .001$. Statistical analyses were performed with independent samples *t* test or Mann-Whitney *U* test according to the sample set. (E): QPCR analysis for expression of *BEST1* on d82 in each analyzed cell line. The columns show the average fold change from at least two independent experiments \pm SEM. (F): Top row: Bestrophin-1 (BEST1) staining for cytospin samples collected from hiPSC5-derived RPE cells. Bottom row: pigmented cells derived from hiPSC5 at d210 in passage 2. (G): Expression of *MITF* and bestrophin-1 proteins on d82. Scatter plots show the percentage of positive cells from one or two independent experiments. The total number of cells counted were as follows for *MITF*/bestrophin-1: hESC1, 326/274; hESC2, 351/337; hESC3, 466/454; hiPSC1, 184/202; hiPSC2, 579/518; hiPSC3, 355/402; and hiPSC4, 288/269. Abbreviations: d, day; hESC, human embryonic stem cell; hiPSC, human induced pluripotent stem cell; ICC, immunocytochemistry; Neg, negative; QPCR, quantitative polymerase chain reaction.

Brachyury T expression is observed on day 3 in END-2 cocultures [32], and the delayed expression peak leads to poor cardiac differentiation efficiency [33, 34]. In this study, the expression peak of *Brachyury T* was extended up to day 6 with hiPSCs, which was associated with a lower lowest number of beating areas than in hESCs. However, high variation in cardiac differentiation efficiency was also detected between different passages/differentiation experiments within the same cell line, indicating that the cell line characteristics change over time in culture.

The neural differentiation protocol used here has been used routinely with several hESC lines previously [35, 36]. Both hESC and hiPSC lines were successfully differentiated toward neural cells regardless of their origin. Previous studies have, however, demonstrated the differences between the innate differentiation propensities within hESC and hiPSC lines [11, 16–18, 35] and between hESC and hiPSC lines [6]. In contrast, two other studies have suggested that in general, hESCs and hiPSCs have similar differentiation capacity toward neural cells, but line-specific variation can be detected in both groups [16, 17]. Our results were more compatible with the latter view.

Electrophysiological properties are an essential aspect of the characterization of neuronal cells. In the present study, all the cell lines differentiated into neuronal networks that were able to display some form of spontaneous electrical activity regarded as a feature of functional neuronal networks [27, 37]. However, obvious maturation stage-related functional variability was observed. None of the gene or protein level markers of neuronal differentiation directly correlated with the functional properties of the derived neuronal networks. Thus, it is difficult to predict the efficiency of a particular cell line to produce functional neuronal networks without electrophysiological analyses.

Lastly, we differentiated the hPSCs into another ectodermal cell type, RPE cells. During mammalian development, RPE is derived from optic neuroepithelium by approximately the seventh week of gestation [38], and RPE cell fate specification *in vitro* has been shown to follow a time course reminiscent of normal retinal development [39]. All the cell lines examined produced pigmented cells within 3 weeks after initiation of differentiation. On average, hiPSC lines produced pigmented cells slightly more slowly than hESC lines. This is compatible with the findings by Meyer et al., who also reported longer differentiation times with hiPSCs than hESCs [39]. hESC3 produced pigmented cells the fastest. This cell line also produced eventually mature RPE cells. Two hiPSC lines also produced mature RPE cells, suggesting that the time of pigment appearance is not a crucial factor for the later maturation of RPE cells.

Consistent reactivation of the *OCT4* transgene was observed in all retrovirally induced hiPSC lines during RPE differentiation (Fig. 1B; supplemental online Fig. 2B). The reactivation was most dramatic in hiPSC1. In addition, the *NANOG* and *LIN28* transgenes were also reactivated in hiPSC1 during the RPE differentiation. On the contrary, transgene reactivation was not observed with the Sendai virus-induced iPSC5 line (supplemental online Fig. 3). Interestingly, hiPSC1 was differentiated successfully into both HLCs and cardiomyocytes, and transgene reactivation was not seen during those experiments. During RPE differentiation, hiPSC1 appeared to produce a high number of MITF and bestrophin-1-positive cells. However, hiPSC1-derived RPE cells peeled off from the culture membranes easily, allowing only one successful experiment to be completed. The RPE differentiation protocol is much (almost 3 months) longer and more spontaneous than the other protocols, which could be

one explanation for the difference. Obviously, these observations raise concerns about the safety of hiPSCs that have integrated transgenes in their genome.

CONCLUSION

Part of the variation in the differentiation efficiency between the individual hiPSCs could be explained by residual activity of viral transgene *KLF4* in hiPSC4 and the reactivation of several transgenes during RPE differentiation. In contrast, the hiPSC line that was derived through the nonintegrating Sendai virus technology differentiated well into both HLCs and RPE cells and did not show signs of transgene expression. Our study strongly suggests that many of the “first-generation” retrovirally derived iPSC lines are hampered by potential transgene reactivation, with specific effects on their further differentiation properties. These findings highlight the need for integration-free reprogramming technologies, resulting in transgene-free iPSCs, which could also be potentially therapeutically applicable, unlike the retrovirally derived cells used in this study. Several such technologies have been established, in addition to Sendai viruses [40]: polycistronic minicircle vectors [41], PiggyBac transposons [42], and modified mRNA-based [43] or protein transduction-based methods [44]. Future studies should focus on nontransgenic iPSC lines generated through these methods.

ACKNOWLEDGMENTS

We are grateful to the following individuals for technical assistance: Markus Haponen, Maria af Hällström, Merja Lehtinen, Henna Venäläinen, Elina Konsén, Hanna Koskenaho, Outi Melin, Jarkko Ustinov, and Eila Korhonen. We thank Juha Heikkilä and Meeri Mäkinen for assistance with MEA measurements. This study was supported by funding from Biocenter Finland for the national platform on stem cells and biomaterials. Additional grant support was received from the Academy of Finland (to H.S., S.N., K.A.-S., T.O.), the Competitive Research Funding of the Pirkanmaa Hospital District (to H.S., S.N., K.A.-S.), the Alfred Kordelin Foundation (to K.A.-S.), the Finnish Foundation of Cardiovascular Research (to K.A.-S.), the Finnish Funding Agency for Technology and Innovation (to K.A.-S.), the Päivikki and Sakari Sohlberg Foundation (to H.S.), the Sigrid Jusélius Foundation (to T.O.), and the Competitive Research Funding of the Uusimaa Hospital District (to T.O.).

AUTHOR CONTRIBUTIONS

S.T., M.O., A.H., T.I., K.R., and R.Ä.: conception and design, collection and assembly of data, data analysis and interpretation, manuscript writing; M.P.-M.: conception and design, data analysis and interpretation; K.L.: conception and design, collection and assembly of data; J.P.: collection and assembly of data, data analysis and interpretation; J.W. and R.T.: provision of study material, collection and assembly of data; O.S.: conception and design, financial support; H.S.: conception and design, financial support, data analysis and interpretation, final approval of manuscript; S.N.: conception and design, financial support, provision of study material, final approval of manuscript; K.A.-S. and T.O.: conception and design, financial support, provision of study material, data analysis and interpretation, manuscript writing, final approval of manuscript.

DISCLOSURE OF POTENTIAL CONFLICTS OF INTEREST

The authors indicate no potential conflicts of interest.

REFERENCES

- 1 Robinton DA, Daley GQ. The promise of induced pluripotent stem cells in research and therapy. *Nature* 2012;481:295–305.
- 2 Thomson JA, Itskovitz-Eldor J, Shapiro SS et al. Embryonic stem cell lines derived from human blastocysts. *Science* 1998;282:1145–1147.
- 3 Takahashi K, Tanabe K, Ohnuki M et al. Induction of pluripotent stem cells from adult human fibroblasts by defined factors. *Cell* 2007;131:861–872.
- 4 Yu J, Vodyanik MA, Smuga-Otto K et al. Induced pluripotent stem cell lines derived from human somatic cells. *Science* 2007;318:1917–1920.
- 5 Cao N, Liu Z, Chen Z et al. Ascorbic acid enhances the cardiac differentiation of induced pluripotent stem cells through promoting the proliferation of cardiac progenitor cells. *Cell Res* 2012;22:219–236.
- 6 Hu BY, Weick JP, Yu J et al. Neural differentiation of human induced pluripotent stem cells follows developmental principles but with variable potency. *Proc Natl Acad Sci USA* 2010;107:4335–4340.
- 7 Si-Tayeb K, Noto FK, Nagaoka M et al. Highly efficient generation of human hepatocyte-like cells from induced pluripotent stem cells. *Hepatology* 2010;51:297–305.
- 8 Vaajasaari H, Ilmarinen T, Juuti-Uusitalo K et al. Toward the defined and xeno-free differentiation of functional human pluripotent stem cell-derived retinal pigment epithelial cells. *Mol Vis* 2011;17:558–575.
- 9 Takahashi K, Yamanaka S. Induction of pluripotent stem cells from mouse embryonic and adult fibroblast cultures by defined factors. *Cell* 2006;126:663–676.
- 10 Chin MH, Mason MJ, Xie W et al. Induced pluripotent stem cells and embryonic stem cells are distinguished by gene expression signatures. *Cell Stem Cell* 2009;5:111–123.
- 11 Bock C, Kiskinis E, Verstappen G et al. Reference maps of human ES and iPS cell variation enable high-throughput characterization of pluripotent cell lines. *Cell* 2011;144:439–452.
- 12 Matsui T, Leung D, Miyashita H et al. Proviral silencing in embryonic stem cells requires the histone methyltransferase ESET. *Nature* 2010;464:927–931.
- 13 Lister R, Pelizzola M, Kida YS et al. Hotspots of aberrant epigenomic reprogramming in human induced pluripotent stem cells. *Nature* 2011;471:68–73.
- 14 Hu Q, Friedrich AM, Johnson LV et al. Memory in induced pluripotent stem cells: Reprogrammed human retinal-pigmented epithelial cells show tendency for spontaneous redifferentiation. *STEM CELLS* 2010;28:1981–1991.
- 15 Ieda M, Fu JD, Delgado-Olguin P et al. Direct reprogramming of fibroblasts into functional cardiomyocytes by defined factors. *Cell* 2010;142:375–386.
- 16 Kim K, Zhao R, Doi A et al. Donor cell type can influence the epigenome and differentiation potential of human induced pluripotent stem cells. *Nat Biotechnol* 2011;29:1117–1119.
- 17 Boulting GL, Kiskinis E, Croft GF et al. A functional characterized test set of human induced pluripotent stem cells. *Nat Biotechnol* 2011;29:279–286.
- 18 Osafune K, Caron L, Borowiak M et al. Marked differences in differentiation propensity among human embryonic stem cell lines. *Nat Biotechnol* 2008;26:313–315.
- 19 Zhang J, Wilson GF, Soerens AG et al. Functional cardiomyocytes derived from human induced pluripotent stem cells. *Circ Res* 2009;104:e30–e41.
- 20 Mikkola M, Olsson C, Palgi J et al. Distinct differentiation characteristics of individual human embryonic stem cell lines. *BMC Dev Biol* 2006;6:40.
- 21 Skottman H. Derivation and characterization of three new human embryonic stem cell lines in Finland. *In Vitro Cell Dev Biol Anim* 2010;46:206–209.
- 22 Hussein SM, Batada NN, Vuoristo S et al. Copy number variation and selection during reprogramming to pluripotency. *Nature* 2011;471:58–62.
- 23 Lahti AL, Kujala VJ, Chapman H et al. Model for long QT syndrome type 2 using human iPS cells demonstrates arrhythmogenic characteristics in cell culture. *Dis Model Mech* 2012;5:220–230.
- 24 Hay DC, Fletcher J, Payne C et al. Highly efficient differentiation of hESCs to functional hepatic endoderm requires ActivinA and Wnt3a signaling. *Proc Natl Acad Sci USA* 2008;105:12301–12306.
- 25 Passier R, Oostwaard DW, Snapper J et al. Increased cardiomyocyte differentiation from human embryonic stem cells in serum-free cultures. *STEM CELLS* 2005;23:772–780.
- 26 Huttunen TT, Sundberg M, Pihlajamäki H et al. An automated continuous monitoring system: A useful tool for monitoring neuronal differentiation of human embryonic stem cells. *Stem Cell Studies* 2011;1:71–77.
- 27 Heikkilä TJ, Yla-Outinen L, Tanskanen JM et al. Human embryonic stem cell-derived neuronal cells form spontaneously active neuronal networks in vitro. *Exp Neurol* 2009;218:109–116.
- 28 Stadtfeld M, Maherali N, Breault DT et al. Defining molecular cornerstones during fibroblast to iPS cell reprogramming in mouse. *Cell Stem Cell* 2008;2:230–240.
- 29 Lei H, Oh SP, Okano M et al. De novo DNA cytosine methyltransferase activities in mouse embryonic stem cells. *Development* 1996;122:3195–3205.
- 30 Mikkelsen TS, Hanna J, Zhang X et al. Dissecting direct reprogramming through integrative genomic analysis. *Nature* 2008;454:49–55.
- 31 Sridharan R, Tchiew J, Mason MJ et al. Role of the murine reprogramming factors in the induction of pluripotency. *Cell* 2009;136:364–377.
- 32 Beqqali A, Kloots J, Ward-van Oostwaard D et al. Genome-wide transcriptional profiling of human embryonic stem cells differentiating to cardiomyocytes. *STEM CELLS* 2006;24:1956–1967.
- 33 Bettiol E, Sartiani L, Chicha L et al. Fetal bovine serum enables cardiac differentiation of human embryonic stem cells. *Differentiation* 2007;75:669–681.
- 34 Pekkanen-Mattila M, Ojala M, Kerkela E et al. The effect of human and mouse fibroblast feeder cells on cardiac differentiation of human pluripotent stem cells. *Stem Cells Int* 2012;2012:875059.
- 35 Lappalainen RS, Salomaki M, Yla-Outinen L et al. Similarly derived and cultured hESC lines show variation in their developmental potential towards neuronal cells in long-term culture. *Regen Med* 2010;5:749–762.
- 36 Sundberg M, Jansson L, Ketolainen J et al. CD marker expression profiles of human embryonic stem cells and their neural derivatives, determined using flow-cytometric analysis, reveal a novel CD marker for exclusion of pluripotent stem cells. *Stem Cell Res* 2009;2:113–124.
- 37 Pine J. Recording action potentials from cultured neurons with extracellular microcircuit electrodes. *J Neurosci Methods* 1980;2:19–31.
- 38 Fuhrmann S. Eye morphogenesis and patterning of the optic vesicle. *Curr Top Dev Biol* 2010;93:61–84.
- 39 Meyer JS, Shearer RL, Capowski EE et al. Modeling early retinal development with human embryonic and induced pluripotent stem cells. *Proc Natl Acad Sci USA* 2009;106:16698–16703.
- 40 Fusaki N, Ban H, Nishiyama A et al. Efficient induction of transgene-free human pluripotent stem cells using a vector based on Sendai virus, an RNA virus that does not integrate into the host genome. *Proc Jpn Acad Ser B Phys Biol Sci* 2009;85:348–362.
- 41 Jia F, Wilson KD, Sun N et al. A nonviral minicircle vector for deriving human iPS cells. *Nat Methods* 2010;7:197–199.
- 42 Woltjen K, Michael IP, Mohseni P et al. piggyBac transposition reprograms fibroblasts to induced pluripotent stem cells. *Nature* 2009;458:766–770.
- 43 Warren L, Manos PD, Ahfeldt T et al. Highly efficient reprogramming to pluripotency and directed differentiation of human cells with synthetic modified mRNA. *Cell Stem Cell* 2010;7:618–630.
- 44 Kim D, Kim CH, Moon JI et al. Generation of human induced pluripotent stem cells by direct delivery of reprogramming proteins. *Cell Stem Cell* 2009;4:472–476.



See www.StemCellsTM.com for supporting information available online.

Comparative Analysis of Targeted Differentiation of Human Induced Pluripotent Stem Cells (hiPSCs) and Human Embryonic Stem Cells Reveals Variability Associated With Incomplete Transgene Silencing in Retrovirally Derived hiPSC Lines

Sanna Toivonen, Marisa Ojala, Anu Hyysalo, Tanja Ilmarinen, Kristiina Rajala, Mari Pekkanen-Mattila, Riikka Äänismaa, Karolina Lundin, Jaan Palgi, Jere Weltner, Ras Trokovic, Olli Silvennoinen, Heli Skottman, Susanna Narkilahti, Katriina Aalto-Setälä and Timo Otonkoski

Stem Cells Trans Med 2013;2;83-93; originally published online January 22, 2013;
DOI: 10.5966/sctm.2012-0047

This information is current as of February 21, 2013

**Updated Information
& Services**

including high-resolution figures, can be found at:
<http://stemcellstm.alphaamedpress.org/content/2/2/83>

Supplementary Material

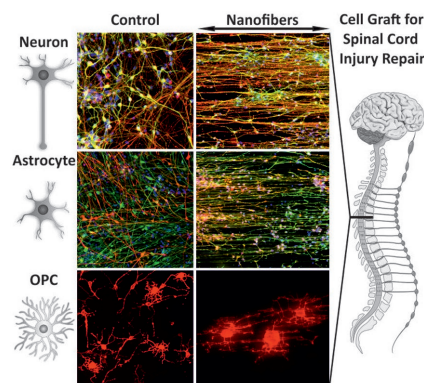
Supplementary material can be found at:
<http://stemcellstm.alphaamedpress.org/content/suppl/2013/01/21/sctm.2012-0047.DC1.html>

 **AlphaMed Press**

Aligned Poly(ϵ -caprolactone) Nanofibers Guide the Orientation and Migration of Human Pluripotent Stem Cell-Derived Neurons, Astrocytes, and Oligodendrocyte Precursor Cells In Vitro

Anu Hyysalo,* Mervi Ristola, Tiina Joki, Mari Honkanen, Minnamari Vippola, Susanna Narkilahti

Stem cell transplantations for spinal cord injury (SCI) have been studied extensively for the past decade in order to replace the damaged tissue with human pluripotent stem cell (hPSC)-derived neural cells. Transplanted cells may, however, benefit from supporting and guiding structures or scaffolds in order to remain viable and integrate into the host tissue. Biomaterials can be used as supporting scaffolds, as they mimic the characteristics of the natural cellular environment. In this study, hPSC-derived neurons, astrocytes, and oligodendrocyte precursor cells (OPCs) are cultured on aligned poly(ϵ -caprolactone) nanofiber platforms, which guide cell orientation to resemble that of spinal cord in vivo. All cell types are shown to efficiently spread over the nanofiber platform and orient according to the fiber alignment. Human neurons and astrocytes require extracellular matrix molecule coating for the nanofibers, but OPCs grow on nanofibers without additional treatment. Furthermore, the nanofiber platform is combined with a 3D hydrogel scaffold with controlled thickness, and nanofiber-mediated orientation of hPSC-derived neurons is also demonstrated in a 3D environment. In this work, clinically relevant materials and substrates for nanofibers, fiber coatings, and hydrogel scaffolds are used and combined with cells suitable for developing functional cell grafts for SCI repair.



A. Hyysalo, Dr. M. Ristola, T. Joki, Dr. S. Narkilahti
NeuroGroup
BioMediTech and Faculty of Medicine and Life Sciences
University of Tampere
Lääkärintätkatu 1 FI-33520, Tampere, Finland
E-mail: anu.hyysalo@staff.uta.fi
Dr. M. Honkanen, Prof. M. Vippola
Department of Materials Science
Tampere University of Technology
Korkeakoulunkatu 6 FI-33720, Tampere, Finland

1. Introduction

Spinal cord injury (SCI) repair has been extensively studied for decades, however, major clinical challenges remain.^[1] Stem cell transplantation therapies are a promising approach for treating patients with SCI because stem cell-derived neural cells have the ability to replace the damaged tissue. The main cell types from the central nervous system, neurons, astrocytes, and oligodendrocytes, can

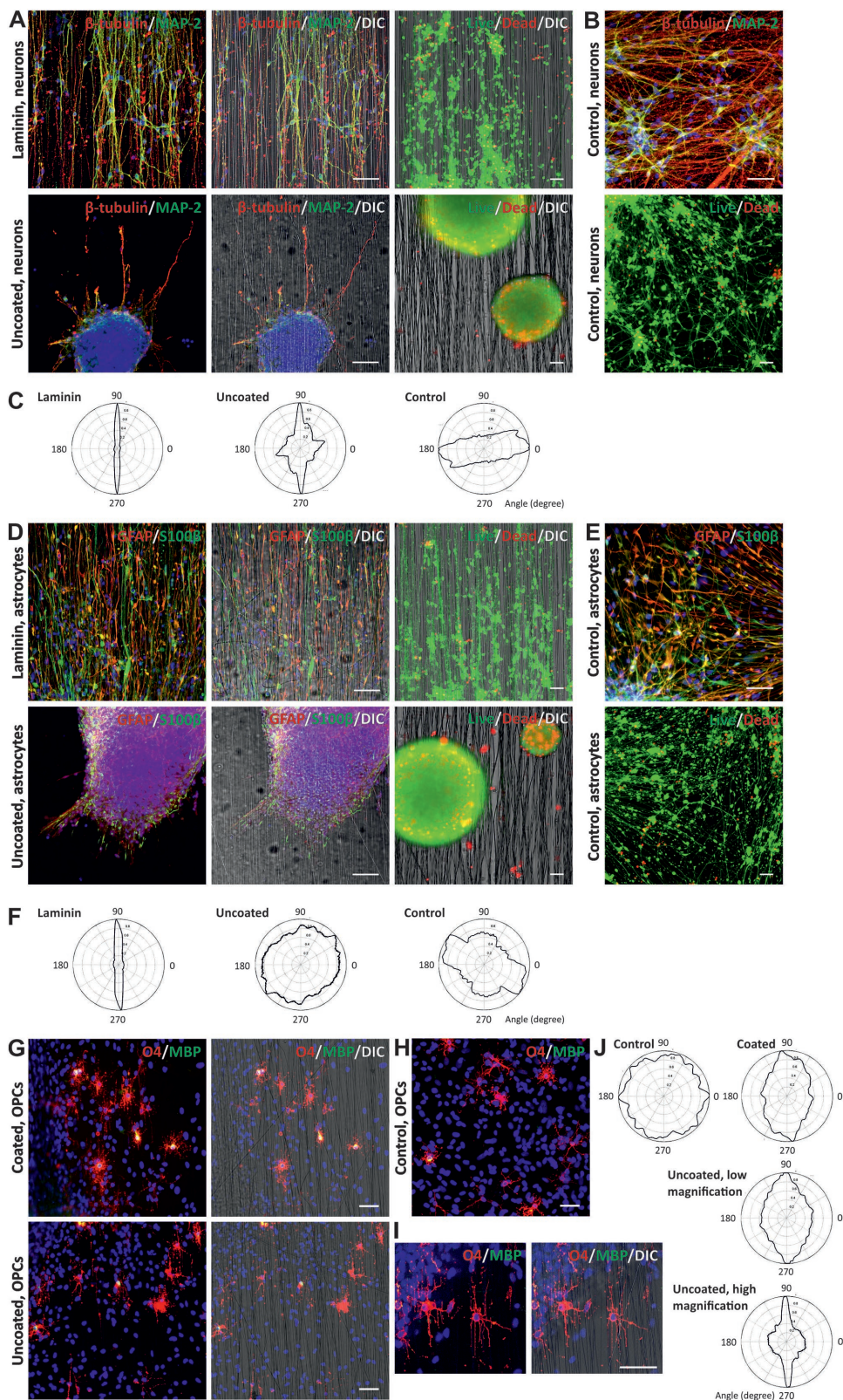


Figure 1. hPSC-derived neurons, astrocytes, and OPCs cultured on uncoated and ECM protein-coated nanofiber platforms. A) hPSC-derived neurons cultured on uncoated and laminin-coated nanofiber surfaces. Live-dead and immunocytochemical staining demonstrates the viability and migration of the neurons on laminin-coated nanofibers. B) Neuron control cultures on laminin-coated 2D polystyrene. C) Orientation distribution of hPSC-derived neurons on laminin-coated and uncoated nanofiber platforms and control cultures. D) hPSC-derived astrocytes

be produced from human pluripotent stem cells (hPSCs) via targeted differentiation, making them suitable for transplantation.^[2–4] Previous studies have shown that the viability, migration, and integration of the transplanted cells into the target tissue are generally poor and inefficient.^[5] To overcome these challenges and to promote SCI repair, supporting biomaterial scaffolds are beneficial. Topographical guidance is crucial for the migration and orientation of the transplanted cells in the target tissue, and nanofabricated electrospun polymer substrates have been shown to mimic the natural cellular environment in the central nervous system (CNS).^[6] Neural cells have been successfully cultured on nanofiber surfaces and extracellular matrix molecule coatings have been used to increase cell viability, migration, and functionality.^[7] Cell electrospinning has also been utilized for encapsulating living cells into fiber structures during fabrication.^[8,9] SCI often results in the formation of a cavity encapsulated by glial scar tissue at the injury site.^[10,11] Thus, more 3D-like scaffolding, in combination with the guiding feature of the nanofibers for transplanted cells, would be essential, enabling proper cell orientation typical of the spinal cord structure.^[12] The integration of guiding nanofibers with soft and porous hydrogels provides a potential structure for such constructs.^[13] Importantly, when cell culture platforms and scaffolds are designed for CNS repair, clinical grade components are needed.

In the present study, we describe culturing of human pluripotent stem cell-derived neurons, astrocytes, and oligodendrocyte precursor cells (OPCs) on aligned poly(ϵ -caprolactone) (PCL) nanofibers. PCL is an FDA-approved material and has previously been studied and utilized in a wide range of tissue engineering applications, including neural cells.^[14] Here, all cell types were shown to efficiently spread over the nanofiber surface and orient according to the nanofiber alignment. We also generated a 3D environment in combination with the nanofiber platform using hydrogel scaffolds with controlled thicknesses. We used clinically relevant materials and substrates for the nanofibers, fiber coatings, and hydrogel scaffolds in order to further develop cell grafts for SCI repair.

2. Results and Discussion

Aggregates of differentiated neurons and astrocytes attached to uncoated PCL fibers, however, the cell

viability was low and cell migration out of the initially plated aggregates was very limited with both cell types (Figure 1A,D, upper row). Previously, extracellular matrix (ECM) molecule coatings on nanofibers have been shown to enhance neural cell growth.^[7] Here, the nanofibers were coated with mouse laminin, which is routinely used as a coating material for hPSC-derived neurons and astrocytes in different *in vitro* applications.^[15,16] A considerable increase in cell viability was detected with both neurons and astrocytes on laminin-coated PCL fiber surfaces compared to uncoated fibers (Figure 1A,D, lower row). Viability on the coated fiber surfaces was similar to the control conditions on laminin-coated polystyrene (Figure 1B,E). Both cell types also efficiently migrated out of the aggregates over the culture area along the laminin-coated nanofibers and oriented according to the fiber alignment (Figure 1A,D, lower row). The mean orientations detected from the neurons and astrocytes on laminin-coated fiber surfaces were 89° and 92° and the circular variances were 0.49 and 0.56, respectively. The mean orientations of neurons and astrocytes on control surfaces were 9° and 146° and the circular variances were 0.70 and 0.88, respectively. (Figure 1C,F) This was an indication of strict orientation of the cells according to the laminin-coated fibers, as the mean orientation of the fibers in the images was 90°. Scanning electron microscopy (SEM) analysis revealed in more detail how the neurons and astrocytes were contacting the laminin-coated nanofibers (Figure S1, Supporting Information). Cell somas mostly attached to the nanofibers instead of the underlying polystyrene. In the neuronal cultures, some cell somas were even elongated, as a result of the cell orientation according to the fibers (white arrowheads). Neuronal processes were migrating on the surface of the nanofibers, but astrocytes wrapped processes around single nanofibers covering the fibers entirely (white arrows). Additionally, the processes deviating and crossing over fibers were detected with both cell types, which can most likely be explained by the laminin coating that was not exclusively specific for the fibers in the cultures.

The culturing of hPSC-derived OPCs has not previously been reported on PCL nanofibers. Here, OPCs were cultured on uncoated PCL nanofiber surfaces and PCL nanofibers coated with a mixture of ECM proteins routinely used in our laboratory for culturing hPSC-derived OPCs on 2D polystyrene.^[3] OPC aggregates attached well to nanofibers and migrated out of the aggregates on both uncoated and coated nanofiber surfaces

cultured on uncoated and laminin-coated nanofiber surfaces. Live-dead and immunocytochemical staining demonstrates the viability and migration of the astrocytes on laminin-coated nanofibers. E) Astrocyte control cultures on laminin-coated 2D polystyrene. F) Orientation distribution of hPSC-derived astrocytes on laminin-coated and uncoated nanofiber platforms and control cultures. G) hPSC-derived OPCs cultured on nanofiber surfaces without additional coating and coated with ECM protein mixture. H) OPC control cultures on 2D polystyrene coated with ECM protein mixture. I) Higher magnification image of OPCs on uncoated nanofiber platform. J) Orientation distribution of hPSC-derived OPCs on coated and uncoated nanofiber platforms and control cultures. Scale bar = 50 μ m.

(Figure 1G). OPCs also mainly oriented according to the fiber alignment, but this result was partly masked by contaminating, nonorienting cells in the differentiated OPC population. A higher magnification image of the OPCs on nanofiber surfaces shows the distribution of more distinct orientation according to the fibers (Figure 1I,J). The mean orientations of OPCs on noncoated and coated fiber surfaces were 95° and 86° , respectively, with circular variances of 0.88 and 0.86, respectively (Figure 1J), indicating a higher variation in the orientation compared to neurons and astrocytes. However, a clear difference was detected in the OPC orientation on nanofiber surfaces compared to control surfaces, for the corresponding orientation and circular variance values for the control cultures were 64° and 0.99, respectively (Figure 1H,J). No difference in the attachment or migration of OPCs on noncoated and coated nanofibers (Figure 1G) was detected as opposed to the behavior of neurons and astrocytes (Figure 1A,D).

Since laminin coating was shown to be required for the survival and efficient spreading of hPSC-derived neurons and astrocytes on PCL nanofibers, xeno-free, and defined recombinant human laminin substrates on nanofiber surfaces were studied. Previously, the use of clinically relevant ECM-coating substrates on nanofiber surfaces has not been reported with human neural cells. Our previous study demonstrated that recombinant human laminin isoforms containing the $\alpha 5$ -chain, or even a fragment of the concerned laminins, supported the viability, growth, and functional development of hPSC-derived neurons more efficiently than traditionally used mouse laminin.^[17] A corresponding study has been performed with hPSC-derived astrocytes, with similar results (unpublished data). Here, we have used laminins (LN)521, LN511, and LN411, as well as the E8 fragment of LN511, for coating the nanofibers.

Both neurons and astrocytes attach and migrate out of the aggregates efficiently on nanofiber surfaces coated with laminin $\alpha 5$ substrates (LN521, LN511, and LN511-E8) (Figure 2A,B). Cell alignment along the fibers was also similar to what was detected on mouse laminin-coated fiber surfaces (Figure 1A,D, lower row). The mean orientations and circular variances on nanofiber surfaces coated with laminin $\alpha 5$ substrates were 90° – 91° and 0.52–0.58 with neurons, and 90° – 92° and 0.50–0.56 with astrocytes, respectively. Furthermore, LN411, previously detected as a nonsupportive coating material for hPSC-derived neurons and astrocytes in 2D cultures on polystyrene,^[17] also failed to enhance cell migration on nanofiber surfaces (Figure 2, Supporting Information). Thus, clinically relevant human recombinant laminin substrates are compatible with PCL nanofibers and can be used for efficient culturing of hPSC-derived neurons and astrocytes on PCL nanofibers.

Previously, hydrogels of different materials have been utilized for embedding the fibers into a 3D scaffold.^[11] These scaffolds have been studied using rodent-derived neural cells, and SH-SY5Y cells, but the results cannot be directly applied to native human cells.^[13,18] Furthermore, human mesenchymal and PSCs in neural differentiation medium have been cultured in a nanofiber-hydrogel scaffold, but the neural differentiation of the cells in these conditions was insufficiently demonstrated.^[19] In this study, we concentrated on hPSC-derived neurons on a hydrogel-nanofiber scaffold. We used commercial PuraMatrix, a self-assembling peptide as a hydrogel with the PCL nanofibers. A peptide-based Puramatrix hydrogel has been shown to support the growth of viable neural cells in 3D conditions and currently clinical grade Puramatrix is commercially available.^[20] Two different thicknesses, 15 and 75 μm , of hydrogel were used and neurons were plated either on top of the thin hydrogel or encapsulated in the thick hydrogel scaffold (Figure 3A). Thin hydrogel was used to investigate whether neurons can sense the effective stiffness and topography of the nanofibers through a thin layer of hydrogel,^[21] as the stiffness of the Puramatrix is considerably lower (storage moduli and loss moduli in range of 5–150 and 1–50 Pa, respectively)^[22,23] compared to PCL nanofibers (Young's modulus in range of 4–60 MPa).^[24,25] Using thick hydrogel, we aimed to discover whether hPSC-derived neurons orient according to the fiber alignment in the 3D hydrogel environment.^[26] Here, the nanofibers were not coated with laminin since Puramatrix itself is a supportive substrate for hPSC-derived neurons.^[27] Laminin coating on nanofibers within the hydrogel could, however, enhance the neurite's contact with the fibers.^[13]

When the cells were plated on top of the thin hydrogel layer, the neurons spread and migrated vertically along the surface of the hydrogel more efficiently than into the hydrogel (Figure 3B). The thin hydrogel (15 μm) on top of the fiber surface isolated the cells from direct contact with the nanofibers, and thus, no processes were detected to follow fiber alignment. Effective stiffness of the fibers did not influence the cells on top of the hydrogel. When the neurons were encapsulated into the thick hydrogel (75 μm), neurons migrating out of the clusters close (<10 μm) to the nanofiber surface started to orient according to the fiber alignment (Figure 3C). However, the cells migrating out of the same cluster a few micrometers further from the nanofiber surface (>10 μm) did not attach to the fibers or adapt to the fiber orientation. The 3D rendered images with pseudocolored depth coding demonstrate the distribution of the cells on the thin and within the thick hydrogel (Figure 3D). Evidently, the cells needed to be initially brought in close contact with the fibers in order to adapt to the fiber orientation in a 3D environment.

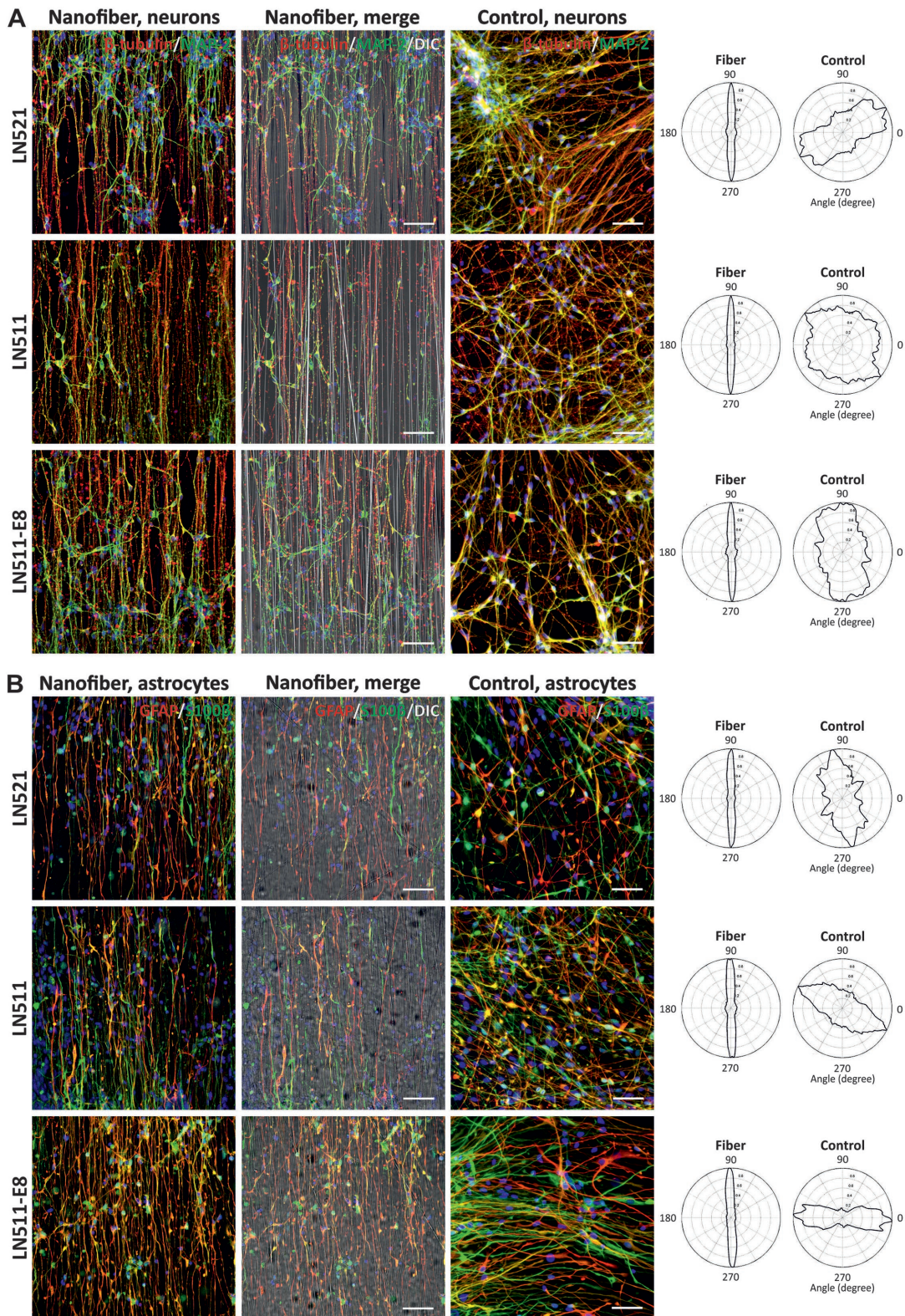
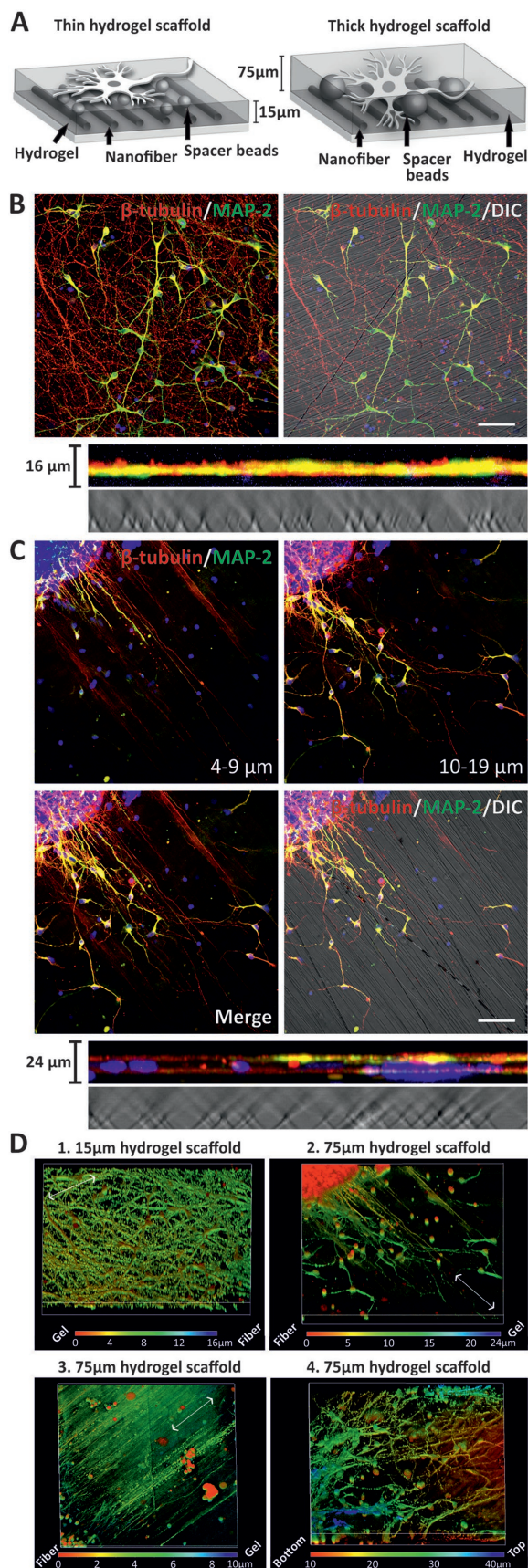


Figure 2. hPSC-derived neurons and astrocytes cultured on recombinant human laminin-coated nanofiber platforms. A) hPSC-derived neurons and B) astrocytes were cultured on nanofiber platforms coated with LN521, LN511, and LN511-E8. The behavior of both cell types on nanofiber platforms with recombinant laminin substrates resembled that of 2D polystyrene control cultures. The orientation distributions of hPSC-derived neurons and astrocytes on nanofibers and control cultures coated with different human recombinant laminin substrates are shown. Scale bar = 50 μ m.



3. Conclusions

In conclusion, we demonstrated that hPSC-derived neurons, astrocytes, and OPCs can be successfully cultured on PCL nanofibers. ECM protein coating for the fibers was required for efficient attachment and spreading of neurons and astrocytes, whereas growth of OPCs was achieved on nanofibers without additional coating. Previously, CNS cells of different origins have been cultured on nanofiber platforms in various conditions, whereas human astrocytes and oligodendrocytes have not been studied on aligned nanofibers.^[28] Furthermore, our results indicate that coculturing of human CNS cells on PCL nanofiber platforms is feasible. The result is of clinical relevance since the coculturing of neurons with astrocytes and OPCs has previously been shown to improve neuronal functional development.^[29,30] We also studied the behavior of hPSC-derived neurons in 3D conditions by embedding nanofibers and encapsulating neurons into a Puramatrix hydrogel. We showed that when using Puramatrix as a hydrogel component, cell seeding by encapsulation into the hydrogel was essential for the development of a 3D neuronal network. We demonstrated that hPSC-derived neurons orient according to fiber alignment in a 3D hydrogel, however, to do so, the cells required initial close contact (<10 μm) with the fibers. Our results are compatible with previous findings concerning the alignment of neural cells in nanofiber-hydrogel scaffolds.^[13,18] Overall, in this work we combined clinically relevant cells and materials, which could be further utilized to develop functional cell grafts for SCI repair.

Figure 3. hPSC-derived neurons cultured on nanofiber-hydrogel scaffolds. A) Schematic presentation of neurons cultured on thin (15 μm) and in thick (75 μm) hydrogel scaffolds on nanofiber platforms. The illustration is not in scale. B) hPSC-derived neurons on top of thin (15 μm) hydrogel-nanofiber scaffold. Cross section of the scaffold presents planar neuronal network on top of the nanofiber surface. Scale bar = 50 μm. C) hPSC-derived neurons in thick (75 μm) hydrogel-nanofiber scaffold. The image has been separated into 4–9 μm image stack from the bottom of the hydrogel scaffold close to the nanofiber surface, and 10–19 μm image stack from the higher level in the hydrogel. Merged images show 24 μm thick stacks with a DIC image of the nanofibers. A cross section of the scaffold demonstrates the neuronal network on two distinct levels in the hydrogel, with the lower level overlapping with the nanofibers. Scale bar = 50 μm. D) 3D rendered images with pseudo colored depth coding demonstrate neuronal growth patterns in more detail on thin and in thick hydrogel-nanofiber scaffold. Images D1 and D2 are depth coding presentations of the same locations presented in images (B) and (C), respectively. Fiber orientation is demonstrated with a white arrow. Images D3 and D4 are separate stacks from one location in the hydrogel-nanofiber scaffold; 1–10 μm image stack from the bottom of the hydrogel scaffold close to the nanofiber surface, and 10–40 μm image stack from a higher level in the hydrogel.

4. Experimental Section

Production of Neurons, Astrocytes, and Oligodendrocyte Precursor Cells: The human embryonic stem cell (hESC) line, Regea 08/023, derived and characterized at the Institute of Biosciences and Medical Technology (BioMediTech, University of Tampere, Finland)^[31] was used for differentiation. The maintenance of pluripotent stem cells was performed as previously described with minor modifications.^[32] The cell lines were quality controlled with frequent protein expression analysis and karyotype and mycoplasma assays. The institute has obtained permission from the Finnish Medicines Agency (FIMEA) to conduct research with human embryos and to derive hESC lines (1426/32/300/05), and a supportive statement from the ethical committee of the Hospital District of Pirkanmaa to derive, culture, and differentiate hESC lines (R05116).

The directed differentiation toward neurons, astrocytes, and OPCs was performed according to previously published protocols with minor modifications.^[3,15]

Cell Culture on Nanofiber Platform: Predifferentiated neural spheres were mechanically dissected into small aggregates, and allowed to randomly distribute and attach to the nanofiber platforms (NanoAligned 24-well plates and 24-well plate inserts, Nanofiber Solutions, Columbus, OH, USA). Cells migrated out of the attached aggregates and spread over the culture area. The mean diameter of a single fiber was ≈ 700 nm, and plasma surface treatment was applied to improve the hydrophilic features of the fibers (<http://www.nanofibersolutions.com/products.html>). The 24 or 48-well polystyrene plates (Nunc/Thermo Fisher Scientific, Rochester, NY, USA) were used as a control platform. Neurons and astrocytes were cultured in NDM with or without 0.1×10^{-6} M LDN193189 (Stem Cell Technologies, Vancouver, Canada) where basic fibroblast growth factor (bFGF) was withdrawn.^[15] Oligodendrocyte precursor cells were cultured in neural stem cell (NS) medium supplemented with 40 ng mL⁻¹ 3,3',5-triiodo-L-thyronine (Sigma-Aldrich, St. Louis, MO, USA), 200×10^{-6} M L-ascorbic acid 2-phosphate (Sigma-Aldrich), 20 ng mL⁻¹ epidermal growth factor (Prospec, Rehovot, Israel), 10 ng mL⁻¹ bFGF (R&D Systems, Minneapolis, MN, USA), 100 ng mL⁻¹ insulin-like growth factor-1 (Prospec), 20 ng mL⁻¹ platelet-derived growth factor-AA (Prospec), and 1 mg mL⁻¹ laminin (Sigma-Aldrich), with or without 0.1×10^{-6} M LDN193189.^[3] The medium was changed three times per week.

Neurons and astrocytes were cultured on nanofiber platforms for two weeks and OPCs for four weeks, and the neurons encapsulated into the hydrogel were cultured for three weeks. Phase-contrast imaging was used to evaluate the attachment and growth of the cells. Cells were imaged using a Nikon T2000S microscope with a DS-Fi1 camera (Nikon Instruments, Amsterdam, Netherlands).

ECM Protein Coatings for the Nanofibers: Laminin from Engelbreth-Holm-Swarm murine sarcoma basement membranes ($2 \mu\text{g cm}^{-2}$, Sigma-Aldrich) was used for coating the nanofibers for neurons and astrocytes. A mixture of laminin ($10 \mu\text{g mL}^{-1}$), collagen IV ($10 \mu\text{g mL}^{-1}$, Sigma-Aldrich), and nidogen(1) ($1 \mu\text{g mL}^{-1}$, R&D Systems) was used for coating the nanofibers for OPCs. Furthermore, xeno-free and defined recombinant human laminins LN411, LN511, and LN521 ($2 \mu\text{g cm}^{-2}$, BioLamina, Sundbyberg, Sweden), or the LN511-E8 fragment (iMatrix-511, $1 \mu\text{g cm}^{-2}$,

Clontech, Takara Bio Inc., Shiga, Japan) were used for coating the nanofibers for neurons and astrocytes. All coatings were prepared by incubating the coating solutions on the nanofiber wells or inserts at $+4$ °C overnight.

Preparation of Hydrogel Scaffolds: Commercial PuraMatrix hydrogel was used on top of nanofibers, according to manufacturer's instructions (Corning, Corning, NY, USA). Hydrogel scaffolds were prepared according to a previously published method, with further modifications.^[21] Briefly, glass coverslips treated with hydrochloric acid (HCl) were incubated in poly(L-lysine) (PLL, 20 kDa) grafted with poly(ethylene glycol) (PEG, 2 kDa) (0.1 mg mL⁻¹, SuSoS AG, Dübendorf, Switzerland) for 30 min at room temperature (RT). Hydrogels were polymerized while sandwiched between a PLL-PEG-treated cover slip and nanofiber insert or nontreated cover slip. A 0.25% Puramatrix was used for hydrogel scaffolds and cell culture medium was used to initiate the polymerization process. The mixture was polymerized at 37 °C for 2 h. The gel thickness was controlled with $15 \mu\text{m}$ polystyrene microspheres (Thermo Fisher Scientific) or $75 \mu\text{m}$ silica microspheres (Corpuscular Inc., Cold Spring, NY, USA), serving as physical spacers between the glasses. Before polymerization, a weight was placed on top of the nanofiber insert or nontreated cover slip in order to remove excess hydrogel. Thus, the diameter of the spacer beads defined the thickness of the gel. After polymerization, the hydrogel scaffolds were carefully detached from the PLL-PEG-treated cover slips and transferred into NDM. Cells were seeded as small aggregates either on top of the hydrogel after polymerization ($15 \mu\text{m}$ hydrogels) or encapsulated into the hydrogel before polymerization ($75 \mu\text{m}$ hydrogels). For encapsulation, cell aggregates (mean diameter $50 \mu\text{m}$) were mixed with final concentration of 0.25% Puramatrix, 5% sucrose, and silica microspheres in dH₂O. The mixture was pipetted on PLL-PEG-treated cover slip and sandwiched with nanofiber insert or nontreated cover slip (Figure 3A).

Cell Viability Assay: A LIVE/DEAD Viability/Cytotoxicity Kit for mammalian cells (Thermo Fisher Scientific) was used according to the manufacturer's instructions for qualitative analysis of cell viability. Briefly, the cells cultured on nanofiber platform were incubated in culture medium supplemented with calcein AM (0.1×10^{-6} M, emission 515 nm) and ethidium homodimer-1 (0.5×10^{-6} M, emission 635 nm) to stain live and dead cells, respectively. After a 30 min incubation at RT in a light-protected area, the cells were imaged with an Olympus IX51 fluorescence microscope equipped with DP71 camera (Olympus Corporation, Tokyo, Japan).

Immunocytochemistry: To investigate the protein expression of neural markers, immunocytochemical characterization was performed as previously described.^[15] Neurons were stained with rabbit anti-microtubule associated protein (MAP-2, 1:400, Merck Millipore) and rabbit anti- β -tubulin isotype III (1:2000, GenScript, Piscataway, NJ, USA). Astrocytes were stained with chicken anti-gial fibrillary acidic protein (GFAP, 1:4000, Abcam, Cambridge, UK) and mouse anti-S100 β (1:500, Abcam). OPCs were stained with mouse anti-oligodendrocyte marker O4 (1:100, R&D Systems), rabbit anti-myelin basic protein (MBP, 1:200, Merck Millipore), or rat anti-MBP (1:100, Abcam).

Immunocytochemical samples were imaged using a fluorescence microscope (IX51, Olympus) with DP71 camera (Olympus) or Zeiss LSM 780 LSCM confocal microscope (Zeiss, Oberkochen, Germany). Visualization of the imaging data was performed using Adobe Photoshop (Adobe Systems Inc., San Jose, CA),

Huygens Essential (Scientific Volume Imaging B.V., Hilversum, Netherlands), Zeiss Microscope Software Zen (Zeiss), and ImageJ (U.S. National Institutes of Health, Bethesda, MD, USA). Qualitative analysis of cell migration was performed by assessing spreading of DAPI-positive cell somas around the initially plated aggregates (Figure S3, Supporting Information). The distribution of cell orientations was analyzed from immunocytochemical samples using the spectral analysis software CytoSpectre.^[33] Cell alignment was quantified as the dominant orientation in degrees, with 0° corresponding to the horizontal level in the image and 90° corresponding to the vertical level along with the fiber alignment. Circular variance presents the spread of the orientation distribution. A lower circular variance indicates higher anisotropy, while a value of 1 indicates evenly spread distribution.

Scanning Electron Microscopy: Surface morphology and cell growth and orientation on the nanofibers were studied in more detail using a field emission scanning electron microscope (FESEM, Zeiss ULTRApplus). The cells were fixed with 5% glutaraldehyde for 1 h at RT. Thereafter, samples were washed with deionized water and dehydrated in a graded ethanol series. Dehydrated samples were carbon glued on the FESEM aluminum stubs followed by carbon coating (turbo carbon coater, Agar Scientific, Stansted, UK) to avoid sample charging during the FESEM studies. In the imaging, an accelerating voltage of 3 kV was used and the samples were tilted ≈55° to observe the 3D structures more easily.

Supporting Information

Supporting Information is available from the Wiley Online Library or from the author.

Acknowledgements: Teemu Ihalainen, Ph.D., is acknowledged for his assistance with the hydrogel scaffold preparation. Outi Paloheimo, M.Sc. and University of Tampere Imaging Core enabled the confocal imaging of the nanofiber samples. Risto-Pekka Pölönen, M.Sc., is acknowledged for his assistance in image analysis with CytoSpectre and M.Sc. student Elina Haukkavaara for her assistance with immunocytochemical analyses. This work was financially supported by Doctoral Programme in Biomedicine and Biotechnology (BioMediTech, University of Tampere), the Finnish Funding Agency for Innovation (Tekes), Finnish Cultural Foundation and the Finnish MS Foundation.

Received: December 13, 2016; Revised: February 6, 2017;
Published online: ; DOI: 10.1002/mabi.201600517

Keywords: 3D environment; differentiated neural cell; human pluripotent stem cell; nanofiber; orientation

- [1] A. S. Kramer, A. R. Harvey, G. W. Plant, S. I. Hodgetts, *Cell Transplant.* **2013**, *22*, 571.
- [2] A. Kirkeby, S. Nolbrant, K. Tiklova, A. Heuer, N. Kee, T. Cardoso, D. Ottosson, M. Lelos, P. Rifés, S. Dunnett, S. Grealish, T. Perlmann, M. Parmar, *Cell Stem Cell* **2017**, *20*, 135.
- [3] M. Sundberg, A. Hyysalo, H. Skottman, S. Shin, M. Vemuri, R. Suuronen, S. Narkilahti, *Regener. Med.* **2011**, *6*, 449.
- [4] A. Shaltouki, J. Peng, Q. Liu, M. S. Rao, X. Zeng, *Stem Cells* **2013**, *31*, 941.
- [5] A. L. Carlson, N. K. Bennett, N. L. Francis, A. Halikere, S. Clarke, J. C. Moore, R. P. Hart, K. Paradiso, M. Wernig, J. Kohn, Z. P. Pang, P. V. Moghe, *Nat. Commun.* **2016**, *7*, 10862.
- [6] J. H. Bell, J. W. Haycock, *Tissue Eng., Part B* **2012**, *18*, 116.
- [7] D. Han, K. C. Cheung, *Polymers* **2011**, *3*, 1684.
- [8] A. Townsend-Nicholson, S. N. Jayasinghe, *Biomacromolecules* **2006**, *7*, 3364.
- [9] S. N. Jayasinghe, *Analyst* **2013**, *138*, 2215.
- [10] Y. Zhong, R. V. Bellamkonda, *J. R. Soc. Interface* **2008**, *5*, 957.
- [11] M. Kamudzandu, P. Roach, R. A. Fricker, Y. Yang, *J. Neurorestoratol.* **2015**, *3*, 123.
- [12] D. E. Koser, E. Moeendarbary, J. Hanne, S. Kuerten, K. Franze, *Biophys. J.* **2015**, *108*, 2137.
- [13] R. J. McMurtrey, *J. Neural Eng.* **2014**, *11*, 066009.
- [14] M. A. Woodruff, D. W. Huttmacher, *Prog. Polym. Sci.* **2010**, *35*, 1217.
- [15] R. S. Lappalainen, M. Salomaki, L. Ylä-Outinen, T. J. Heikkilä, J. A. Hyttinen, H. Pihlajamäki, R. Suuronen, H. Skottman, S. Narkilahti, *Regener. Med.* **2010**, *5*, 749.
- [16] L. Ylä-Outinen, C. Mariani, H. Skottman, R. Suuronen, A. Harlin, S. Narkilahti, *Open Tissue Eng. Regener. Med. J.* **2010**, *3*, 1.
- [17] A. Hyysalo, M. Ristola, M. Mäkinen, S. Häyrynen, M. Nykter, S. Narkilahti, Submitted.
- [18] A. Weightman, S. Jenkins, M. Pickard, D. Chari, Y. Yang, *Nanomedicine* **2014**, *10*, 291.
- [19] N. Shelke, P. Leed, M. Anderson, N. Mistrya, R. Nagaralee, X. Mag, X. Yu, S. Kumbar, *Polym. Adv. Technol.* **2016**, *27*, 42.
- [20] L. Ylä-Outinen, T. Joki, M. Varjola, H. Skottman, S. Narkilahti, *J. Tissue Eng. Regener. Med.* **2014**, *8*, 186.
- [21] A. Buxboim, K. Rajagopal, A. E. Brown, D. E. Discher, *J. Phys. Condens. Matter.* **2010**, *22*, 194116.
- [22] P. Allen, J. Melero-Martin, J. Bischoff, *J. Tissue Eng. Regener. Med.* **2011**, *5*, e74.
- [23] K. Shroff, E. L. Rexeisen, M. A. Arunagirinathan, E. Kokkoli, *Soft Matter* **2010**, *6*, 5064.
- [24] F. Croisier, A. S. Duwez, C. Jerome, A. F. Leonard, K. O. van der Werf, P. J. Dijkstra, M. L. Bennink, *Acta Biomater.* **2012**, *8*, 218.
- [25] S. R. Baker, S. Banerjee, K. Bonin, M. Guthold, *Mater. Sci. Eng., C* **2016**, *59*, 203.
- [26] B. M. Baker, C. S. Chen, *J. Cell Sci.* **2012**, *125*, 3015.
- [27] H. Aligholi, S. M. Rezayat, H. Azari, S. E. Mehr, M. Akbari, S. M. M. Mousavi, F. Attari, F. Alipour, G. Hassanzadeh, A. Gorji, *Brain Res.* **2016**, *1642*, 197.
- [28] H. Cao, T. Liu, S. Y. Chew, *Adv. Drug Delivery Rev.* **2009**, *61*, 1055.
- [29] R. Krenck, J. P. Weick, Y. Liu, Z. J. Zhang, S. C. Zhang, *Nat. Biotechnol.* **2011**, *29*, 528.
- [30] K. Sakai, K. Shimba, K. Kotani, Y. Jimbo, *Conf. Proc. IEEE Eng. Med. Biol. Soc.* **2015**, *2015*, 7127.
- [31] H. Skottman, *In Vitro Cell. Dev. Biol.: Anim.* **2010**, *46*, 206.
- [32] K. Rajala, H. Hakala, S. Panula, S. Aivio, H. Pihlajamäki, R. Suuronen, O. Hovatta, H. Skottman, *Hum. Reprod.* **2007**, *22*, 1231.
- [33] K. Kartasalo, R. P. Polonen, M. Ojala, J. Rasku, J. Lekkala, K. Aalto-Setälä, P. Kallio, *BMC Bioinf.* **2015**, *16*, 344.